

Jafer Sami Ibrahim Abdelkader Ibrahim

Koekoekspolder geothermal field development with long-term sustainability



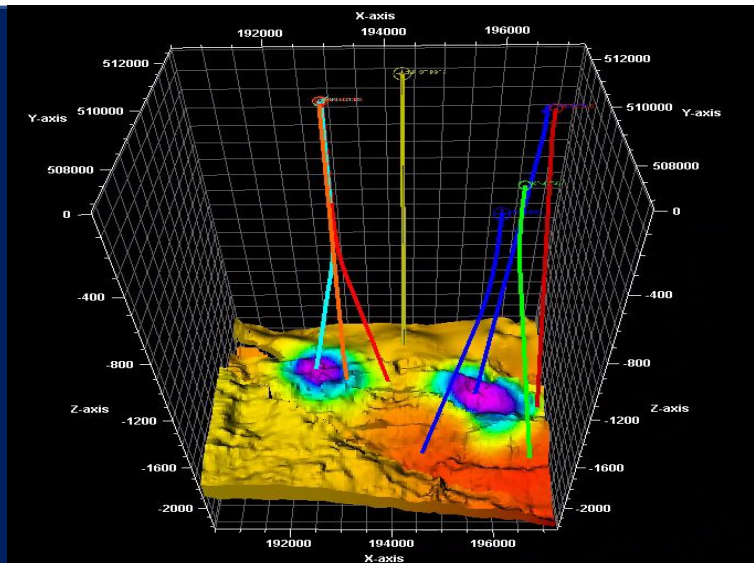
Koekoekspolder geothermal field development with long-term sustainability

Slochteren Formation

Jafer Sami Ibrahim Abdelkader Ibrahim

Msc-thesis

Delft university of Technology



Koekoekspolder geothermal field development with long-term sustainability

By

Jafer Sami Ibrahim

in partial fulfilment of the requirements for the degree of

Master of Geo-Energy Engineering
in Applied earth science

at the Delft University of Technology,
to be defended publicly on Tuesday September 05, 2023 at 16:00 PM.

Supervisors:	Prof. dr. S. (Sebastian) Geiger	TU Delft
	Prof. W.R. Rossen	TU Delft
Thesis committee:	Prof. A. W. Martinius	TU Delft

An electronic version of this thesis is available at <http://repository.tudelft.nl/>.

Acknowledgements

Thank God, I'm grateful for taking this opportunity, I would like to thank all parties involved in this research project for their support. Thank you so much, Prof. Bill Rossen and Prof. Sebastian Geiger. I would like to thank TNO for sharing their static model to be a constructive starting point for dynamic modeling. My gratitude to my TU Delft University, Alexandria University, and my schools (Saint Marc and Saint Gabriel). I appreciate the tremendous efforts of my parents to arrive at this stage. I would like to thank myself for being consistent and never giving up to overcome many technical challenges related to this study. I'm convinced that a true Geo-energy-engineer is a person who is capable of reaching the target of any project feasibly by minimizing as much as he can the disturbance of the naturally existing and balanced system by predicting sustainable strategies that avoid possible problems as much as he can.

Abstract

Revealing an optimal geothermal development strategy attempt with long-term sustainability (upcoming 100 years) based on a real 3D model derived from seismic data is considered one of the main contributions of this research study. The heat extraction and thermal recharge of the reservoir must be in balance to extend the productive lifetime of the Koekoekspolder field system. Based on the best results obtained among different unconventional thermal development approaches, the best locations for the new production wells or extra geothermal doublets as well as the timing, injection temperatures, and rate at which the doublets operate are determined. The best strategy to develop the Koekoekspolder field can be achieved by several steps such as understanding the reservoir properties such as the sedimentary facies, porosity, and permeability distribution by analyzing the literature studies and the static model that simulates the Slochteren formation using Petrel software based on the seismic and log data available followed by a dynamic model that mimics the flow of the hot aquifer inside the reservoir using Eclipse 300 software. Both static and dynamic models must be calibrated by the accessible production data to decrease inaccuracy. The thermal boundaries that are taken into consideration for the koekoekspolder field are not mere confining layers. The workflow of this research study ensures a high degree of realism in terms of the input data and output information of the thermal model of the Koekoekspolder field. The best locations for the new production wells or extra geothermal doublets are determined based on the best simulation results obtained from this research study which fulfill the future energy demand increment. The procedures used in this research study give clear guidance on how the Koekoekspolder field or any other geothermal field can be sustainably developed using a robust history-matched model that has reliable predictions. The low-enthalpy deep geothermal system of the koekoekspolder field is optimized and developed using different types and scenarios of operational strategies for doublets which allow adequate periods for operational thermal recharge. This study takes into consideration different thermal parameters that are not common to achieve enhanced predictions. Moreover, it illustrates the importance and benefits of considering reservoir boundary conditions. Finding suitable sustainable geothermal field development for the Koekoekspolder field can be achieved by new well-studied techniques that can ensure adequate thermal recharge periods. The results of this research study show that the energy demand can be fulfilled with low investment costs to increase the profit of the field owner. Long-term (around 1 century) sustainable development of geothermal fields such as Koekoekspolder and the new technology in this research study can partially contribute to achieving the geothermal master plan objectives in the Netherlands as well as enhancing low and high-enthalpy geothermal field development worldwide.

Contents

Abstract	5
*Nomenclature	8
*Glossary	8
1.Introduction	9
1.1 General overview:.....	9
1.2 Research objectives:	9
1.3 Research questions:	10
1.4 Research approach:	10
1.5 Previous work:	12
1.6 Added value:.....	12
2.Important concepts / Assumptions	13
2.1 Regional overview:	13
2.2 Static model overview:.....	17
2.3 Energy content in Slochteren formation:	18
2.4 Boundary conditions:	20
2.5 Thermal boundaries for Slochteren aquifer:	23
2.6 Initial aquifer velocity:	24
2.7 BHP calculations:	25
3.Methodology	26
3.1 Data analysis:.....	26
3.2 Update static modelling:	27
3.3 Geomechanical modelling:.....	28
3.4 History matching:.....	32
3.5 Forecasting model setup:.....	36
3.6 New possible wells locations & Development strategies:	39
3.7 Qualitative uncertainty analysis:.....	44
3.8 Sensitivity analysis:.....	51
4.Results & Discussion	55
4.1 Production guide rate and temperature distribution:.....	55
4.2 Direct & Indirect increase in doublets:.....	59
4.3 Unconventional geothermal field development:.....	60
4.4 Energy demand fulfilment using the discontinuous shut-off operation:	69
4.5 Well placement and stored energy distribution:.....	69
5.Sustainability & Optimization	74
5.1 Direct & Indirect factors on geothermal sustainability:.....	74

5.2	Ranking of different optimized scenarios:	74
5.3	Optimal field operation:	75
6.	Effects of subsurface geothermal engineering.....	76
7.	Feasibility study.....	77
7.1	Predicting the reliable revenues:.....	77
7.2	Computing the capital expenditures:.....	78
7.3	Calculating Operational expenditures:	80
7.4	Obtaining the pure profit in term of net to present value:.....	81
8.	Conclusion	84
9.	Recommendation.....	85
10.	New technology.....	87
11.	References.....	88
12.	Appendices.....	92

*Nomenclature

The following symbols are used within this document:

λ	Thermal conductivity	[W/m/K]
λ_f	Fluid thermal conductivity	[W/m/K]
λ_s	Matrix thermal conductivity	[W/m/K]
θ	Porosity	[-]
ϕ_e	Effective reservoir porosity	[-]
ρ	Density of the material	[Kg/m ³]
ρ_f	Pore filling fluid density	[Kg/m ³]
ρ_s	Rock density	[kg/m ³]
c	Heat capacity	[J/Kg/K]
c_f	Heat capacity of the pore fluid	[J/Kg/K]
c_s	Heat capacity of matrix rock	[J/Kg/K]
ρc	Volumetric Heat capacity	[J/m ³ /K]
ρc_b	Bulk volume heat capacity	[J/Kg/K]
E_R	Stored energy of a geothermal reservoir	[J]
V	volume of the reservoir	[m ³]
T_R	Reservoir temperature	[°C]
T_{ref}	Reference temperature	[°C]
KKP	Koekoekspolder {name of the field} / [O.T.R]	Operational thermal recharge

*Glossary

By knowing that the thermal recharge is always taking place, **Operational thermal recharge**^{*1}[O.T.R] is simply shutting a certain doublet/wells for a defined period to allow thermal recharge without any cooling as a result of water injection in that doublet as in the case of **Discontinuous Shut-off geothermal development strategy**^{*2} and **Continuous shut-off geothermal development strategy**^{*3} or by injecting a small amount of cold water as in the **Low pressure gradient geothermal development strategy**.

Discontinuous Shut-off geothermal development strategy^{*2}:shutting off the doublet under [O.T.R] for instance for 1 year or for few months then operating the doublet for the following year, and so on.

Continuous shut-off geothermal development strategy^{*3}:continuous [O.T.R] by shutting off the wells for a certain continuous period without any injected or produced water.

Low pressure gradient geothermal development strategy^{*4}:operating the doublet which are under [O.T.R] with a small difference in bottom hole pressures(low pressure gradient).

Jafer matrix for geothermal operation^{*5}:matrix build from 0 and 1 which simply reflects the shut off periods and operation periods respectively of all doublets that are present in a geothermal field using Discontinuous Shut-off geothermal development strategy^{*2} to allow adequate [O.T.R] that overcome high yearly cooling rate of the geothermal reservoir. This matrix can help the owner of any geothermal field to have less constraints related to the injection temperature.

Filling duration^{*6}:the time that 1 kg of the produced brine water takes from the bottom hole of the production well to the bottom hole of the injection well.

Thermal fatigue^{*7}(**Geothermal fatigue zones**):refers to the parts of the reservoir that are subjected to cooling for a long period of time as in the vicinity of the injection wells or the parts of the reservoir that are subjected to an excessive cooling due to cold front intersections of injection wells. The duration of time that the surface area of 1m² of the reservoir rock is subjected to the continuous flow of injected cold water due to direct contact with the injected brine water through effective pore spaces.

1. Introduction

1.1 General overview:

According to the Geothermal Masterplan in the Netherlands (2018), the aim is to increase the current production of 3 PJ of geothermal energy per year to 50 PJ per year in 2030 and eventually to 200 PJ per year in 2050 to reach the CO₂ reduction goals as stated by the government. Effective development of geothermal fields such as Koekoekspolder can partially contribute to achieving the master plan objectives.

The current doublet in Koekoekspolder field located North-East of Kampen in Overijssel was drilled in 2011. The doublet consists of production well KKP-GT-01 and injection well KKP-GT-02. Both wells target the mid-Permian Slochteren reservoir formation in the upper Rotliegend group at an approximate depth of 1850 meters. The well KAM-01-S1 located near the field area provides core data of the Slochteren formation. Plans to drill an additional production well (KKP-GT-03) are being materialized.

The Slochteren formation is sealed by the Zechstein Group, and it contains a sequence of red to light reddish brown with occasional gray or yellow sandstones and conglomerates with a broad range of grain size, texture, and sedimentary structures (TNO-GSN, 2020). Different mineral compositions are found in the targeted aquifer like gypsum, anhydrite, and iron oxide grains (Ziegler, 2006).

An expert report provided by Pan Terra Geoconsultants in December 2008 states that the field could support 8 doublets based on seismic and petrophysical interpretation as well as the possible drilling trajectories which can reach a maximum inclination of 45 degrees. The underground distance between the injection and the production well is about 1500 m.

For the new doublets, the distance between the injection and the production well can be smaller in case of barriers (less permeable areas) in the reservoir that can hinder the free flow of the injected water. For the current doublet, the production capacity is lower than the injection capacity. For this reason, an extra production well has been included by the permit holder in the production forecast to double the expected energy yield from currently 150,000-170,000 GJ to 350,000 GJ per year. At the top of the Slochteren formation, the reservoir pressure is 196 bar, while the hydrostatic pressure at the same depth is 192 bar, which means that this aquifer was over-pressured. The initial reservoir temperature at the production well is approximately 76.4°C, and the injection temperature is around 35°C.

1.2 Research objectives:

This thesis aims to find a balance between the short-term heat extraction for optimal business development and the long-term sustainability of the KKP geothermal field, because developing a geothermal play in terms of maximizing heat extraction can result in an unsustainable situation where parts of the reservoir are thermally depleted to such an extent that future heat energy demand might not be met from the thermal resources in that geothermal

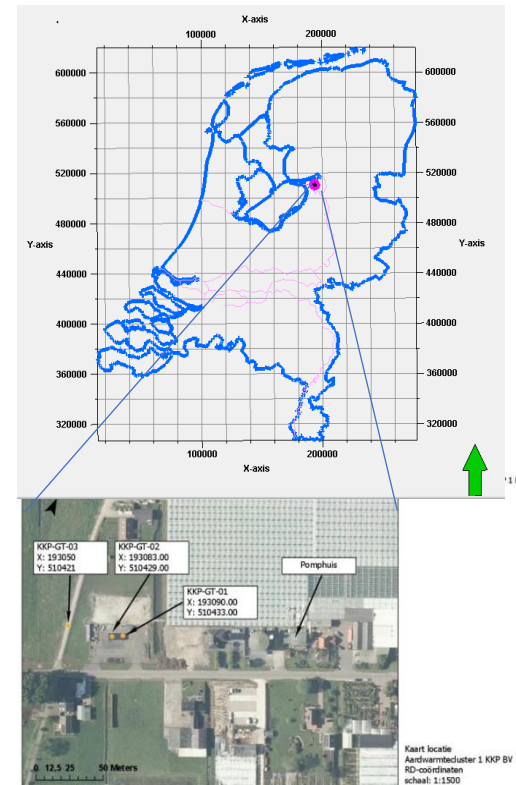


Figure 1: Illustration of the KKP field with wells location from an aerial photo.

aquifer. The goal of this research is to derive scenarios for optimized exploitation with multiple wells in the KKP license area. In order to achieve this objective, the long-term heat demand will be offset by the potential subsurface supply of heat. A stepwise approach is needed for new wells (type, location, timing) that allow optimal and sustainable utilization of the reservoir in combination with economical optimization for the future. Dynamic reservoir model (using Petrel and Eclipse300) was history matched by available production data to model forecasts for the upcoming 50 to 100 years after observing as much as possible the direct and indirect relationship between the effective operation and reservoir parameters with the geothermal heat production as well as maximizing the lifetime of the geothermal system. The final output is a system where field development, energy extraction, and heat regeneration of the subsurface are in an optimum equilibrium to build an effective sustainable development approach for the deep geothermal system at KKP field.

1.3 Research questions:

Based on the research objectives, the following questions need to be answered:

- How are the boundaries for the geothermal reservoir defined in general and especially in the area of Koekoekspolder?
- What are the key factors to define a geothermal reservoir in Koekoekspolder?
- What are limitations (for instance winningsplan, seismic risk, compaction, etc.) that are relevant in the use of a geothermal reservoir in general, and specifically in the Koekoekspolder license area?
- What does a long-term heat balance (influx of heat in the reservoir/type of heat transfer, outflux/extraction of heat look like for a geothermal play in general and specifically for the geothermal play in Koekoekspolder by taking the economic aspects into account? How can this be combined in the model?
- How does the future local heat demand align with the optimal heat supply from the Koekoekspolder reservoir?
- What is the field development plan for Koekoekspolder (number and type of wells, timing of well availability) if thermal regeneration is a prerequisite?
- What are the possible thermal development approaches to optimize a balanced use of the targeted hot aquifer, also looking at possibilities to increase the lifetime of the reservoir under exploitation?

1.4 Research approach:

To answer the defined research questions and to cover all aspects related to the research questions to the extent feasible, the steps indicated in the following chart have been conducted. The research approach steps illustrated in chart 1 help in finding the best strategies to develop KKP geothermal field by:

- Understanding the reservoir properties as permeability distribution, current and long-term development of the injection and production behavior of the doublet to have a better overview of the short and long-term heat delivery.

- Observing as much as possible the direct and indirect relationship between the effective operation and reservoir parameters with the geothermal heat production as well as maximizing the lifetime of the reservoir, moreover, adjusting the created model by the available production data (History matching).

- Identify optimal placement of the second production well and/or a new doublet for KKP aquifer development.

- Applying economical study to be able to predict the revenue from the most effective development strategy.

- Explaining the findings of the study and including recommendations on the optimal development for the Slochteren formation which can be applicable for other doublets in the Netherlands.

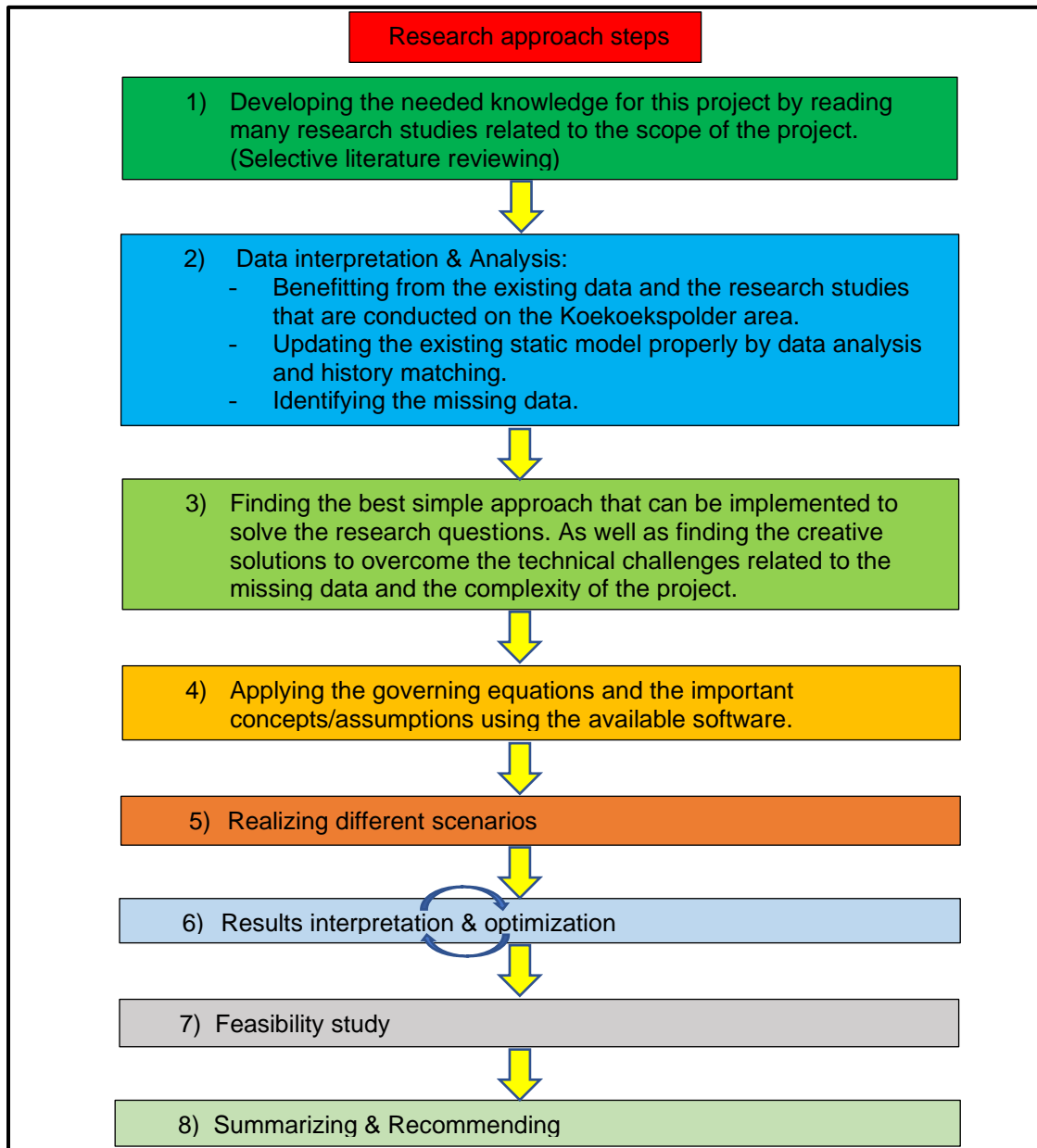


Chart 1: Research approach steps.

The stage of both gathering and evaluation of existing data is very important to deliver accurate and reliable results, this is why more organized inputs are needed to update the existing static model and to construct a geothermal dynamic model that is adjusted by history matching which will help in decreasing the uncertainty related to the placement of new production well or doublets. The data analysis of the KKP field is mainly conducted by quantitative methods. The static model that mimics all the possible details such as the lithology and permeability distribution can be updated using Petrel. The static model can be calibrated by the available production and injection data (History Matching). Furthermore, dynamic modeling can be

achieved by Eclipse software for the optimization of both wells placements and field operation. The analysis of the injectivity and productivity can be conducted with Excel software. By using Python software for the geomechanical modeling, the maximum injection pressure for field operation can be quantitatively computed with Mohr coulomb criteria as well as the minimum production pressure to avoid any effects of subsurface engineering as induced seismicity.

1.5 Previous work:

A static model of the KKP field by TNO (Redjosentono, 2014) was the starting point for the dynamic modeling simulation of the Slochteren formation in the KKP field performed for this thesis. The Rotliegend is an Aeolian sandstone with bimodal horizontal parallel lamination based on the core, seismic, and well data interpretation. The Rotliegend Aeolian reservoirs contain zones of high density which indicates the presence of anhydrite /gypsum, and these zones may reach thicknesses up to 15 meters that can be interpreted as nodular gypsum growth or as gypsum dunes. The static model is based on object modeling and multiple points statistic techniques with input data from logs and core studies. Moreover, the case study area is covered by high-resolution seismic imaging. Based on the history matching process and a detailed study of the reservoir properties for this thesis, the net to gross ratio is adjusted, and the static model of the KKP field by TNO (Redjosentono, 2014) is updated to understand the flow through the Slochteren aquifer. (Franco and Donatini, 2017) described a simple method to compute the energy of the geothermal reservoir, which is used in this research study with few modifications. Despite the presence of many different methods and reliable perspectives that are tested and used, it is challenging to obtain a collective and general view of computing the energy of the subsurface geothermal reservoir that connects between the parameters of geothermal plant design, reservoir characteristics, and reservoir engineering. The methods estimate simply the thermal energy content in the reservoir by taking into consideration the contribution from the solid rock and liquid phase. (Chen, Liu and Liao, 2019) studied the reservoir boundary conditions for the enhanced geothermal system by establishing a thermal-hydraulic-mechanical coupled model to compare the performance of fracture reservoir under 'recharge' boundary conditions with that under 'no-flow' during the heat extraction process. The recharge boundary conditions permit fluxes of mass and heat across the reservoir boundaries which will affect the geothermal reservoir lifetime. Heat compensation from surrounding rocks "under recharge boundary conditions " has a strong influence on the lifespan of the reservoir. The efficiency of energy generation is positively correlated to the reservoir permeability and water production rate.

1.6 Added value:

Next to this detailed case study of Slochteren formation in the KKP field, recommendations are made for the translation of the site-specific results to the larger scale Slochteren play in the Netherlands by providing a sustainable development catalog that balances between preliminary revenue and long-term sustainable heat extraction for geothermal projects and better strategies for sustainable geothermal field development accompanied with a new technology of geothermal field development. In this report, a broader and profound analysis of sustainable heat production and development terms is taken into consideration, which includes compatible development with recharging characteristics of the aquifer as well as the effects of the subsurface as induced seismicity and subsidence that can be an obstacle or contradict the sustainable development concept.

2. Important concepts / Assumptions

2.1 Regional overview:

To have realistic boundary conditions for the Koekoekspolder dynamic model, the regional study was the first step. The Slochteren aquifer of the KKP field is located adjacent to the eastern side of the Texel-IJsselmeer High basement rock (TYH).

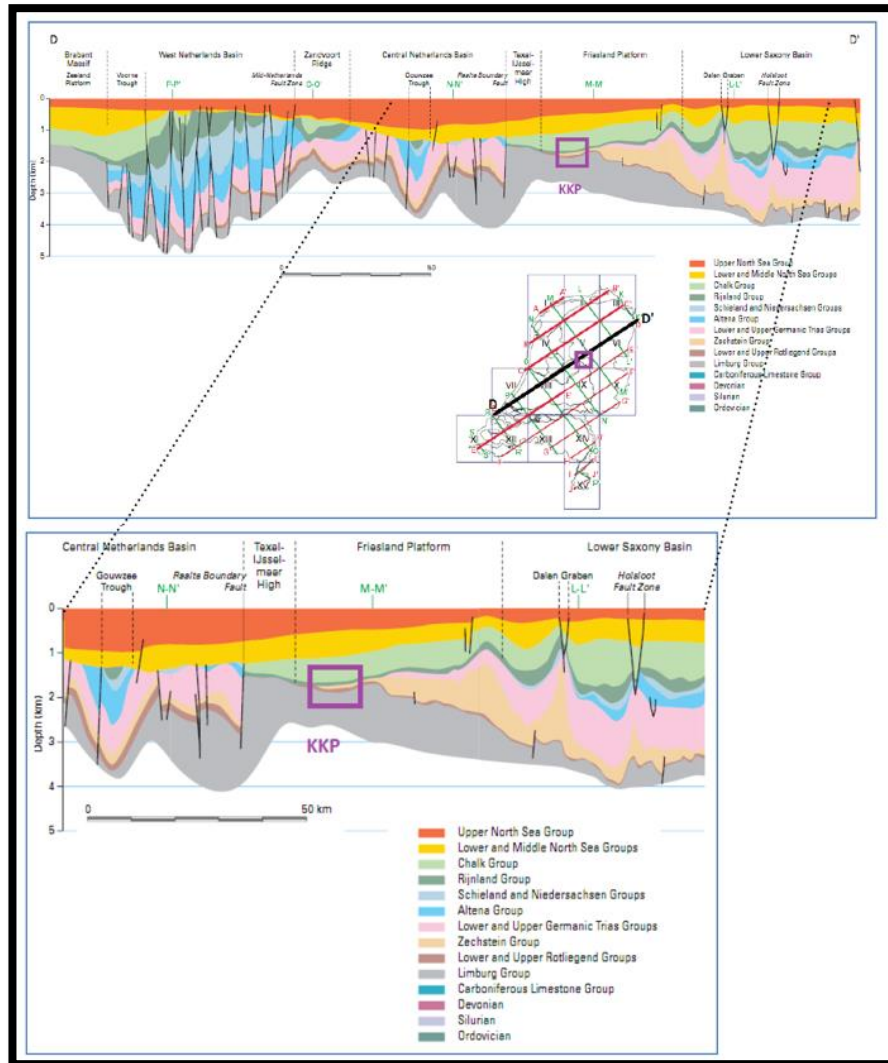


Figure 2: shows the position of koekoekspolder subsurface area according to the regional cross-section (Redjosentono, 2014).

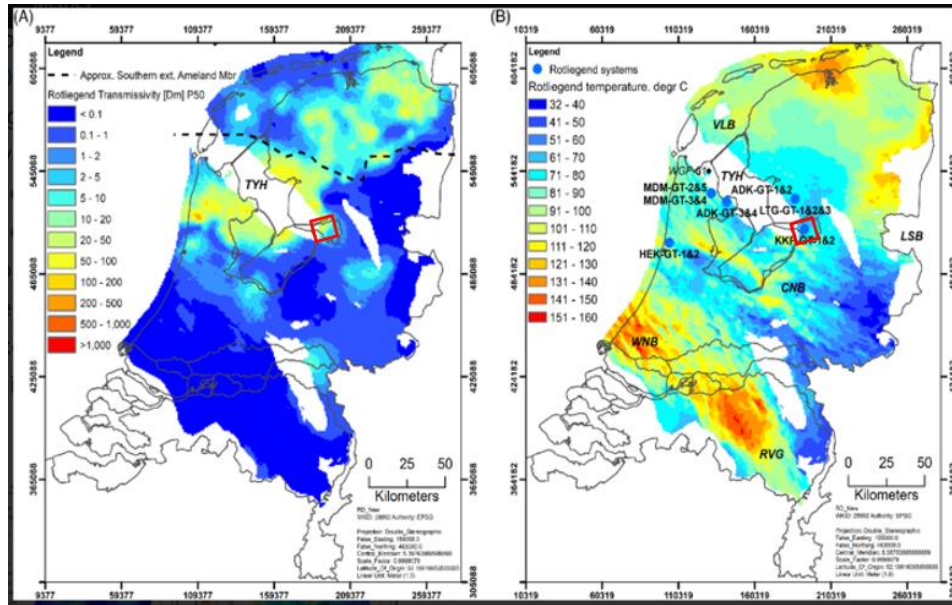


Figure 3: A) Transmissivity distribution of Rotliegend Slochteren formation, B) Temperature pattern of Rotliegend systems in the Netherlands (Bonté, Van Wees and Verweij, 2012).

Based on the Slochteren formation distribution, the Slochteren formation disappears toward the western side of the Koekoekspolder field. Multi-well pressure-depth plots, salinity maps, regional fluid overpressure maps, and hydraulic-head maps are used to evaluate the present-day pressure and fluid flow conditions in the Rotliegend reservoir (Verweij et al., 2011) to determine which boundaries allow heat and mass flow. It's very important to study the hydrodynamics of the Slochteren formation on a regional scale to determine the distribution of current pressure and fluid-flow conditions. This can provide realistic assumptions for the northern and southern boundary conditions as in figure 4.

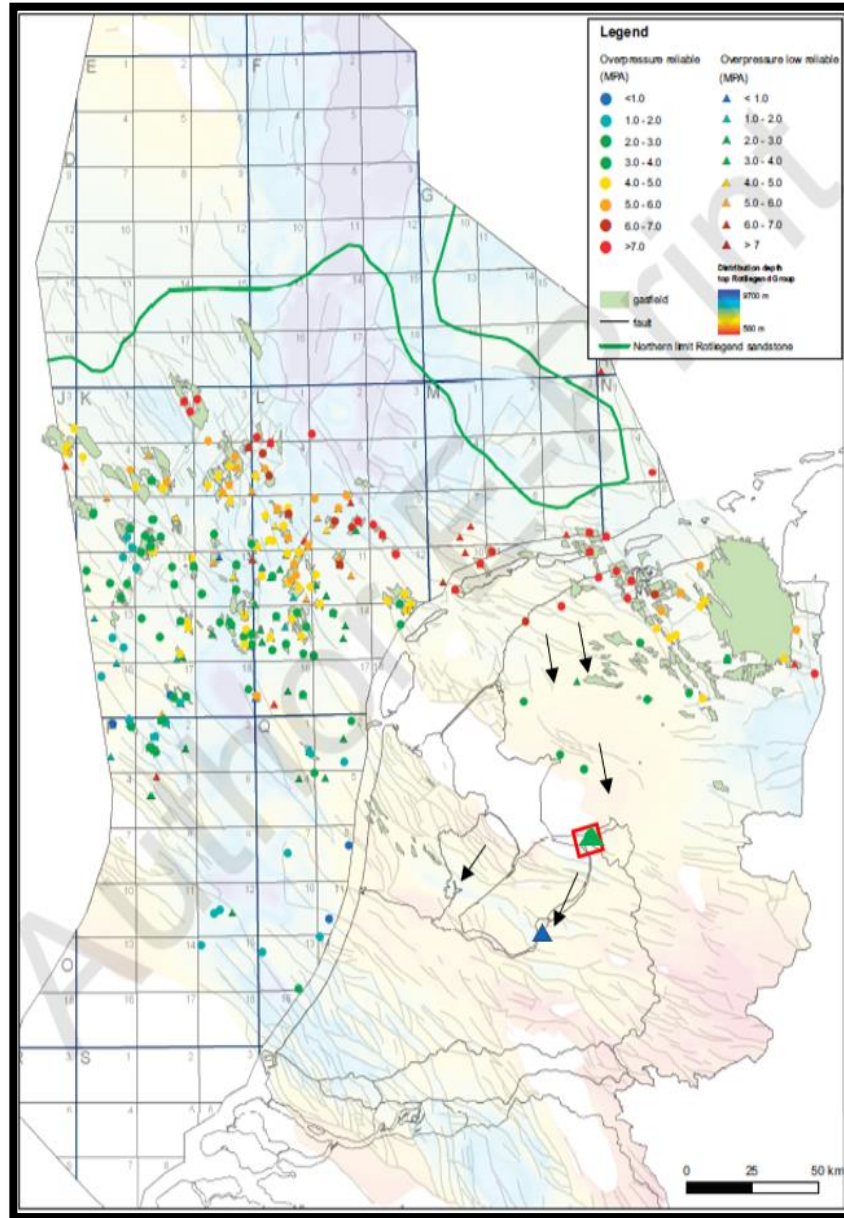


Figure 4: Distribution of fluid overpressures in the upper Slochteren formation. Red square represents the KKP field area, black arrows represent the estimated direction of the natural aquifer flow (Simmelink & Underschultz, 2015; Verweij et al., 2011).

As shown on the map in figure 4, there are different levels and ranges of overpressure from near-hydrostatic pressures mainly in the southern part of the Netherlands (Excess pressure < 1 MPa) and high overpressures (Excess pressure > 40 MPa) in the northern part. The pressure gradient results in a potential general trend for aquifer flow in the Slochteren from the northeast to the south (Verweij et al., 2011). At the western side of the Koekoekspolder field, Texel-IJsselmeer High is located where the aquifer pinches out.

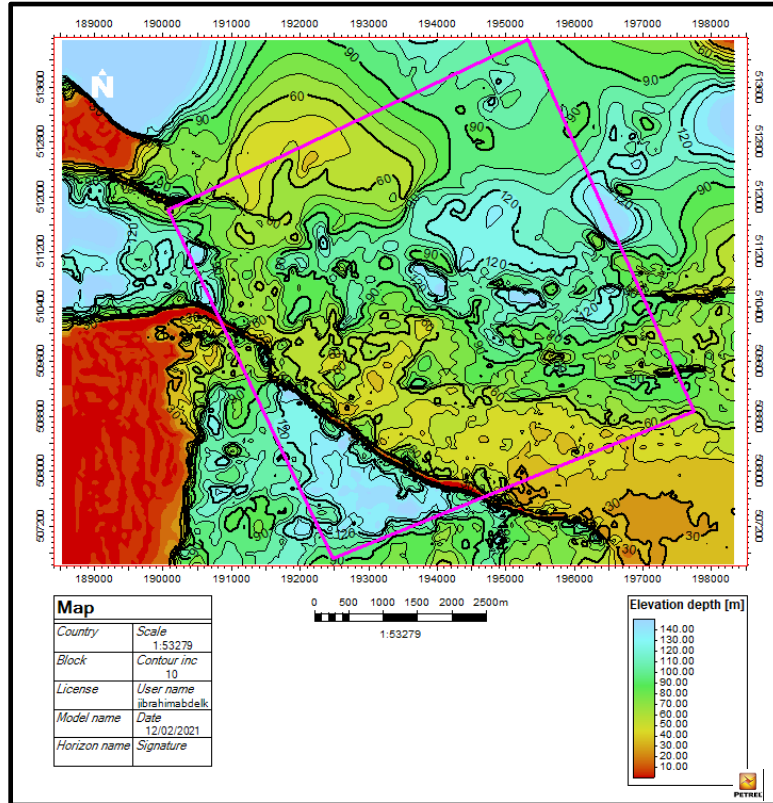


Figure 5: Thickness map of Rotliegend which illustrates parts of no thickness indicated by the red colour due to changes in formation or lithology (Redjosentono, 2014).

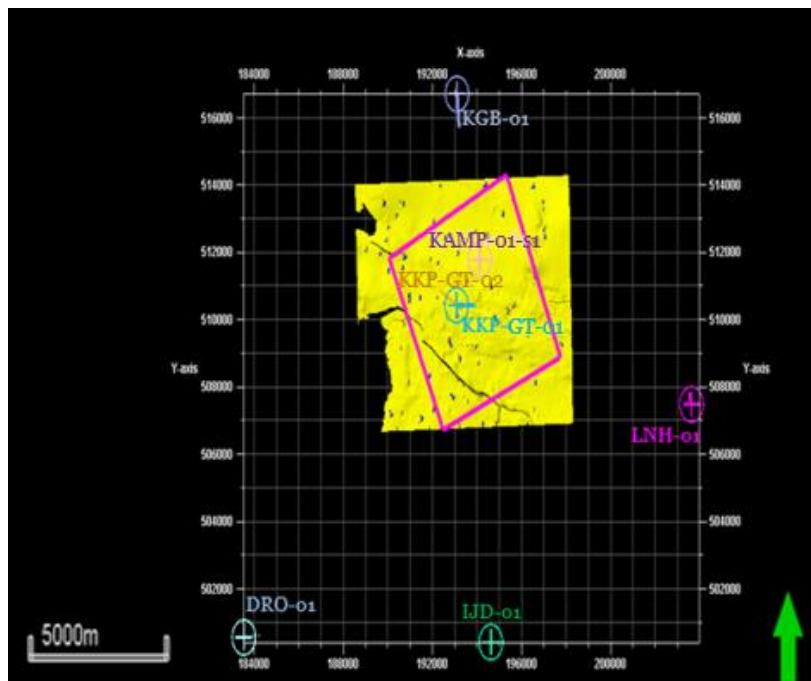


Figure 6: shows the well locations inside and outside the Koekoekspolder license area.

2.2 Static model overview:

The facies model consists of gypsum bodies with Aeolian sandstone as background and the facies modeling of the static model has been done by object-based modeling with input data from logs and core (Redjosentono, 2014). The 3 drilled wells in the KKP field and different parts of the thickness map indicated in figure 5 after applying time-depth conversion (Redjosentono, 2014) show that the thickness of the Slochteren formation increases toward the NE direction which may emphasize that the wind direction was in the same NE direction during the deposition of aeolian sand (Kiersnowski, 2013) which can indicate that the permeability in the NE direction is higher than the other permeability directions.

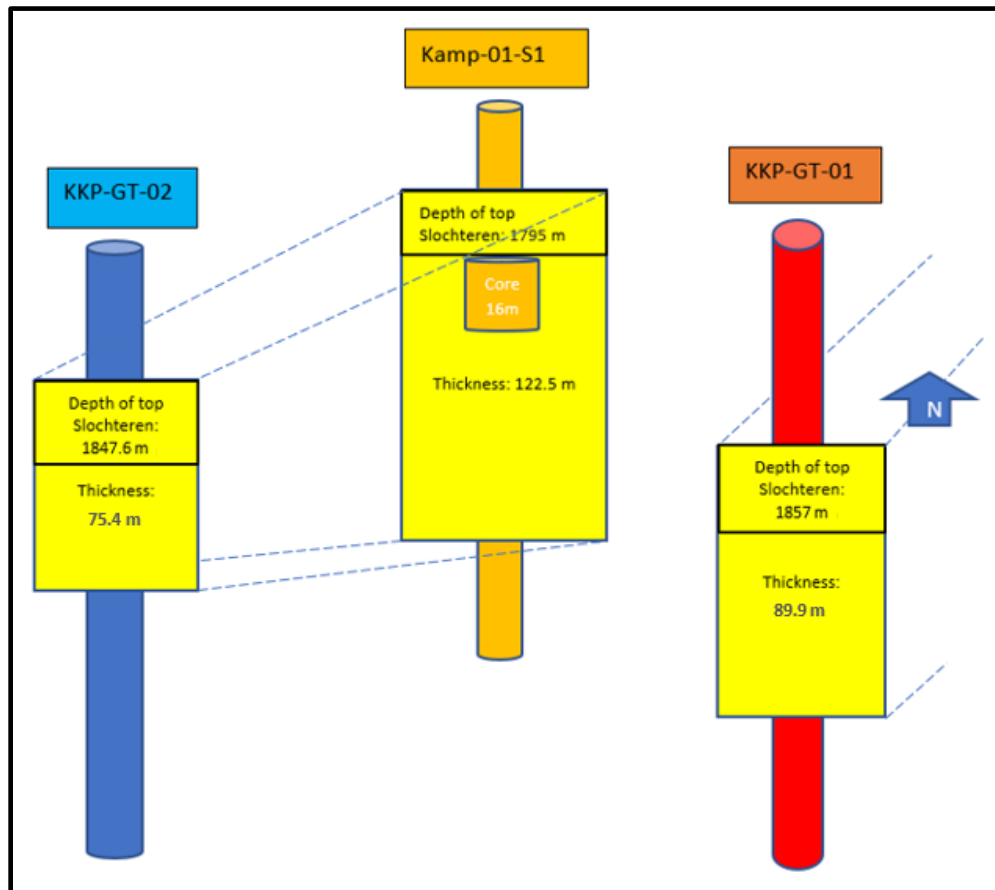


Figure 7: Borehole data indicates the direction of thickness increase (north-east).

The Aeolian sandstones of the Slochteren formation were deposited under a North-East constant wind direction (Glennie, 1982; Redjosentono, 2014). Middle Rotliegend is the best zone because it has high porosity and permeability (Willems, Cees; Donselaar, Rick; Weltje, 2014):

- 1- Upper zone has low porosity and permeability
- 2- Middle zone has high porosity and permeability
- 3- Lower zone has very low porosity and permeability

The gypsum sections in the 2 wells (KKP-GT-01 and KKP-GT-02) are not present in the well Kamp-01-S1 which favored the concept of nodular gypsum presence. The geometry of these gypsum bodies (Gypsum nodulars or enthorlitic) are based on the seismic amplitude response

(Redjosentono, 2014). Based on the porosity-permeability relationship, the areas with high porosity values have higher permeability as well.

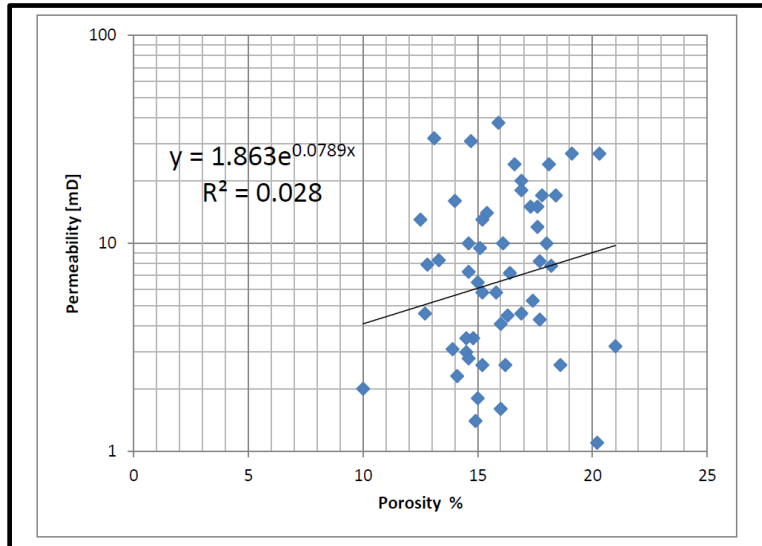


Figure 8: shows the porosity-permeability cross-plot based on the porosity and permeability measurements from the Kampen core plug (TNO; Minister of Economic Affairs and Climate, no date; Redjosentono, 2014).

The relation between porosity and permeability based on laboratory experiments is used as a petrophysical guideline to estimate the permeability of similar reservoir units in the areas around wells with no cores available. The following equation describes the relationship between porosity and permeability based on a cross-plot of the average porosity and the average permeability from different wells (Redjosentono, 2014):

$$(1) \quad K = 1.1978 * e^{27.093\phi}$$

The majority of faults have an orientation from NW to SE due to rifting before the Permian period. The existing faults in the Koekoekspolder concession were subjected to the Alpine Inversion. The direction of compression was from south and North which resulted in the inverted blocks in the KKP area. The permeability of faults can be very low due to the intense friction that occurred along the different faults in KKP and the high clay content in the Silverpit and Ruurlo formations which are the confining layer of the Slochteren aquifer. Based on the well logs interpretation of the injection well KKP-GT-02 and the production well KKP-GT-01, the static model consists of aeolian sandstone, which represents approximately 88.12 %, and gypsum nodules that make 11.88 % of the total reservoir volume. There might be fractures inside the gypsum nodules of the Slochteren formation, but in this study, the gypsum volume which accounts for 11.88 % of the Slochteren geothermal reservoir based on the well logs interpretation is considered as impermeable bodies.

2.3 Energy content in Slochteren formation:

It's relevant to understand how the heat energy of the reservoir can be obtained and this can be achieved by computing at the beginning the total volumetric heat capacity of the targeted aquifer that represents all the components of the reservoir, then computing the energy of the aquifer by multiplying the volume of the reservoir with the representative heat capacity and the difference between reservoir and surface temperature. The energy of the reservoir varies through the different subsurface locations of the aquifer. Firstly, the heat capacity is defined as the amount

of heat that is needed to raise the temperature of a material unit volume (1 m³) or mass (1 kg) by 1 kelvin with no change in phase. Thus, the specific heat capacity { c_s } can be expressed in energy per unit weight for every one-degree change in temperature (J/Kg/K), and the volumetric heat capacity is the energy per unit volume for every one-degree change in temperature (J/m³/K). The volumetric heat capacity { $c_v = \rho \cdot c_s$ } in [J/m³/K] can be obtained by multiplying the specific heat capacity by the density of the material in (Kg/m³). The bulk volume heat capacity of the Slochteren geothermal play represents the total volume heat capacity of the reservoir rock and the occupying pore fluid. All the components of reservoir rock must be taken into consideration in the calculation of the bulk volumetric heat capacity. The bulk volume heat capacity c_b can be calculated using the following equation (assuming full saturation of the pore volume).

$$(2) \quad c_b = \phi \rho_f c_f + (1 - \phi) \rho_r c_r$$

ϕ : porosity, ρ_f and ρ_r : are respectively the pore filling fluid and matrix rock density [kg/m³], c_f is the specific heat capacity of the pore fluid, and c_r expresses the specific heat capacity of matrix rock [J/kg/K].

Furthermore, the bulk volumetric heat capacity is computed based on the average porosity and the average proportion of rock components, but the porosity and lithologies vary along the horizontal and the vertical directions of the reservoir. The following equation represents the total bulk matrix capacity and density of the Slochteren formation.

$$(3) \quad c_r = F_1 * c_{sandstone} + F_2 * c_{Gypsum}$$

$$(4) \quad \rho_r = F_1 * \rho_{sandstone} + F_2 * \rho_{Gypsum}$$

Where c_r and ρ_r are the total bulk matrix capacity and the total matrix bulk density, respectively, $c_{sandstone}$ is the sandstone heat capacity and c_{Gypsum} is the gypsum heat capacity, while $\rho_{sandstone}$ is the sandstone density, and ρ_{Gypsum} is the gypsum density.

Based on well log interpretation, F_1 is the volume percentage of the sandstone matrix component, F_2 represents the volume percentage of the gypsum matrix component. The density of Gypsum is around 2360 kg/m³, while the density of sandstone is approximately 2350 kg/m³ (Arisona *et al.*, 2018). The specific heat capacity of sandstone is around 850 J/kg/k (Kirk and Williamson, 2012). The heat capacity of Gypsum is around 1090 J/kg/k (Evans, 2016). The above equations can be developed for any subsurface aquifer with different fluid types or phases as well as heterogeneous rock composition to be as follow.

$$c_b = \underbrace{\phi * X_1 * \rho_{f1} c_{f1}}_{1^{st} \text{ term}} + \underbrace{\phi * X_2 * \rho_{f2} c_{f2}}_{2^{nd} \text{ term}} + \underbrace{F1 * (1 - \phi) \rho_{s1} c_{s1}}_{3^{rd} \text{ term}} + \underbrace{F2 * (1 - \phi) \rho_{s2} c_{s2}}_{4^{th} \text{ term}} + \dots \dots \dots \underbrace{\dots \dots \dots}_{N^{th} \text{ term}}$$

Where ϕ is the porosity, X_1 and X_2 are the degrees of saturation of the first and second fluid types or phases. ρ_{f1} and ρ_{f2} are the fluid densities of the first and second fluid types or phases. c_{f1} and c_{f2} are the specific heat capacities of the first and second types or phases of pore fluids. F_1 and F_2 are the volume percentages of the first and second types of lithologies. ρ_{s1} and ρ_{s2} are the densities of the first and second types of lithologies. c_{s1} and c_{s2} are the specific heat capacities of the first and second types of lithologies. Depending on the number of lithology types, fluid, and phase types, the number of terms related to the lithologies types, fluid types and/or phases can increase. The accuracy of the estimated stored energy of a geothermal reservoir depends on taking into consideration:

- All the conceivable types of lithologies in the reservoir as well as rock matrix and cement mineralogy.

- All the types and phases of the fluids that are present in the pore-spaces of the geothermal reservoir.

The stored energy of a geothermal reservoir can be obtained using the following equation (Franco and Donatini, 2017).

$$(5) \quad E_R = c_b * V * (T_R - T_{ref})$$

Where c_b is the bulk volume heat capacity, V represents the volume of the reservoir, T_R is the reservoir temperature, and T_{ref} indicates the reference temperature (surface temperature).

The average salinity of the brine water (concentration of salt) inside the Slochteren formation is approximately 15 %. The total fraction of the reservoir that is permeable and porous in the case of the Koekoekspolder license area is around 0.8812. The saturation of the brine water is equal to 1. The average porosity based on the well logs is equivalent to 18.25 %. Using equation (2), the volumetric heat capacity calculated for Slochteren formation is obtained.

2.4 Boundary conditions:

One of the main steps of this research study is to establish a thermal-hydraulic-mechanical coupled model with realistic assumptions that are very close to the subsurface reservoir conditions to have reliable results for temperature, pressure, and energy distribution. The Slochteren thermal-hydraulic-mechanical coupled model has many parts of the **following Boundary conditions chart.**

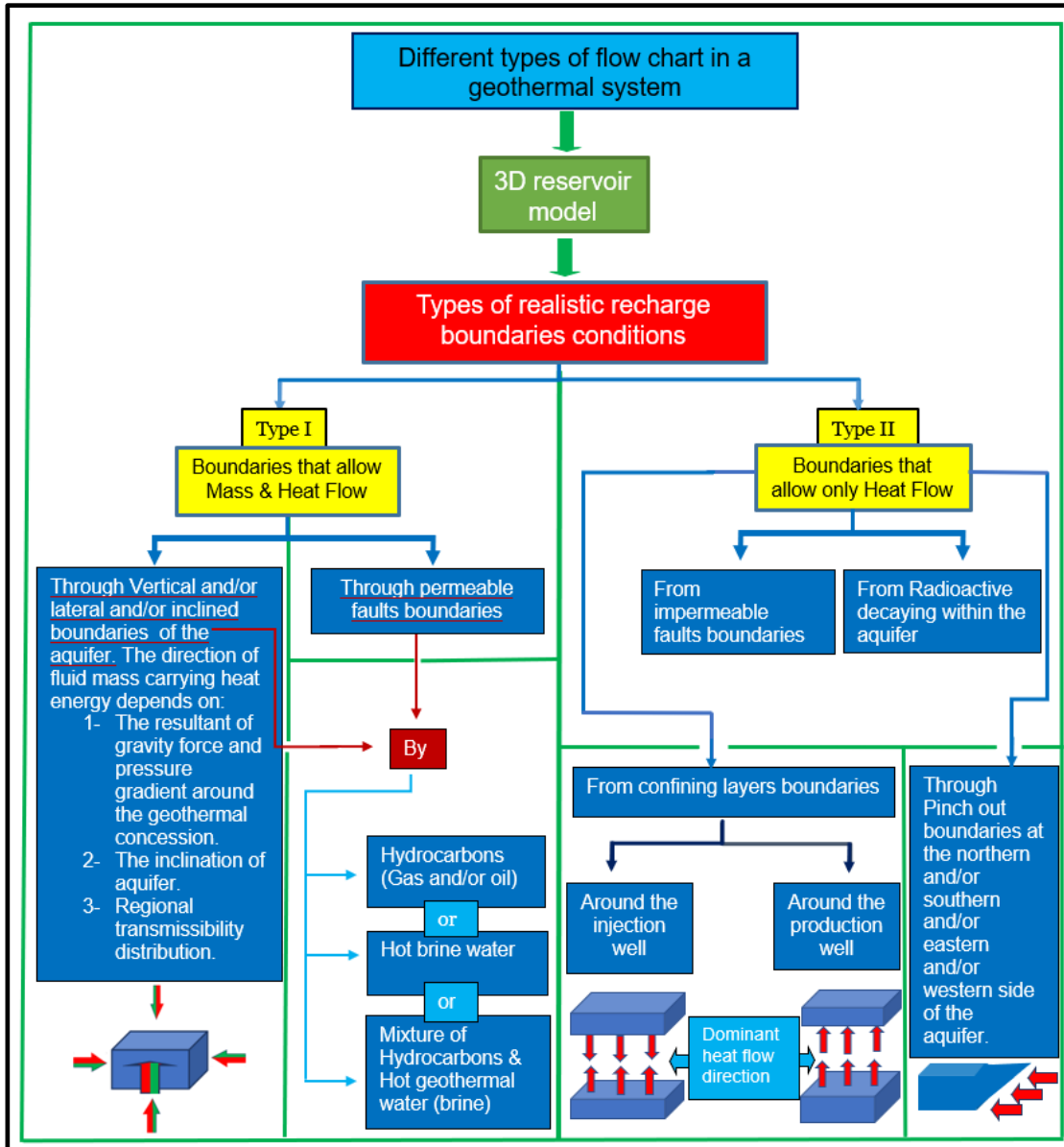


Chart 2: represents the possible realistic recharge boundary conditions in a geothermal system.

Chart 2 elucidates the various types of recharge boundary conditions that can be present in a geothermal model. Furthermore, this chart helps in defining the different possible boundary conditions in the Koekoekspolder geothermal model and its related uncertainties. As indicated in the chart above, realistic types of recharge boundaries conditions can be only related to heat flow or a combination of mass and heat flow. By one or mixture of fluid types, the mass and heat flow can be transmitted through permeable faults and/or vertical and/or lateral and/or inclined boundaries of the aquifer based on the structure of the reservoir (The mass flow is indicated by the green color in the arrow while the red color indicates only heat flow, a combination of red and green color in an arrow illustrates mass and heat flow). However, some boundaries allow only heat flow from impermeable faults boundaries and/or radioactive decaying within the aquifer and/or pinch out boundaries at any side orientation of the aquifer and/or confining layers boundaries by taking into consideration that the dominant heat flow direction in the vicinity of the injection well is different than the dominant heat flow around the production well as shown in

Chart 2. The geothermal model of the KKP field has different types of realistic boundary conditions. As known, the Koekoekspolder extraction area is around 5.2 km², and to determine whether the Slochteren geothermal play is under “recharge” or “no flow” boundary conditions, the reservoir properties as transmissivity and pressure distribution of Slochteren formation are needed to be investigated at different scale as in figure 9.

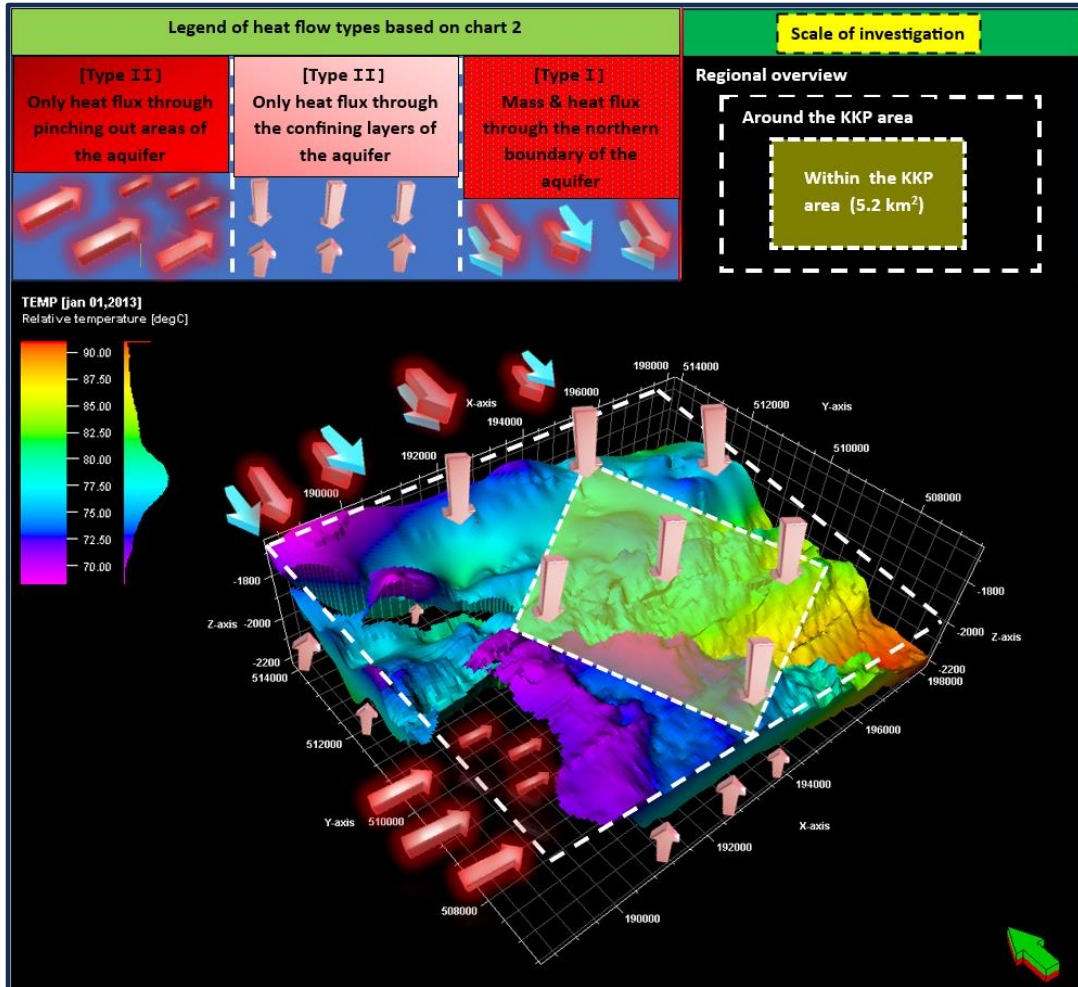


Figure 9: represents the different scales of investigation and the thermal boundary conditions taken into consideration in the case of the Slochteren aquifer.

The heat influx in Slochteren formation which is under “recharge boundary condition” obtains heat compensation through conduction and convection from the surrounding rocks (Chen, Liu and Liao, 2019). The ideal assumptions for the boundary conditions that can be used in the dynamic modeling of the Slochteren formation in the Koekoekspolder geothermal field for thermal recharge are as follows:

- 1- The northern boundaries of the heat model permit heat and mass inflow due to the initial north-south aquifer flow as a result of the fluid overpressures distribution pattern in the upper Slochteren formation as indicated in the figure (4).
- 2- The western reservoir model boundary allows only heat inflow (no mass inflow) based on the Slochteren distribution.
- 3- The southern boundaries allow heat flow and mass outflow.

4- There is a possibility that the faults connect the Slochteren formation with the Limburg group formations as shown in the cross-section of figure (2) permitting heat and mass inflow (gas convection heat flow).

5- The confining layers of the Slochteren aquifer act as recharge boundary conditions which allow heat fluxes to inflow by taking into consideration that the heat flow pattern around the injector well is different than that near the production well as shown in the chart (2).

Those boundary conditions and assumptions are based on the regional interpretation, the vertical and lateral extension of Slochteren aquifer at different scales and the available initial Koekoekspolder static model as well as field data, and many of those boundary conditions are creatively implemented into Eclipse 300 simulator as indicated in the methodology section to create a realistic and robust model for Koekoekspolder geothermal play. Those boundary conditions and assumptions must be well studied by sensitivity and uncertainty analysis to monitor their impacts.

2.5 Thermal boundaries for Slochteren aquifer:

To have reliable thermal boundary conditions that describe the heat influx into the Slochteren formation, the confining layers of the Slochteren formation and the western impermeable Texel-Ijsselmeer High must be included because they have direct contact with the geothermal aquifer block of the Koekoekspolder field. Based on the available well data from the KKP field from NLOG, the confining layers of the Slochteren aquifer are the Silverpit formation, which consists of a silt/claystone sequence, and the Ruurlo formation which comprises a succession of silty claystone with a variable number of coal seams. In the Koekoekspolder geothermal field, the average depths of Silverpit and Ruurlo formations top surfaces at KKP-GT-01 and KKP-GT-02 are around 1851 m and 1935.44 m, respectively. For every thermal boundary condition in Eclipse 300, the direction of heat loss from the reservoir must be specified. Thus, the initial upper thermal boundary has heat loss from the Slochteren reservoir with a bottom-up direction while the initial lower thermal boundary has a top-down heat loss direction from the Slochteren reservoir. The thermal conductivity of shale and siltstone varies between 0.7 and 5 W/m/K (Chekhonin *et al.*, 2012). The thermal conductivities that are chosen for the Silverpit and Ruurlo formations are 3.2 W/m/K and 2.85 W/m/K, respectively. Furthermore, the thermal conductivity of the Texel-Ijsselmeer high is approximately 1.89 W/m/K (Verweij *et al.*, 2010). The average geothermal gradient in the Dutch subsurface is approximately 31 °C/km (0.031 °C/m) and the surface temperature is around 10.1 °C (Bonté, Van Wees and Verweij, 2012).

$$(6) \quad T = \text{Surface temperature} + \text{Depth} * \text{Geothermal Gradient}$$

The bottom hole temperature at the Slochteren formation is approximately 76.5 °C. The temperature of Slochteren formation in the KKP field is higher than the temperature at the same depth in other fields according to the average geothermal gradient which means that there might be a connection between the Slochteren formation and deeper reservoir through faults which allows gas migration and convection heat flow into Slochteren aquifer or/and due to the local basement highs, salt. Also, it is possible that the geothermal gradient is approximately 35.8 °C/km in the area of the KKP field which means that the temperature at Silverpit formation is about 76.36 °C and 79.388 °C for the Ruurlo formation by using equation (6). The heat capacities of the Silverpit formation, Ruurlo formation and Texel-Ijsselmeer high are 1009 J/kg/k, 1017.4 J/kg/k and 1021.6 J/kg/k, respectively (Verweij *et al.*, 2010). According to the available well log data of Kamp-01-S1 in NLOG.nl that cover the confining layers of the Slochteren formation, the densities of the Silverpit and Ruurlo formations are sequentially equal to 2600 kg/m³ and 2400 kg/m³ with extremely low porosity. Moreover, the density that represents Texel-Ijsselmeer high is about 2700 kg/m³ (Verweij, Echternach and Witmans, 2010). These high densities values with extremely low porosity and based on the fact that the injected flow rates are equal to the produced flow rates from 2013 to 2022 indicate that the

confining layers of the Slochteren formation and the western Texel-Ijsselmeer high can be considered impermeable formations that permit only heat flow and no mass inflow or outflow and act as a seal for the aquifer.

Volumetric heat capacity (KJ/m ³ /K)	Silverpit formation	Ruurlo formation	Texel-Ijsselmeer high
Value	2623.4	2441.76	2758.32

Table 1: shows the volumetric heat capacities of different formations that represent the thermal boundary conditions for the Slochteren formation.

The thermal properties such as the rock thermal conductivity and the rock-specific heat capacity of the Silverpit, Ruurlo, and Texel-Ijsselmeer High formations surrounding the Slochteren aquifer are taken into consideration during modeling based on the assumption that there is a continuous thermal recharge from the formations surrounding the Slochteren aquifer. The property data for the formations surrounding the Slochteren aquifer requires initial temperatures. The average initial temperature of the confining layers and the Texel-Ijsselmeer high are obtained based on equation (6). The heat losses from the rocks surrounding the geothermal aquifer are computed numerically by Eclipse 300 simulator. The simulator assumes the outside edges of the grid blocks on the boundaries are not at fixed temperature which might give realistic thermal recharge. The overburden and underburden layers are not explicitly modeled. The bottom surface of the Silverpit formation and the upper surface of the Ruurlo formation as well as the pinching out surface of the Texel-Ijsselmeer high act as thermal recharge boundaries for the Slochteren aquifer.

2.6 Initial aquifer velocity:

Based on the available data from the Koekoekspolder field, there is no direct measurement for the initial aquifer properties. A 2D numerical model using Phytion software is developed to calculate the average velocity of the aquifer with the following assumptions:

- The fluid of the aquifer is considered incompressible and the buoyancy effect is not taken into consideration.
- The pressure gradient drives the fluid motion in the Slochteren permeable aquifer with a constant fluid density.
- The pressure at the northern boundary of the numerical model is higher than the pressure at the southern boundary as indicated in the regional study overview which allows mass and heat flow from north to south direction.

Viscosity of water in Slochteren formation	Average permeability	Pressure at the northern boundary	Pressure at the southern boundary
1*10 ⁻³ Pa.s	0.28 d	1.96 * e ⁷ Pa	1.94 * e ⁷ Pa

Table 2: Input data for the 2D developed numerical model to compute the pressure and velocity distribution.

The governing equation used in the numerical model to predict the velocity of the aquifer is derived from the Darcy model, which describes the incompressible flow in porous media by using the following equation for a source term equal to zero (Mansur, 2018).

$$(7) \quad \mathbf{u} = -\frac{k}{\mu} \nabla p$$

$$\nabla \cdot \mathbf{u} = 0$$

Where \mathbf{u} is the velocity field, k represents the permeability, μ denotes the dynamic viscosity of the fluid, and ∇p indicates the pressure gradient.

Using this approach, the average initial velocity for the KKP field is equal to 1.3e-07 m/s, which is around 0.01 m/day and it is used as described in the methodology section for the 3D aquifer model.

2.7 ***BHP calculations:***

The measured bottom hole pressures and the measured flow rates are needed to obtain a complete history matching. Due to the lack of measured bottom hole pressure values, the average available wellhead pressure of KKP-GT-01 and KKP-GT-02 wells in the KKP field is used to obtain the BHP values by calculating the pressure drop over each borehole. For simplicity, the true vertical depth is used in the calculations of bottom hole pressure. The gravitational head, acceleration losses, and frictional losses have a direct influence on the pressure drop (J.Jansen, 2017; Reinhard, 2019).

The pressure drop equation (J.Jansen, 2017) can be formalized as follows (Reinhard, 2019):

$$(8) \quad \frac{dP}{ds} = -\rho g - \frac{\rho}{2d} f v |v| - \rho v \frac{dv}{ds}$$

Where dP : the pressure drop [Pa], ds : pipe length [m], ρ : density of water at reservoir conditions [kg/m³], g : gravitational acceleration [9.80665 m/s²], d : well diameter [m], f : friction factor [-], v : velocity [m/s].

Based on the available density, gravitational acceleration, true vertical depth, and friction factor data for different flow rates, the computation of pressure drop due to friction and gravity can be obtained over the length of the wellbore. In the case of the production well (KKP-GT-01), the pressure drop is generated from the bottom level of the electric submersible pump (ESP) to the top aquifer screen depth but in the case of the injection well (KKP-GT-02), the pressure drop is created from surface level to the top aquifer screen depth (See Appendices 1 and 2 for the wells schematics). The term related to the acceleration losses is neglected because there is one brine water phase that barely expands (Reinhard, 2019). Only the wellhead pressure data for the last 2 months of 2020 and the first month of 2021 were available. The reference depth which indicates the top screen depth for the injection well (KKP-GT-02) and the production well (KKP-GT-01) are respectively 1848 m and 1846 m. The ESP depth of the producer well (KKP-GT-01) is equal to 413 m and the density of the produced or injected brine water is equivalent to 1.140 g/cc. The dynamic viscosity is about 0,37 cp. The inner diameter of the injection well is equal to 8,8681 inches from the surface to a depth of 1010 m, then it changes to 6,276 inches from 1010 m to 1773 m, afterwards, the inner diameter is 4,052 inches. For the production well, the value of the inner diameter is 8,835 inches from the surface to a depth of 833 m then it changes to 4,052 inches for the remaining depth interval.

Date	Average flow rate per hour Q (m ³ /h)	Average well head pressure THP (bar)	Velocity (m/s)	Friction factor	Pressure losses dp friction [bar]	Head losses dp gravity [bar]	Approximated Flowing bottom hole pressure BHP [bar]
nov-2020	104,63	15,07	1,6380	0,0192	0,0013	0,09316	224,770
dec-2020	114,89	19,36	1,79	0,01859	0,0033	0,09316	229,532
jan-2021	118,67	20,55	1,85	0,0186	0,0035	0,09316	232,706

Table 3: Available input data and the computed BHP for the injection well KKP-GT-02.

3.Methodology

3.1 Data analysis:

The first step was to analyze the data provided. The following graphs show the monthly production and injection volume as well as the co-produced gas volumes that are available on NLOG. The injected water volume is equal to that of the produced water.

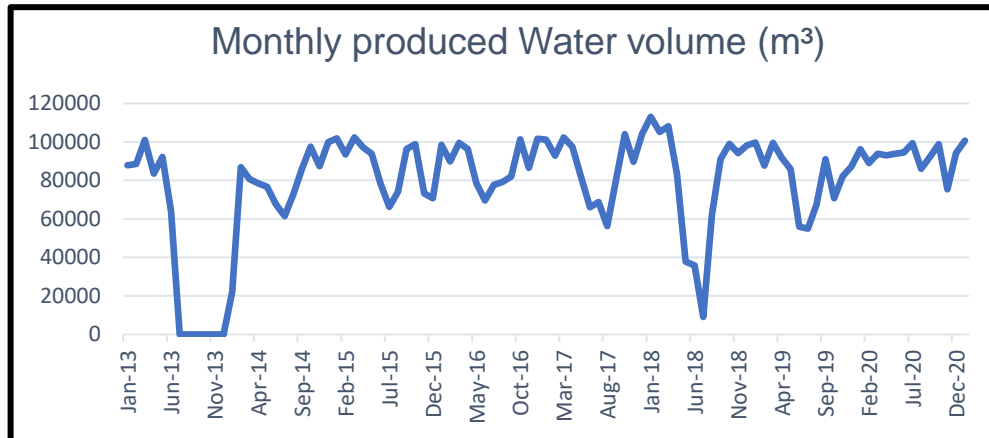


Figure 10: Monthly produced water from 2013 to 2021.

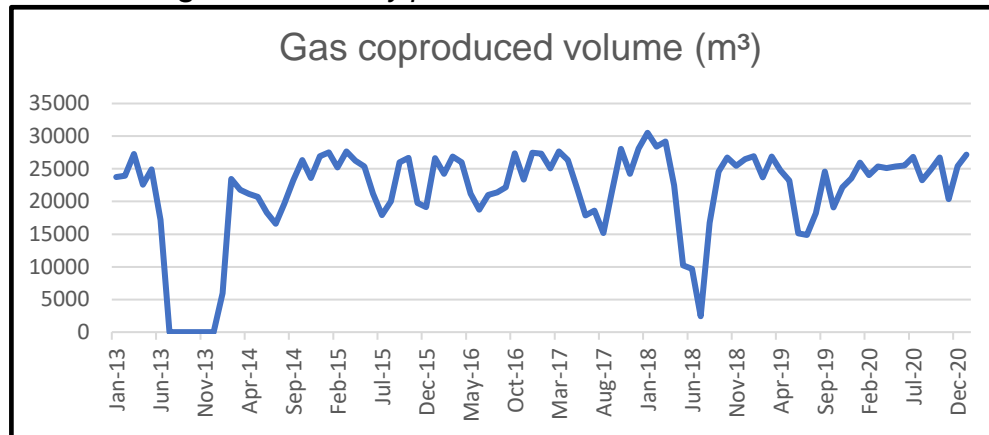


Figure 11: Monthly co-produced gas from 2013 to 2021.

The data provided represent the monthly produced and injected volumes from 2013 to 2021 with an approximated flowing bottom hole pressure that covers only 3 months. To overcome the lack of measured THP or BHP data in the period between January/2013 and November/2020, the implemented solution was to find a polynomial equation that describes and relates the injected and produced volumes with the BHP (available data) to be able to hindcast approximately the BHP related to the addressed rates or vice versa at any time. Using Excel, a strong positive and negative correlation are obtained between the BHP and the injected and produced volume rates respectively.

The flow rate which is currently being produced is around 130 m³/hour with an injection temperature of 35°C and the maximum flow rate is 150 m³/hour (approximately 3200 m³/day assuming that the KKP field operates with the maximum flow rate for a total duration of 2 months per year), and the annual yield of energy is around 170000 GJ which is the same energy used for the period between 2021 and 2024 because the third production well (KKP-GT-03) is not yet drilled. According to the permit holder plan, the proposed flow rate for the period

between 2024 and 2027 is 260 m³/hour (around 6240 m³/day). The permit holder will increase the amount of energy produced to 400000 GJ per year from 2024, while the amount of gas will remain the same. This is due to the planned addition of a heat pump to the system, which will further cool the produced water to 20°C. After that, there will be another increment in the energy from (400000 to 600000 GJ per year) which is related to a possible expansion of the system with a second doublet from 2027 (Klimaat and Warmte en Ondergrond; TNO, 2019a). By knowing that the annual yield of energy depends on the flow rate and the injection temperature, a linear relationship between the desired energy output and its corresponding produced flow rate, as well as its corresponding temperature, is obtained for winter and summer seasons. The 2 equations that represent this relationship are linearly optimized (By summation of the 2 equations) in the case of winter and summer seasons. The predicted flow rate that can yield annual energy of 600000 GJ with an injection temperature of 20°C based on the linearly optimized equation for winter season is around 11526,94361 m³/day. Moreover, the predicted flow rate that can yield the average annual energy demand from 2024 to 2127 updated by the permit holder in 2021 which is around 708819 GJ is approximately 14403.546 m³/day. The predicted flow rate that can yield the average annual energy demand used for heating greenhouses represents the flow rate used for the winter season based on the history flow rate data. From 2021 to 2024, the average summer flow rate based on the available flow rate data before 2021 is around 2200. The summer energy demand from 2024 to 2027 is approximately 51501 GJ which represents 12.87525 % of the total annual expected energy (400000 GJ) and will yield a flow rate of about 5176,47 m³/day. By assuming that the summer energy yield will represent 12.87525 % of the annual expected desired energy from 2027 to 2127 which is equal to 708819 GJ, the expected summer energy will be around 91262.2183 GJ using linearly optimized equation for summer season. Thus, the summer flow rate from 2027 will be around 13169,377 m³/day. The difference between the winter flow rate and the summer flow rate from 2027 is 1234.169 m³/day, and this value is divided to be subtracted from the winter flow rate to obtain the summer flow rates.

3.2 Update static modelling:

Finding the balance between Scaling and the right representation of the reservoir properties is considered one of the major challenges in reservoir simulation due to the heterogeneity in the subsurface. If the upscaling (coarser resolution of the geothermal model) is implemented on the model, the coarser cell will represent many finer cells which leads to a lack of details related to the heterogeneity of the lithology and permeability distribution as well as the thermal properties distribution even by the representative elementary volume technique. At coarser (upscaled) resolution, the same representative value of any type of the input properties will be used for multiple finer cells that might have different values. This is why there was no upscaling implemented on the static model to have a high resolution and accurate dynamic results at a relatively fine scale. The initial total number of grid cells was equal to 1338600 cells (n_I x n_J x n_K =194 x 150 x 46). First, the grids were adjusted because the skewed grids were preventing the dynamic simulation. For the purpose of making adjustments for the grids, all the workflow that was done for the static model must be repeated. Numerous grids around the faults had severe skewness (irregular geometry and the cells were inside out) and by using the Petrel software calculator, the grids were eliminated by a simple code as shown in Appendix 3. The skewed grids were concentrated around the faults. After different iterations, the grid edges were adjusted by a specific number of nodes as shown in appendix 4 because they were the second obstacle for dynamic simulation subsequent to the skewed grids. Furthermore, the volume percentage of gypsum that is used in the updated static model is calibrated based on the well log gross ratio which was around 11.88%. The value of the total net to gross ratio which is used as an input for the dynamic simulation was equal to 88.8812. By contrast, the total gypsum net

to gross ratio represents only 1% in the initial static model volume (Redjosentono, 2014). The input data for the upper, lower, and western thermal boundaries as shown in Appendix 5-a, 5-b, and 5-c are obtained from the initial temperature, conductivity, and volumetric heat capacity data of the formations that are in direct contact with Slochteren aquifer as described in section 2.5. The calculation of heat loss is done by the Numerical method in Petrel.

3.3 ***Geomechanical modelling:***

Swift movement of subsurface layers on preexisting faults can lead to a crustal earthquake (J Byerlee, 1978). Thus, the vertical and horizontal stresses needed to be computed to determine the maximum injection pressure suitable for the targeted Slochteren formation safely without any failure or induced seismicity. The density log data are plotted in relation to depth. By using the bulk density log data, the vertical stress (σ_v) at the subsurface can be calculated. Subsequently, the horizontal stress can be obtained using the vertical stress and the different stratigraphic groups Poisson ratios. The geomechanical calculations are done for the top of Slochteren formation and the combined basic geomechanical outputs are represented as in figure 12:

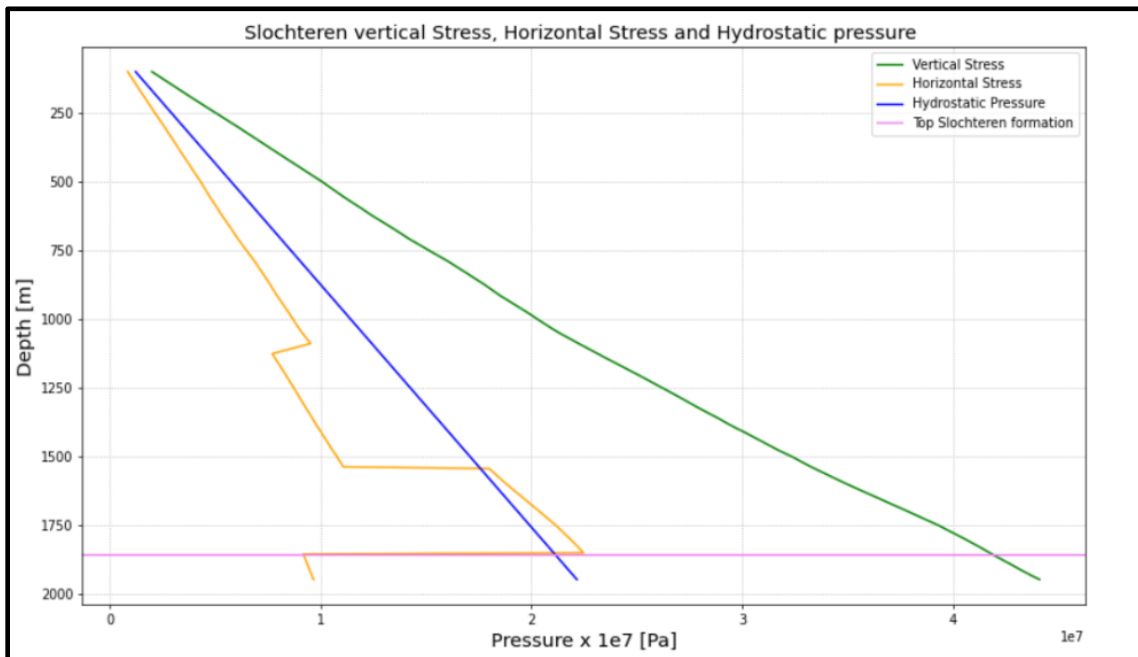


Figure 12: Profile of vertical and horizontal stresses as well as hydrostatic pressure at the depth of top reservoir.

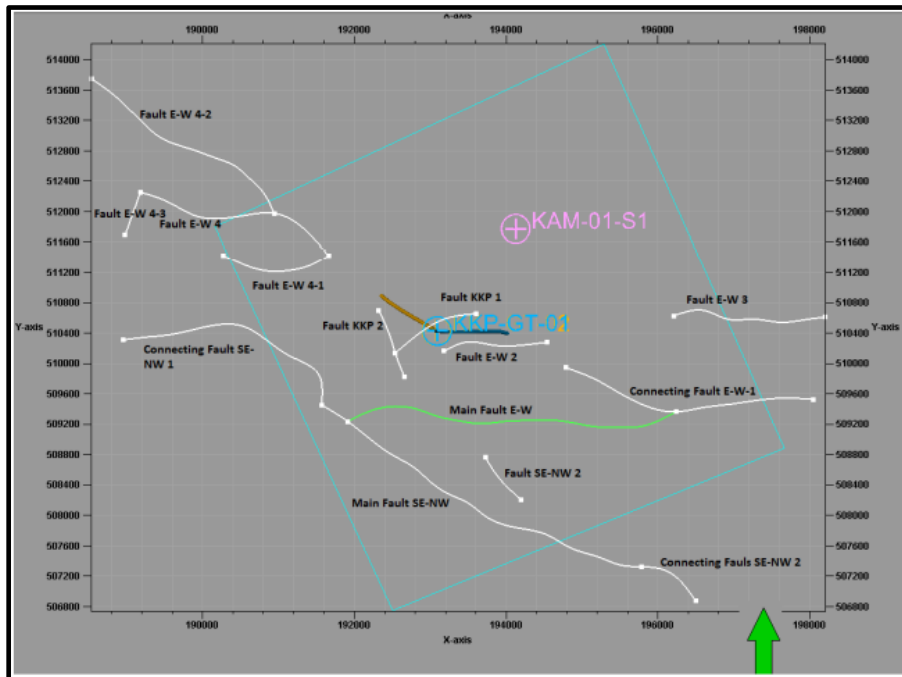


Figure 13: shows the different faults in the KKP field (Redjosentono, 2014).

Several faults have different dip angles that range from 30 degrees to 90 degrees. Within the same fault, different dip angles can be present. Therefore, the existent failure envelope shown in figure 14 must pass by the origin to indicate that there is zero cohesion in the area of the faults. This means that any injection and/or production pressure (energy exerted) on the reservoir beyond the critical injection or production pressure tends to reactivate the existing fault rather than create a new one. In order to determine under what conditions movement will happen as well as determine the variation of the initial friction, the slope of the failure envelope is obtained from the plotted shear stress experimental results for different rock types at normal pressures up to 1000 bars as a function of normal stress for the initial friction (Byerlee, 1978a) by drawing the best-fit line along and between the quartzite symbols. The slope of the failure envelope in the Slochteren formation is around 0.8 due to the large amount of sandstone in the formation. The pore pressure is subtracted from the vertical and horizontal stresses to obtain the effective horizontal and vertical stresses that determine the position of the Mohr circle according to the failure envelope. The center of the circle indicates the value of normal stress (σ_n). The maximum injection pressure is determined by examining when the Mohr circle will start to touch the failure envelope since this is the moment that a fault can rupture, and induced seismicity may happen. The maximum injection pressure without surpassing the failure envelope is equal to 166 bar and the initial aquifer pressure is approximately 196 bar which shows that the faults have been being reactivated with aseismic slip before even operating the Koekoekspolder field and they are critically stressed. The next step considering the geomechanical modeling of the KKP field is to describe the entire fault slip process and to predict whether seismic or aseismic slip will happen after fault reactivation (Kang, Zhu and Zhao, 2019a). It is important to determine the type of movement along the fault to predict if induce seismicity will take place. The first type of movement is the stable sliding along the fault and most likely doesn't induce seismicity, however, the stick-slip sliding along the fault can induce seismicity in the subsurface. The pore pressure value at the target reservoir is needed to be able to obtain Mohr coulomb criteria and to indicate the maximum injection pressure before hitting the failure envelope. But even after the circle of Mohr-Coulomb hits the failure envelope,

a fault slip that doesn't induce seismicity can occur. This fault slip movement depends on 2 factors called frictional parameters (a & b factors). Thus, the frictional parameters (a-b) perform a critical role in the fault frictional stability (Kang, Zhu and Zhao, 2019b). The frictional parameters (a-b) are influenced by the mineralogy, fluid pressure, sliding velocity, and temperature (Ikari, Saffer and Marone, 2007; Rutqvist *et al.*, 2008; Scuderi and Colletini, 2016; Kang, Zhu and Zhao, 2019b). In case of injection pressure higher than 196 bar in the KKP field that leads to an (a-b) value > 0, the fault is velocity strengthening which means that the friction rises with the slip velocity, and there is aseismic slip "The fault is stable" (Kang, Zhu and Zhao, 2019b). On the contrary in the case of injection pressure higher than 196 bar in the KKP field that leads to an (a-b) value < 0, the fault is velocity weakening which indicates unstable or conditional stable behavior and there is a possibility of seismic slip "The fault can be unstable" (Kang, Zhu and Zhao, 2019b). Based on the historical hindcasted bottom hole pressures from 2013 to 2021, the maximum injection pressure value was equal to 207.82 bar and there was no induced seismicity recorded which means that there is a stable sliding (aseismic slip) that has been occurring till a maximum injection pressure of 207.82 bar. Further studies and experiments are needed to understand if there will be unstable slip behaviour or stable slip behaviour of faults around the injection wells in the KKP field with higher injection pressure that range from 207.82 bar to the maximum bottom hole pressure of 252 bar allowed by SODM.

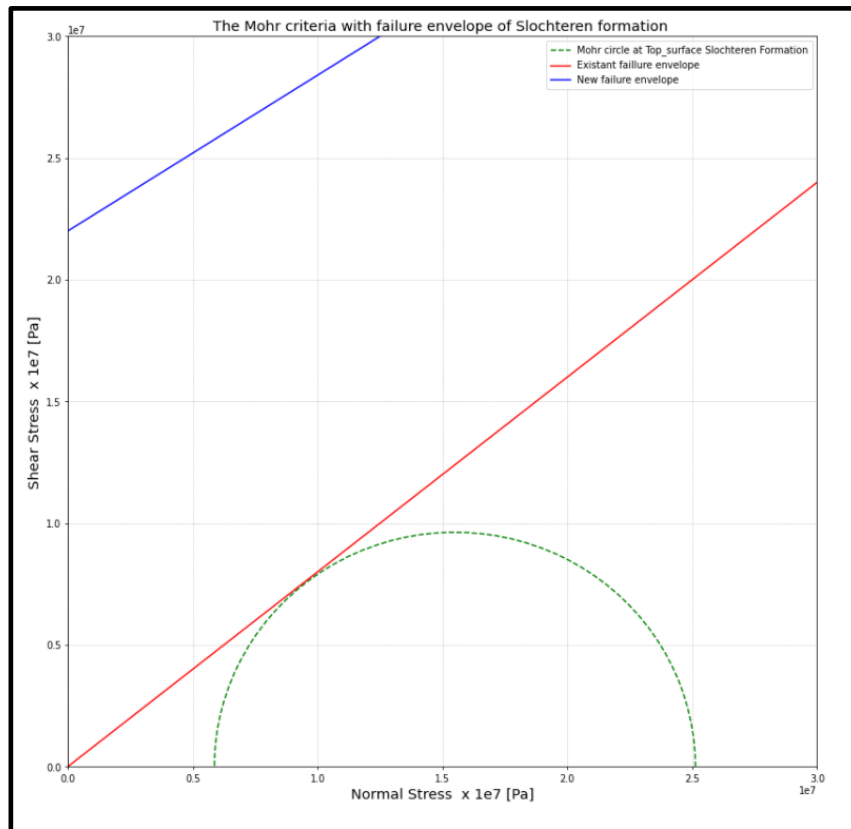


Figure 14: shows the maximum injection pressure without surpassing the failure envelope.

The direction of the current maximum horizontal stress (S_h max) is not parallel to the orientation of the fractures accompanied by the faults. This is why there are possibilities that the opening of the fractures can be reduced.

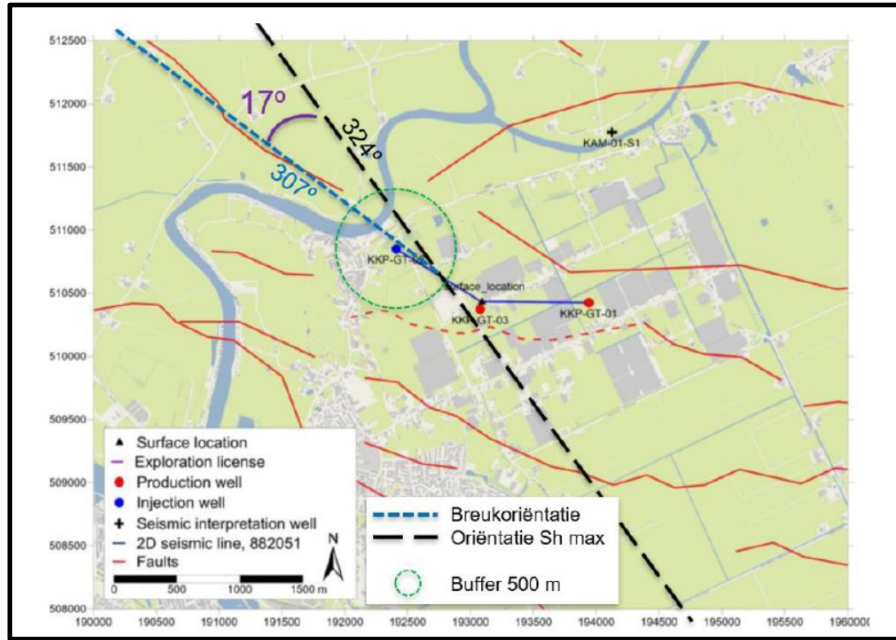


Figure 15: shows the orientation of the maximum horizontal stress indicated by the black dashed line, and the orientation of the fractures which are parallel to the direction of the faults that are marked by the blue dashed line (EN KLIMAAT & WARMTE EN ONDERGROND; TNO, 2019).

In addition to stress change due to declined or increased pore pressure from well operations, the stress change can take place due to a reduction in reservoir temperature as a result of the effect of the cold injected water which is currently around 35.4°C then it will change to 20°C in 2024. According to the Geysers field that produces steam from over 350 wells for power production (Power Technology, 2012) and has a high-enthalpy geothermal system with natural steam (~235°C) hosted in the fractured metagraywacke reservoir (Hulen, Jeffrey B., 1995; Peacock *et al.*, 2019), (Segall and Fitzgerald, 1998) found that if the cooling rate ($\frac{dT}{dt}$) is -0.3 °C/year (a net temperature decrease of 6 °C/20 years), a stressing rate of 0.09 MPa/year will be generated which is adequate to produce critical thermoelastic stresses. Induced earthquakes can be generated from such a magnitude of stress changes in the critically stressed crust (Kang, Zhu and Zhao, 2019b). Despite that the 0.3°C/year criterion may be different for sedimentary formations as in the KKP field because the Geysers field is geologically and operationally different than the KKP field, the geomechanical modelling showed that the KKP field is critically stressed. Based on the predicted results of the Koekoekspolder model using the optimal development strategy in this research study, the cooling rate for the wells “KKP-GT-01” and “KKP-GT-03” is lower than the cooling rate that can induce seismicity because it probably corresponds to stressing rate of 0.06 MPa/year. The KKP field has been operating under pressure constraints with a maximum injection pressure of 252 bar that is derived from the SodM protocol (TNO-AGE; SodM, 2013) and a minimum production pressure of 153 bar based on the lowest bottom hole pressure value for the period between 2013 and 2021.

3.4 History matching:

The flow rates and bottom hole pressure data from 2013 to 2021 were used in history matching. The first step was to obtain the historical data which is the monthly produced and injected brine water volumes as well as the hindcast and approximated BHP from 2013 to 2021 as already explained in section 3.1. Then a suitable history strategy based on the observed production and injection rates was generated using Petrel.

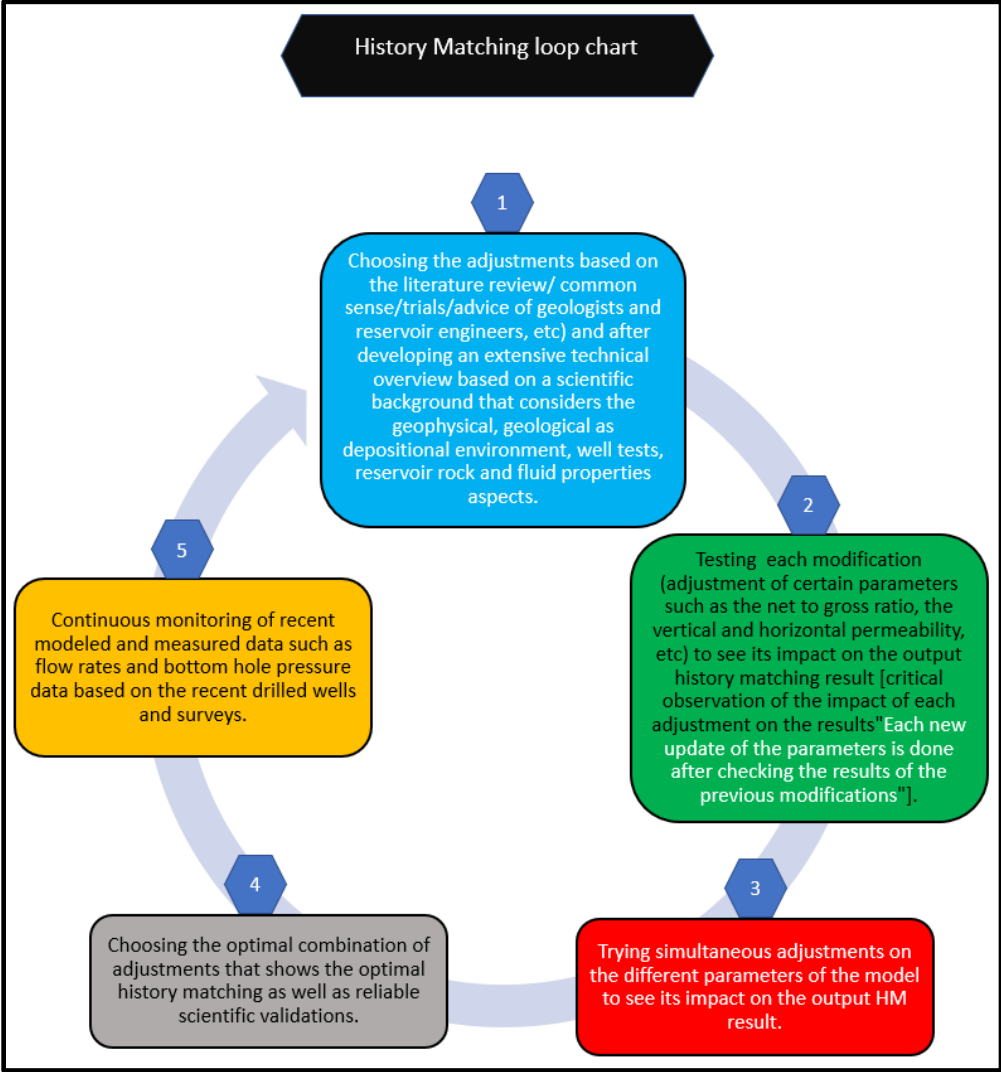


Chart 3: shows the steps of a scientific history matching.

In history matching, the observed production, and injection rates as well as the hindcast and approximated bottom hole pressures for the KKP field were compared to those obtained by forward modelling.

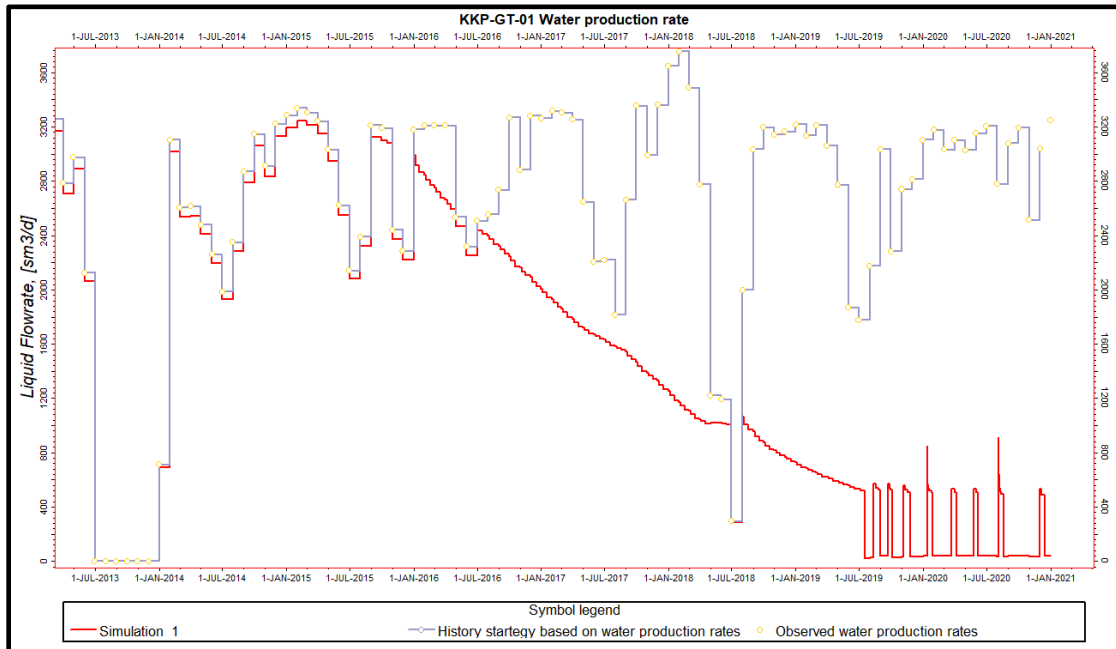


Figure 16: shows an example of history mismatched water production rates model.

Due to the large discrepancy of measured values of porosity and permeability from the well KAM-01-S1 core plug as shown in figure 8, the permeability model is modified and the porosity distribution is not altered because the porosity values are acquired from well logs. Based on the kampen core description and the depositional environment of the Slochteren formation aeolian sandstone, the reservoir is considered to have the same facies which extends over large areas with the presence of a very low porous gypsum enterolithics bodies (Redjosentono, 2014). The initial input data for the dynamic model that simulate the history of the Slochteren aquifer consisted of the permeability in the 3 principal directions, effective porosity, and net to gross ratio of 0.8812. In the beginning, the historic water rates result obtained were slightly similar from January 2013 till January 2016 but after that, the rates began to have big differences. This is why an adjustment was needed for different input parameters to have a robust model of the Koekoekspolder geothermal field. The permeability (in i, j, k) of the entire aquifer and/or in the vicinity of the injector well and/or around the producer well were calibrated by different factors to reach the model with the most accurate history matching results for both flow rates and BHP. The gradual manual change was a systematic way of history matching to avoid overestimation or underestimation as well as the simultaneous adjustment of input parameters. Moreover, different parameters as shown in table 4 are updated according to the literature review of the reservoir description such as that the vertical permeability is significantly lower than the horizontal permeability and the relatively homogenous depositional environment of the Aeolian sandstone which is reflected in the manual and uniform adjustments (whether an increment or a decrement) of the reservoir heterogenous parameters in the model to reach history matching.

Parameters	Addressed values range	Motivation	Optimal change	Motivation
Vertical permeability	Manually multiplied by (0.2/0.25/0.3/0.4/0.6/0.8)	Due to the small vertical-to-horizontal permeability ratio [KV/KH] (Henares <i>et al.</i> , 2014).	The vertical permeability is equal to the horizontal permeability multiplied by 0.25	Showed the optimal history matching results together with the other optimal adjustments.
Horizontal permeability in x and Y directions	Manually multiplied by (8/7/6/5/4/3/2)	Uniform adjustments because the reservoir is considered to have the same facies which extends over large areas with the presence of a very low porous gypsum enterolithics bodies (Redjosentono, 2014).	The entire permeability distribution for i and j directions was multiplied by a factor value of 3	Showed the optimal history matching results together with the other optimal adjustments.
Permeability in the vicinity of the injection well (KKP-GT-02)	Manually multiplied by (1.5/0.83/0.5/0.4/0.3/0.2)	According to the permit holder, the skin factor has positive values around 1.85 (Klimaat and Warmte en Ondergrond; TNO, 2019b).	The permeability in the vicinity of the injection well KKP-GT-02 is multiplied by 0.83	Showed the optimal history matching results together with the other optimal adjustments. Moreover, the Kh computed based on Multi-rate KKP-GT-02 well test is around 581.5 while that in the vicinity of the injection well is approximately 477.69.
Permeability in the vicinity of the production well (KKP-GT-01)	(8/7/4/2/1.5/0.72/0.5)	According to the permit holder, the skin factor has positive values around 0.22 (Klimaat and Warmte en Ondergrond; TNO, 2019b).	The permeability in the vicinity of the production well KKP-GT-01 is multiplied by 0.72	Showed the optimal history matching results together with the other optimal adjustments.
Net to Gross ratio	0.8812	Based on the wells log interpretation.	0.8812	Based on the wells log interpretation.

Table 4: shows most of the adjustment applied on the initial model to reach history matching.

After 21 simulation case trials of the single phase flow model, the twentieth-second simulation case had the most accurate history matched flow rates and history matched bottom hole pressures as shown in figures 17 and 18. This simulation had the following manual adjustment:

- The vertical heterogenous permeability distribution was equal to the horizontal heterogenous permeability distribution multiplied by 0.25
- The entire heterogenous permeability distribution for i and j directions was multiplied by a factor value of 3
- The permeability in the vicinity of the injection well was multiplied by a factor value of 0.83 while that of the production well is multiplied by a factor value of 0.72

- The permeability values in the vicinity of the injection well was compared to the measured well test hydraulic permeability (Multi-rate well test) and they showed values that are close to each other as shown in table 4.

The adjusted permeability distribution in x, y and z direction are shown in appendices 2a, 2b and 2c.

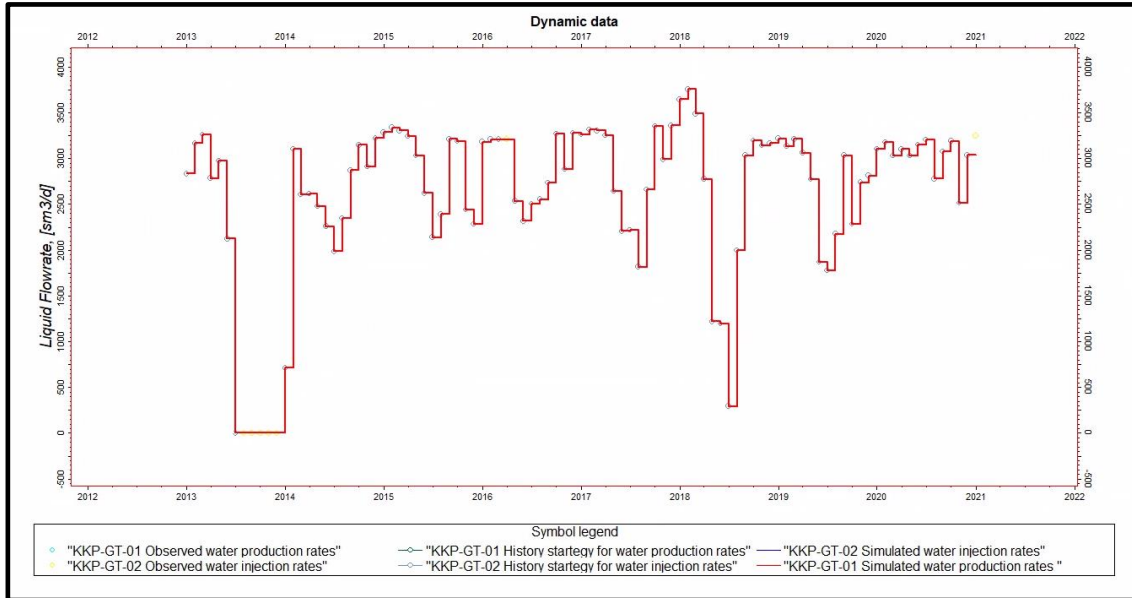


Figure 17: Complete history matching between the simulated and the observed flow rates as well as the history strategy.

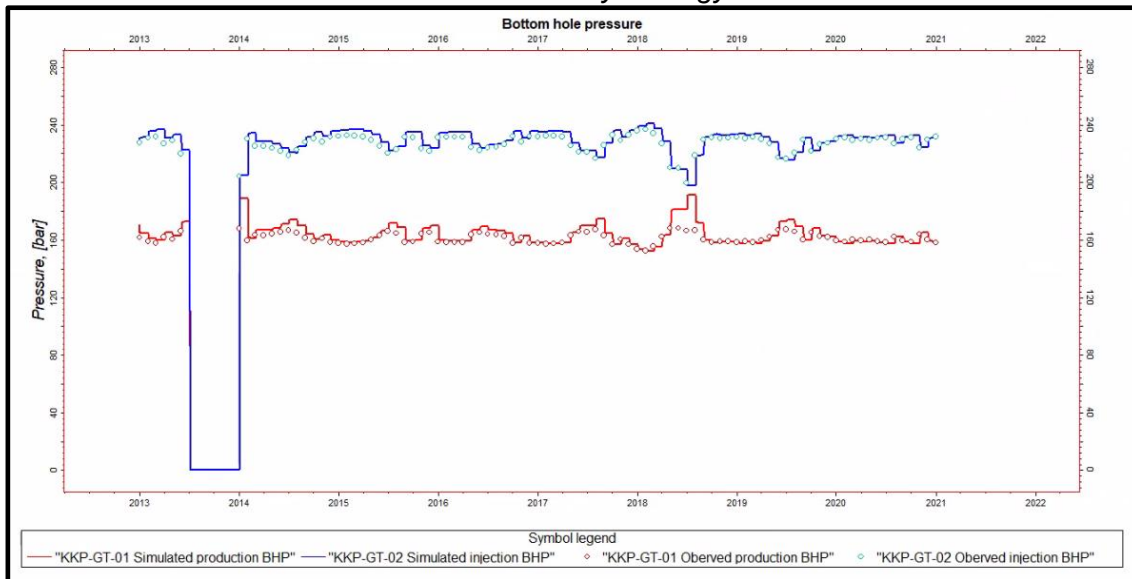


Figure 18: Accurate history matching between the simulated and the observed bottom hole pressures.

The simulation case with the results that showed accurate history matching results for both flow rates and BHP was chosen for the forecasting stage.

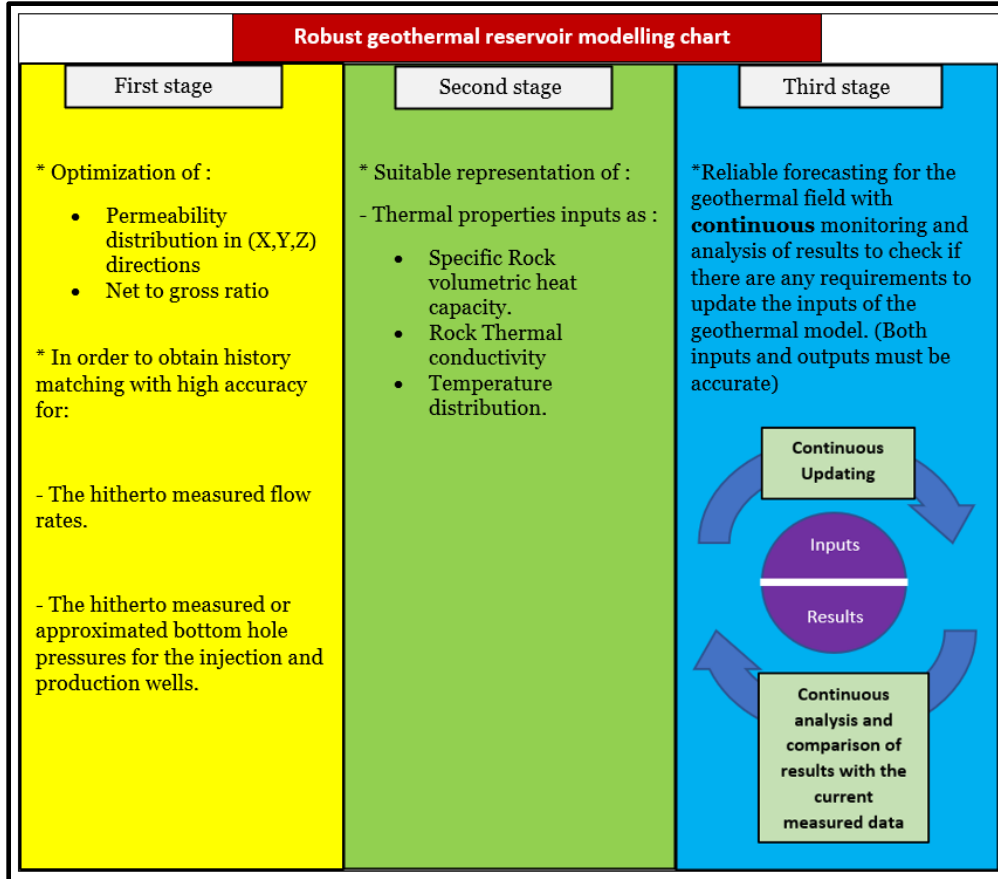


Chart 4: shows the different stages to obtain a robust geothermal model.

3.5 Forecasting model setup:

After obtaining a robust model with high accuracy of history matching for the flow rates and bottom hole pressure from 2013 till 2021, different forecasting models that predict the temperature and heat energy distribution till 2121 are generated. To overcome simulation failure and/or extensive running time of the numerous simulations cases of the next century, smaller sectors of the original model were generated using the ACTNUM keyword in Eclipse 300, which divides the model into active and inactive cells, by applying a code consisting of a few lines as in Appendix 6 without affecting the properties distribution. The new sector model covered most of the KKP field as well as the areas that the owner is interested in as shown in Figure 19 and appendix 6-a. Thus, the inputs for the dynamic forecasting simulator consisted of the new sector model, the thermal boundaries, and the same inputs for the history-matched model as well as the forecasting strategy. The accuracy of temperature or energy distribution for the smaller sector model is tested by subtracting it from the temperature or energy distribution of the bigger model.

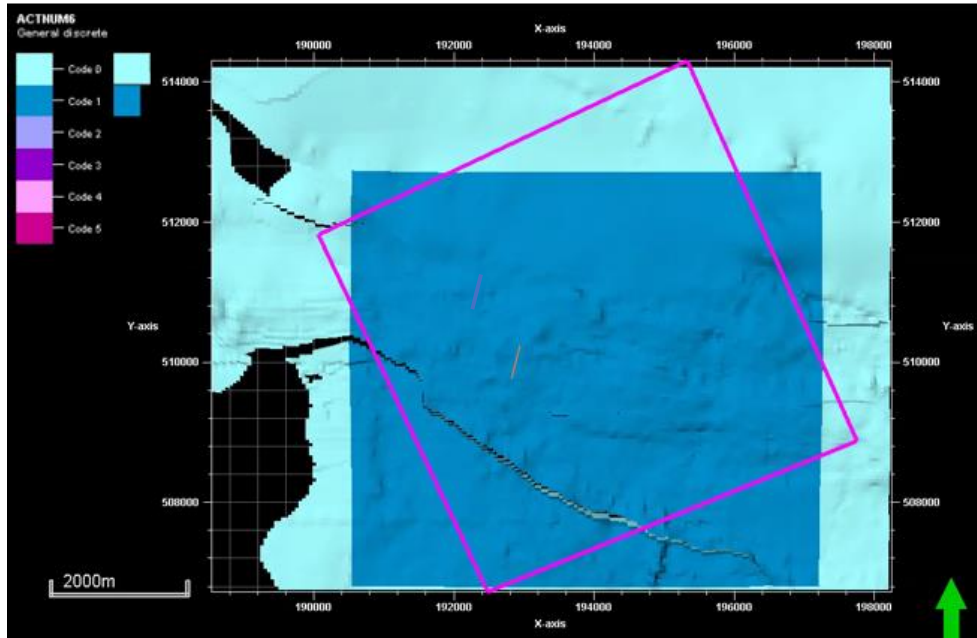


Figure 19: shows the dimensions of the most accurate sector (Actnum 8) that covered the entire 46 layers which are indicated by dark blue colour as well as the entire reservoir dimension that is illustrated by the light blue colour and it includes the new sector and the projection of the KKP concession with purple boundaries.

The new sector model with the same original model boundary conditions is reliable because the result of the subtraction is approximately equal to zero. For better efficiency and reduced running time, the most reliable sector dimensions are shown in figure 19 and Appendix 7. This new sector model (ACTNUM 8) that was used as an input for the dynamic forecasting modeling represents 61.48 % of the original model volume, and it was suitable for the runs with thermal boundary conditions to achieve reliable outputs. When the thermal boundary conditions are taken into consideration, the sector that consists of the entire 46 layers must be used as an input for the dynamic modeling because it's in contact with the confining layers (The lower, upper, and western thermal boundaries). By taking into consideration the direction and velocity of the aquifer flow, the forecasting of the temperature profile, as well as the lifetime of the geothermal doublets, can be affected. Besides the computation of the average velocity as indicated in section 2.6 and assuming that the northern boundary allows heat and mass flow, the spatially constant flux, which is needed for 3D dynamic modeling, can be obtained if the cross-sectional area at the northern boundary, the average effective porosity, and salt concentration are known.

Average velocity (m/day)	Cross sectional area at northern boundary (m ²)	Average effective porosity	Salt concentration	Temperature
0.011	1786.1721 m ²	0.1783	175 kg/m ³	76.4 °C

Table 5: Needed data to generate an aquifer in the Koekoekspolder geothermal model.

The following equation represents how the flux across the aquifer boundary can be obtained.

$$(9) \quad Q = v * \varphi_e * A$$

Where Q is the flux with units of (m³/day), v is the Velocity with units of (m/day), φ_e represents the average effective porosity, and A denotes the cross sectional area with units of (m²).

Using equation (9) and the input data of table 5, the flux for the Koekoekspolder forecasting model is as follows.

$$\text{Flux at the northern boundary (m}^3\text{/day)} = 0.01 * 0.1783 * 1786.1721 = 3.18 \text{ m}^3\text{/day}$$

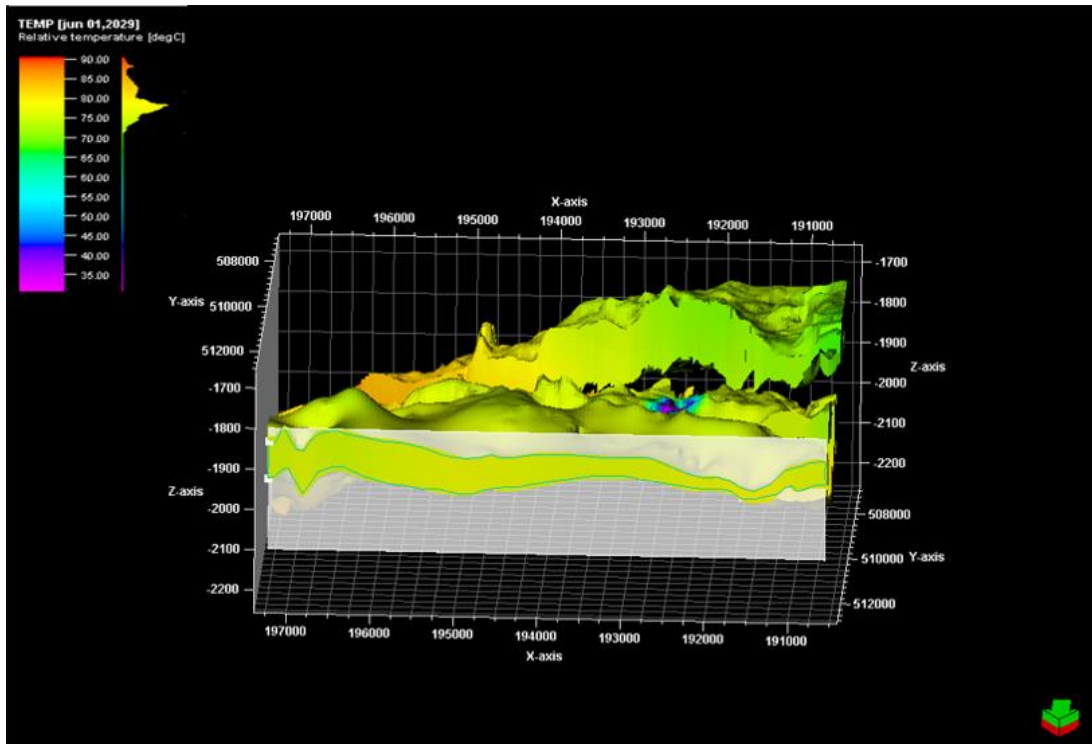


Figure 20: Extent of the cross sectional area at the northern boundary.

Appendix 8 and 9 represent the needed adjustments and inputs for the constant flux aquifer model method available in the reservoir engineering aquifer tool of petrel software.

Input parameters:

Thermal parameters	Values
a- Water specific heat capacity	3.5 kJ/kg.K
b- water thermal conductivity	0.66 W/m*K
c- Rock volumetric specific heat capacity	1997.5 KJ/m ³ /K
d- Rock thermal conductivity	1.98 W/m*K

Table 6: shows the input thermal parameters.

The thermal parameters are updated as follow with a density of 1140 Kg/m³:

- a) The specific heat capacity of water varies with temperature and salinity. The specific heat capacity (SPECHEAT) of the brine water is around 3.5 kJ/kg.K at salinity mass percent of 15% (Warren, 2020).
- b) The remaining simulations have a water thermal conductivity (THCWATER) of around 57.024 kJ/m/day/K (Warren, 2020).
- C) The remaining simulations have a rock volumetric specific heat capacity (SPECROCK) around 1997.5 KJ/m³/K using equation (2).
- d) The remaining simulations have a rock thermal conductivity (THCROCK) around 171.06 kJ/m/day/K.

3.6 New possible wells locations & Development strategies:

It is assumed that from 2024, the proposed production well KKP-GT-03 will produce. The coordinates and depth of the proposed production well KKP-GT-03 according to IF Technology is shown in the following table.

Proposed production well	Coordinates at aquifer depth	Depth
(KKP-GT-03)	X = 193066.20 m/ Y = 510361.60 m	- 1983.77 m

Table 7: Information related to the proposed production well KKP-GT-03 according to IF technology (Dirkx and Buik, 2019).

By 2027, a new doublet will be drilled in the Koekoekspolder field. The proposed wells locations have a distance of more than 500 m from the nearest faults. The distance between KP-GT-04 and KP-GT-05 is around 1773 m and the distance between KP-GT-04 and KP-GT-03 is around 1868.58 m. The coordinates of the new doublets at the surface can be near the first existing doublet to have a connection between the current and new doublets (For more details See the New technology section).

Possible second doublet location	Coordinates at aquifer depth	Depth	Covered Thickness
Injection well (KP-GT-04)	X= 195740.61 m/ Y = 510150.58 m	-2020.26 m	119.8 m
Production well (KP-GT-05)	X = 197142.19 m/ Y = 510049.57 m	-2109.86 m	94 m

Table 8: Information related to the possible second doublet.

The planned current coordinates of KKP-GT-03 were not ideal because the position of the new alternative hypothetical well KP-GT-BB03 can generate higher cumulative production energy than that of KKP-GT-03 well and can help in maintaining the production of KKP-GT-01 for a longer period to meet the future energy demand. An alternative location of the third production well can be drilled with the coordinates indicated in Table 9.

Possible Third well location	coordinates	Depth	Covered Thickness
Production well (KP-GT-BB03)	X = 194285.50 m/ Y = 511544.1 m	-1928.5 m	118.57 m

Table 9: shows the information related to the possible second production well location.

Possible Third doublet location	Coordinates at aquifer depth	Depth	Covered Thickness
Injection well (KP-GT-06)	X= 194565.27 m/Y = 508714.7 m	-2083 m	92.3 m
Production well (KP-GT-07)	X = 196885.61 m/Y = 508578.2 m	-2094.88 m	47.5 m

Table 10: Information related to the possible third doublet.

The locations of the new doublets (KKP-GT-04 & KKP-GT-05/ KKP-GT-06 & KKP-GT-07) are chosen based on the area with the highest temperature in the KKP concession as shown in figure 20 for an effective energy demand fulfilment. The coordinates at aquifer depth of the possible second doublet location (KP-GT-04 & KP-GT-05) and the possible third doublet location (KP-GT-06 & KP-GT-07) shown in appendix 10 and 11 can be optimized after predicting the direction of the natural initial aquifer flow.

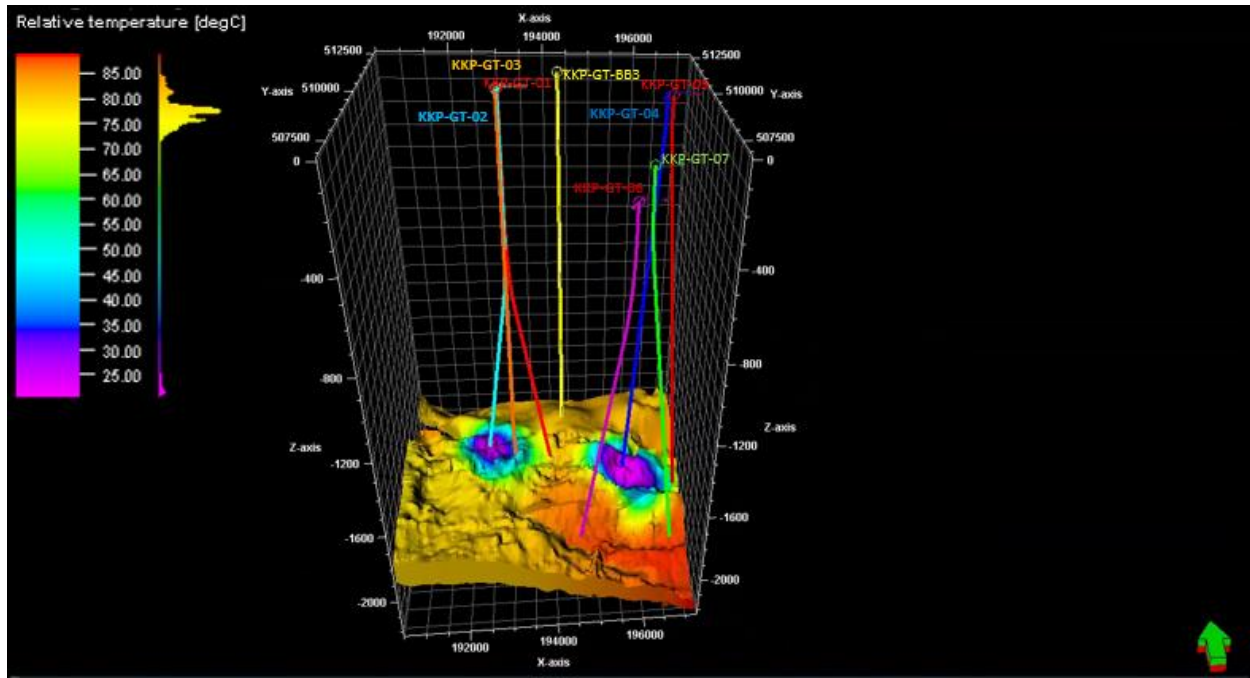


Figure 21: a 3D view that shows the current and predicted wells trajectory and locations from the tables above with temperature distribution at certain timestep generated by the initial geothermal model in KKP field.

To choose the optimal development scenario for the 3 wells (KKP-GT-02, KKP-GT-01, and KKP-GT-03), the scenarios of appendix 12 were tested from 2021 to 2121 while taking into consideration the historic field operation that extends from 2013 to 2021.

As shown in the chart below, three types of operational thermal recharge^{*1} strategies are investigated to stretch out the energy demand fulfillment over the next 100 years and they are continuous shut-off, discontinuous shut-off, and low-pressure gradient. Continuous shut-off simply means continuous operational thermal recharge^{*1} by shutting off the wells for a certain continuous period without any injected or produced water. On the other hand, the discontinuous operational thermal recharge is shutting off the doublet under operational thermal recharge^{*1} for instance for 1 year then operating the doublet for the following year, and so on. Furthermore, the low-pressure gradient means that the doublet operating the zones of the field which are under operational thermal recharge^{*1} have a small difference in bottom hole pressures (low-pressure gradient).

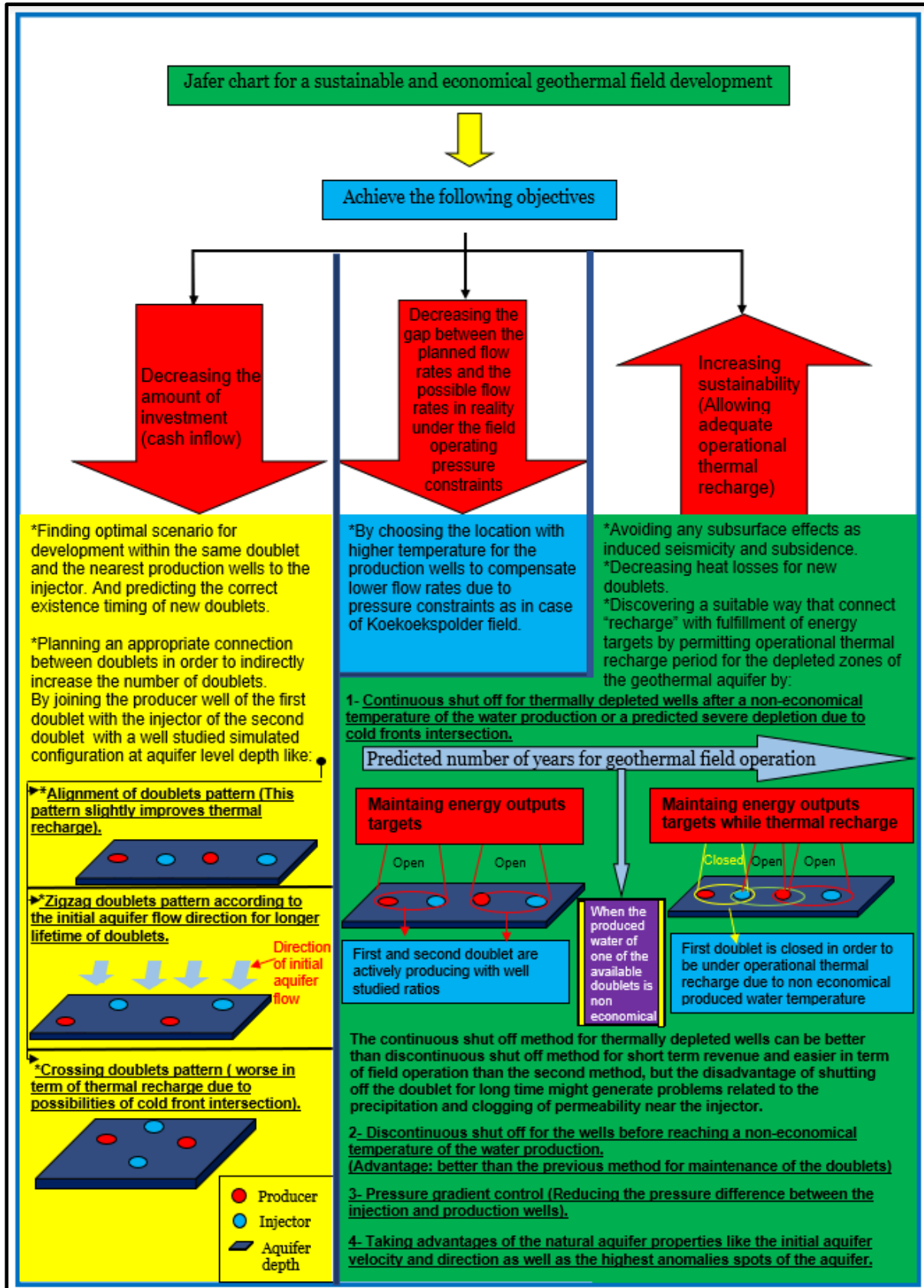


Chart 5: Sustainable and economical geothermal field development.

The table in appendix 13 shows the scenarios related to the second group of simulation cases. The operational thermal recharge¹ periods for the simulations are chosen based on the predicted year of non-economical heat production (non-economical bottom hole temperature) of the wells and the energy demand fulfillment. The permit holder delivered the future yearly desired energy till the year 2121. Based on the results of the optimal scenario from the table shown in appendix 12, the guide rate ratio of the production wells is as follows:

- The guide rate ratio of the first production well KKP-GT-01 = 75%
- The guide rate ratio of the second planned production well KKP-GT-03 = 25%

As mentioned in chart 5 and according to the research questions, one of the goals of this research study is to decrease the cash inflow (economical development) by starting with 1 or 2 doublets for the whole period of development and then testing if the energy supply will fulfil the energy demand as shown in figures 22 and 23.

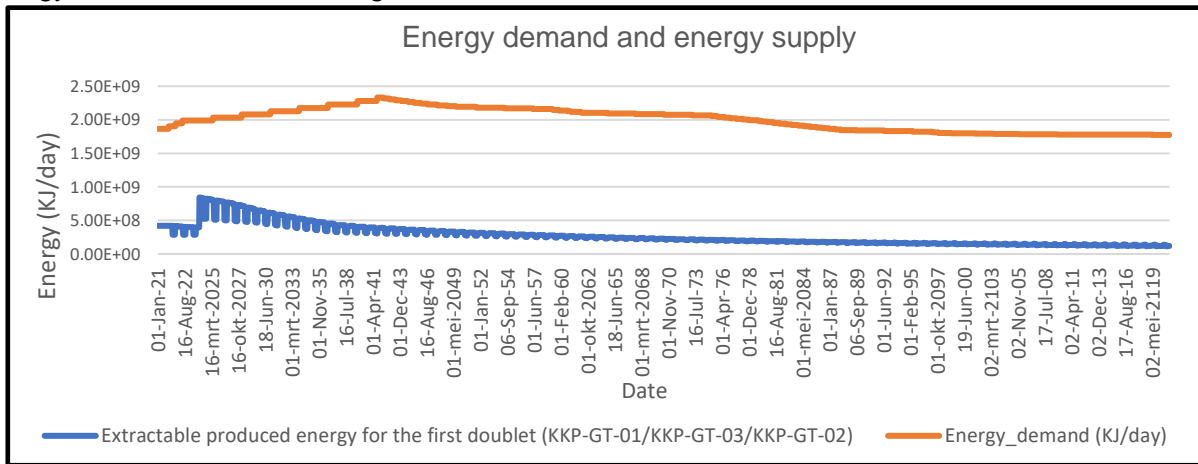


Figure 22: shows the energy demand and energy rate of 1 doublet in total.

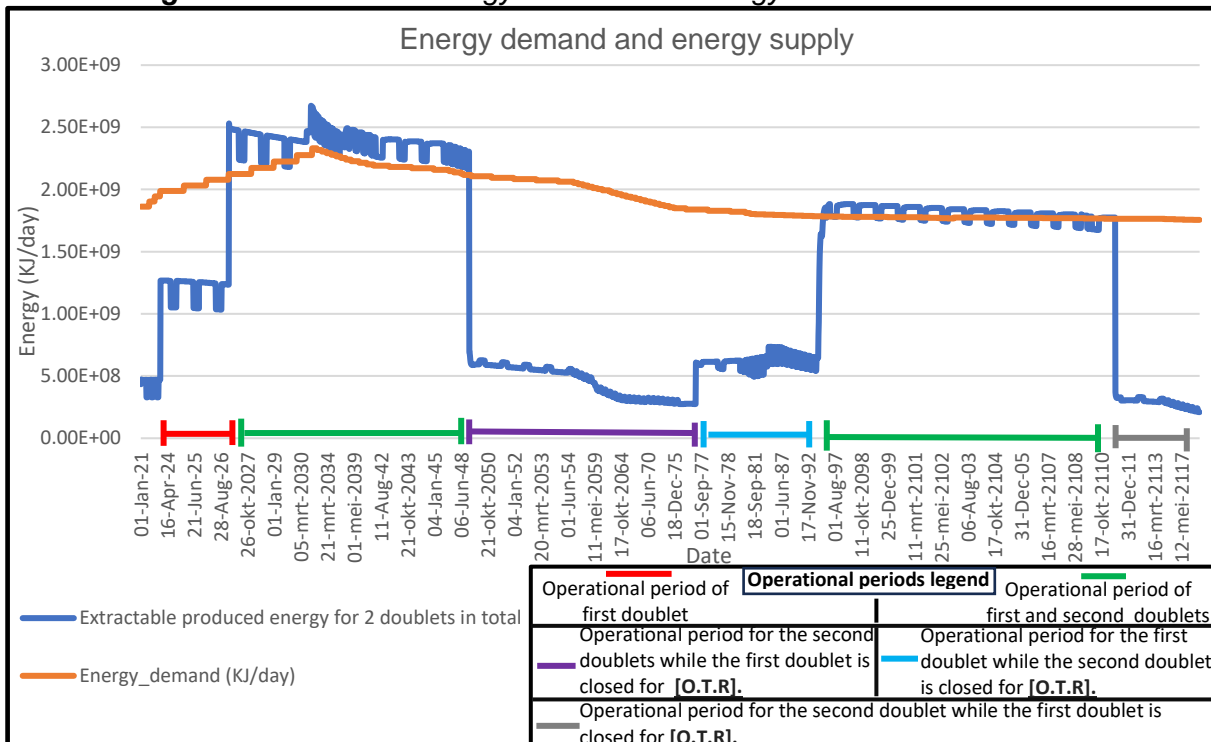


Figure 23: shows the energy demand and energy rate of 2 doublets in total.

Appendix 13-a shows the extractable energy with the energy demand after applying the forecasting scenario of the continuous shut-off strategy using 3 doublets in total. It is found that the field requires 3 doublets in total to fulfil the energy demand of the KKP field with allowing adequate operational thermal recharge^{*1} periods for the thermally depleted areas. In order to fulfill the energy demand from 2024 and to have a sustainable field development that allows adequate operational thermal recharge^{*1}, 3 doublets with the third production well “KKP-GT-03” will be enough. By comparing the energy demand with the predicted extractable energy, the flow rates were adjusted in winter and summer seasons till the year 2121.

The term “direct increase in doublets” means that there is no intention to connect doublets (separated operation of doublets) which means that the injection well of the second doublet has no relation with the production well of the first doublet. The term “indirect increase in doublets” means that there is an intention to connect doublets in such a way that relates the production well of the first doublet with the injection well of the second doublet or vice-versa. The indirect increase in doublets forecasting scenario will split the injected flow rate of the well name “KKP-GT-04” from 2050 on KKP-GT-01 & KKP-GT-05 to achieve an indirect increase in doublets by making the distance between KKP-GT-04 and KKP-GT-05 close at the surface and far away in the subsurface. The geothermal development strategy that allows an indirect increase in doublets as shown in chart 5 by connecting the geothermal wells together may help in achieving lower “Thermal fatigue^{*7}”.

The discontinuous shut-off operation for the 3 wells (KKP-GT-01, KKP-GT-02, and KKP-GT-03) from 2036 to 2077 means that the wells that are under operational thermal recharge^{*1} can operate for 1 year followed by 1 year of continuous shut-off. The discontinuous operational thermal recharge can be yearly based or monthly based. This study tests the yearly based discontinuous shut-off. Discontinuous recharge means that every year of field operation is followed by 1 year of operational thermal recharge^{*1}. But from 2077 to 2080 and from 2094 to 2097 as well as from 2111 to 2114, there is a continuous operational thermal recharge.

Based on the forecasted BHP and the desired flow rates, a relation between BHP and the flow rates of the rest of the wells can be obtained. The mechanism of operational thermal recharge^{*1} under a low pressure gradient can yield different scenarios according to the start datum of operational thermal recharge^{*1} and the desired flow rates during operational thermal recharge^{*1}. The operational thermal recharge^{*1} period of the wells KKP-GT-02, KKP-GT-01, and KKP-GT-03 for the 3 different operational thermal recharge strategies [continuous shut-off/ discontinuous shut-off/ low pressure gradient] are kept identical to choose the optimal operational thermal recharge^{*1} strategy. In the case of low pressure gradient operational thermal recharge strategy, starting operational thermal recharge^{*1} for KKP-GT-01/ KKP-GT-02 /KKP-GT-03 5 years before the start date of continuous operational thermal recharge strategy will make the difference between the injection and production BHP very small which will lead to sustaining a very small difference for BHPs (More restrictions) of the 3 wells (KKP-GT-01/ KKP-GT-02 /KKP-GT-03) compared to starting operational thermal recharge^{*1} for KKP-GT-02/ KKP-GT-01 /KKP-GT-03 10 years before the start date of continuous operational thermal recharge strategy (Fewer restrictions for pressure gradient).

The following steps are used to create the low pressure gradient development strategy which allows operational thermal recharge^{*1} under low pressure gradient strategy for the Koekoekspolder field:

- 1- Starting thermal recharge from 2040 (10 years before the start date of continuous operational thermal recharge strategy (Fewer restrictions for pressure gradient)

- 2- The total winter and summer flow rate of the 3 wells (KKP-GT-02/ KKP-GT-01 /KKP-GT-03) from 2040 to 2050 is distributed across the whole period from 2040 to 2077
- 3- Distribute the flow rates of each period of low pressure gradient operational thermal recharge in a way that maintains the flow rates demand targets
- 4- Obtaining the relation between the flow rates and bottom hole pressures for all wells in the KKP field to determine the suitable bottom hole pressures for the different wells.
- 5- Computing the new guide rate ratio and the new flow rate distribution for the different wells using the same guide ratio distribution used in the continuous operational thermal recharge strategy.
- 6- Minimizing the flow rate planned in the continuous operational thermal recharge strategy from the recent flow rate distribution
- 7- Distributing the total residual flow rate of KKP-GT-04 obtained from step 6 until 2077 to the period from 2077 to 2094
- 8- Distribute the total residual flow rate of KKP-GT-06 obtained from step 6 until 2094 to the period from 2094 to 2110
- 9- Distribute the total residual flow rate of KKP-GT-02 obtained from step 6 to the period between 2077 and 2094 in the period from 2110 to 2121.

In the third scenario for operational thermal recharge^{*1} with continuous doublets shut-offs, the planned operational thermal recharge^{*1} period will extend from 2050 to 2077. In the case of low pressure gradient mechanism for operational thermal recharge^{*1}, the operational thermal recharge^{*1} period extends from 2040 to 2077. The operational thermal recharge^{*1} period in the case of low pressure gradient mechanism will start 10 years before the operational thermal recharge^{*1} period with continuous doublets shut-offs as in the third forecasting strategy in such a way that distributes the flow rates of the wells that will be under operational thermal recharge^{*1} from 2040 to 2050 over the period from 2040 to 2077.

3.7 Qualitative uncertainty analysis:

The approach used in updating the static model and defining the thermal boundary conditions and aquifer flow properties as well as dynamic modeling had a high degree of accuracy and realism purpose despite the lack of different types of data. When the degree of realism and accuracy increase, uncertainty will decrease as in this research study. In case there are a wide range of uncertainties, the number of scenarios increase. From the beginning, the target of this research study was to decrease the uncertainties. The uncertainty is related to the input values as well as the boundary conditions of the model. There are uncertainties related to heat capacity computation due to the inaccuracy of quantifying the gypsum volume, shale, matrix, and cement volumes in the reservoir model which can have an impact on the accuracy of the geothermal doublet lifetime. Moreover, there are uncertainties related to the model outputs. The uncertainties related to the static model, dynamic model, heat model, and geomechanical model as well as other reservoir properties are indicated in the following tables. The idea of the tables below are derived from (Reith, 2019).

Property	Available data	Assumptions	Degree of realism and accuracy with used steps			Degree of uncertainty			Mitigation
			High	Moderate	Low	High	Moderate	Low	
Facies model (Sand dunes + Gypsum nodular (Eneolithic)	-Cuttings for the wells (KKP-GT-01/KKP-GT-02/ KAM-01-S1) -Well logs: GR/RHOB/NP HI/DT -Seismic amplitude (3D seismic cube) - Information on the conceptual model in the literature.	-An ellipse has been used as object geometry with no specific orientation for the gypsum nodulars (Redjosentono, 2014). - The thicknesses of these gypsum nodules are set to be between 1-15 meters (Redjosentono, 2014). -The facies is object based with aeolian sandstone as background deposited under N-E wind direction - Seismic identify the geometry of these gypsum zones bodies. -The gypsum bodies are assumed to be impermeable.	- The presence of gypsum/anhydrite zones that have been deposited is shown by analyzing the cuttings of the wells and the well logs in KKP field (Redjosentono, 2014). -The thicknesses of gypsum bodies are derived from well logs (KKP-GT-01 & KKP-GT-02). The density and neutron -porosity well logs showed that these bodies are impermeable and thick. - Seismic amplitude is projected to know the extension of these gypsum bodies (Redjosentono, 2014).			- The extent of the gypsum zones are not accurately known due to the uncertainty related to the lateral correlation between wells and the uncertainty related to the determination of facies because of the possible errors and inaccuracy of the interpretation of cuttings due to the mix of fragments with the well-bore-fluid as well as the assurance of which depth the fragments are. - Seismic resolution			The Facies model needs to be updated and calibrated based on the existing wells and the new planned wells data of: -KKP-GT-03 -KKP-GT-04 -KKP-GT-05 -KKP-GT-06 -KKP-GT-07
Static model	-3D seismic cube -All wells data -Core data -Information on the depositional environment from literature.	-Well to seismic tie was the first step used to interpret the horizon. A guided picking of seismic reflectors was established based on the well tops [markers] (Redjosentono, 2014).	- Time to depth conversion was applied (Redjosentono, 2014). Degree of realism and accuracy with used steps for the different parts of the static model as facies model (Sand dunes + Gypsum nodular (Eneolithic), N/G ratio, porosity and permeability distribution are identified in the section below. The upscaling of the properties was avoided from the beginning by choosing fine cells model representation for higher accuracy.			Volume uncertainty related to seismic surveys which have restricted vertical and horizontal seismic resolution, the seismic resolution diminish with depth.			Incorporating the new planned wells data of: -KKP-GT-03 -KKP-GT-04 -KKP-GT-05 -KKP-GT-06 -KKP-GT-07 to check if it is required to update the static model or not.

Table 11: shows a qualitative uncertainty analysis of the facies and static model that is used to simulate the KKP field.

Property	Available data	Assumptions	Degree of realism and accuracy with used steps			Degree of uncertainty	Mitigation
			High	Moderate	Low		
N/G ratio	-Cuttings for the wells (KKP-GT-01/KKP-GT-02/ KAM-01-S1) -Well logs: GR/RHOB/NP HI/DT -Seismic amplitude (3D seismic cube)	The N/G ratio is constant	The initial static model had a Net to gross ratio of 99% which was not realistic. This why the net to gross ratio is updated to be equal to 88.12% based on the available well logs.			Interpretation errors of seismic amplitude, well logs measuring errors, volume uncertainty, seismic surveys have restricted vertical and horizontal seismic resolution, the seismic resolution diminish with depth.	Using geostatistical techniques which has a purpose of estimating the local uncertainty at any unsampled area by taking in consideration global parameters like the facies global proportions and variograms (Maharaja, 2007). -Decreasing uncertainty related to the net to gross ratio distribution by integrating all the available data in term of: - Linking the seismic properties with the well logs response -The net to gross ratio needs to be calibrated and updated based on the average net to gross ratio (sand & Gypsum) of the existing and the new planned wells data of: -KKP-GT-03 /KKP-GT-04/KKP-GT-05 KKP-GT-06 & KKP-GT-07 , if a constant net to gross ratio is used for the entire KKP field.
Porosity	-Well logs: GR/RHOB/NP HI/DT -Core data - literature	The porosity model is based on the well logs (NPHI) knowing that the background Aeolian sands have continuous facies that extend out over large areas which means that there is a large correlation length (horizontal spatial continuity) for the porosity and the other properties (Redjosentono, 2014).	The porosity values at the existing wells locations of KKP field are obtained by well logs. Based on the Kampen core, the area of KKP field is assumed to have the same background facies (Aeolian sand). The very low porosity zones coincide with the gypsum/anhydrite bodies. (Redjosentono, 2014)			uncertainty related to the lateral correlation between wells.	Incorporating the new planned wells data of: -KKP-GT-03/KKP-GT-04 -KKP-GT-05 /KKP-GT-06/ KKP-GT-07 to see if there is a calibration required or not. The RMS attribute is directly proportion to the acoustic impedance and it can be related to high porous sands (Emujakporue and Enyenihi, 2020). This why combining well logs with seismic RMS attributes can decrease the uncertainty of the porosity distribution.

Table 12: shows a qualitative uncertainty analysis of the N/G ratio and porosity that are used to simulate the KKP field.

Property	Available data	Assumptions	Degree of realism and accuracy with used steps			Degree of uncertainty			Mitigation
			High	Moderate	Low	High	Moderate	Low	
Permeability	Core plug data	Fractures are assumed to be closed (No fractures are taken in consideration) because the horizontal stress is not parallel to the fractures orientation Moreover, after extension, the basin was subjected to inversion.	The permeability distribution is based on the porosity-permeability relationship (Poro-Perm relations are utilized as a petrophysical guideline to decide the permeability of comparable reservoir units in adjacent wells that have no cores (Redjosentono, 2014). By applying this relation, the permeability can be estimated based on the porosity that is known from well logs (Redjosentono, 2014). The permeability in the x, y and z directions are updated in order to obtain a robust model that have a complete history matching for both flow rates and bottom hole pressures from 2013 to 2021. Moreover realistic adjustment are conducted based on the literatures and measured data that illustrates that the vertical permeability is lower than the horizontal permeability.			uncertainty related to the lateral correlation between wells The seismic data cannot accurately determine to what extent the faults in KKP field influence the transmissivity.			Acquiring more core plugs to measure the permeability for the new planned wells: -KKP-GT-03 -KKP-GT-04 -KKP-GT-05 -KKP-GT-06 -KKP-GT-07 To compare it with the simulated permeability and decide if further adjustments and updates are required for the permeability distribution model of Koekoekspolder field. - FMI (Formation micro imaging log) is needed for the new planned wells in order to add fractures on the existing model (Based on a more reliable data) by taking in consideration the current stress conditions. -Low/mid/high cases scenarios are needed to be generated for the fault transmissivity in the vertical and horizontal components in order to have a more detailed overview to what extent the faults in KKP field influence the transmissivity The combination of seismic attributes, rock properties of the reservoir and confining layers (Shale smear factor) as well as the different faults displacements can have a major contribution in revealing more reliable information to determine to what extent the faults in KKP field influence the transmissivity.

Table 13: shows a qualitative uncertainty analysis of the permeability that is used to simulate the KKP field.

Property	Available data	Assumptions	Degree of realism and accuracy with used steps			Degree of uncertainty			Mitigation
			High	Moderate	Low	High	Moderate	Low	
Dynamic model	<p>Flow rate measured data (m³/day)</p> <p>Tubing head pressure (THP) for only 3 days</p> <p>Permeability distribution in the x, y and z directions.</p> <p>Net to Gross ratio</p> <p>Effective porosity</p>	<p>The dynamic model is based on the:</p> <ul style="list-style-type: none"> - permeability distribution in x, y and z directions. - Net to gross ratio - Effective porosity - The pore spaces is filled with only 1 type and 1 phase of fluid which is brine water. 	<p>-An approximated bottom hole pressures are obtained using equation (8).</p> <p>-The approximated bottom hole pressures are obtained from 2013 to 2021 based on the relationship between flow rates and the available bottom hole pressure.</p> <ul style="list-style-type: none"> - Complete history matching from 2013 to 2021 with high accuracy for both Flow rates and bottom hole pressure. -Taking in consideration the different factors when they are active and inactive as the natural aquifer flow properties assumptions. <p>As shown on the map of figure 4, there are different levels and ranges of overpressure from near-hydrostatic pressures mainly in the southern part of the Netherlands (Excess pressure < 1 MPa) and high overpressures (Excess pressure > 40 MPa) in the northern part. The pressure gradient results in a potential general trend for aquifer flow in the Slochteren from northeast towards the south (Verweij et al., 2011).</p>			<p>No direct bottom hole pressure measurements. There are uncertainties related to the assumption of North-south aquifer flow direction and velocity.</p>			<p>Direct BHP measurements are needed for the new planned wells.</p>

Table 14: shows a qualitative uncertainty analysis of the dynamic model that is used to simulate the KKP field.

Property	Available data	Assumptions	Degree of realism and accuracy with used steps			Degree of uncertainty			Mitigation
			High	Moderate	Low	High	Moderate	Low	
Heat model and energy distribution	<p>Injection temperature</p> <p>Production temperature (intake temperature).</p> <p>Temperature-depth relationship.</p> <p>The rock composition of the aquifer and the confining layers.</p>	<p>Having one input for the following thermal properties of the aquifer:</p> <ul style="list-style-type: none"> -Thermal conductivity of rock -Rock specific heat data <p>Having one input for the average initial temperature and thermal conductivity of the confining layers as well as the western thermal boundary.</p>	<p>A deep understanding of how the input thermal properties are distributed was needed to update the input of the thermal conductivity of the whole reservoir rock as well as the rock-specific heat data in order to reach an accurate distribution of thermal properties.</p>			<p>Uncertainty related to the input parameters.</p> <p>Overestimation of the output results is noticed in term of temperature and energy output.</p> <p>The cement heat capacity is not taken in consideration which can have minor effect on the reservoir energy estimation.</p> <p>There are uncertainties related to heat capacity computation due to the possible inaccuracy of quantifying the matrix and cement volumes in the reservoir model which can give inaccurate value of the geothermal doublet lifetime.</p>			<p>*** continuous monitoring and updating of the thermal properties inputs based on the output measured extractable energy.</p> <p>***Due to the constraints of eclipse 300 software , an overestimation in term of temperature and energy distribution must be taken in consideration.</p> <p>***The heat model is suitable for 2 component of the reservoir (example : Gypsum & sandstone), if another rock composition appeared in the other new planned wells then the uncertainty of the updated heat model will increase.</p> <p>***Validating the output of the simulation with the measured energy data.</p> <p>***In order to decrease the uncertainty related to the prediction of the temperature and energy distribution, the temperature and energy distribution should be simulated based on months and not years.</p> <p>*** Numerical model using Python software can be used to mimic the upwelling of warmer water (convection)from the deeper part in the same Slochteren aquifer.</p>

Table 15: shows a qualitative uncertainty analysis of the heat model and energy distribution that are used to simulate the KKP field.

Property	Available data	Assumptions	Degree of realism and accuracy with used steps			Degree of uncertainty	Mitigation
			High	Moderate	Low		
Geomechanical model	Bulk density data of KKP-GT-01 from 1055 m to 1854.835 m upper section is derived from the density log data of wells ZRP-3A and KGB-01. The Poisson ratios of the different groups used for the geomechanical model of KKP field (Hazel, 2017; Mechelse and Hettema, 2017).	The two horizontal stresses (σ_2 and σ_3) are equal.	<p>-Obtaining the uncovered bulk density of the upper section of KKP-GT-01 from wells ZRP-3A and KGB-01.</p> <p>- The slope of the failure envelope is based on the dominant rock composition of KKP field. The slope of the failure envelope is obtained from the experimental results of (Byerlee, 1978a)</p>			<p>Uncertainty related to the measured bulk density data due to instrumental error.</p> <p>Uncertainty related to the combined data of other locations for the uncovered upper section of KKP-GT-01.</p> <p>Uncertainty related to the maximum injection or minimum production pressure due to the possible variation of reservoir conditions in different reservoir areas.</p> <p>The possible error resulted from the assumption of equal horizontal stresses (σ_2 and σ_3).</p>	<p>- Another experiments are needed for KKP field to determine more accurately the a & b factors and aseismic or seismic slip will occur by realizing different scenarios.</p> <p>-The bulk densities from the surface to the targeted reservoirs needs to be measured for the next wells to lower the uncertainty of the first uncovered part of bulk densities.</p> <p>-More core samples from the reservoir and the above formations are needed to obtain an accurate Poisson's ratio.</p> <p>-Run Extended Leak Off Test (XLOT) for the new planned wells to measure the average in situ stress in KKP field or applying Kirsch equation to be able to determine the magnitude of horizontal stresses.</p> <p>-Applying a 3D Mohr coulomb representation that take in consideration the maximum and minimum horizontal stresses.</p>

Table 16: shows a qualitative uncertainty analysis of the geomechanical model used for the KKP field.

3.8 Sensitivity analysis:

The efficiency of the simulator is related to the sensitivity of the model towards different parameters like temperature, pressure, flow rate, and the velocity of the flow. When the different properties such as thermal boundary conditions and initial aquifer flux are taken into account, a delay in the progression of the cold front is noticed. This reflects the importance of taking the thermal boundaries around the reservoir. The thermal properties distributions are sensitive to the following parameters:

a- Injection temperature:

The sensitivity of the model toward different injection temperatures is based on the optimal guide rate ratios suitable for the first 2 wells (KKP-GT-01 & KKP-GT-03) [The guide flow rate ratio of the first production well (KKP-GT-01) and the second production well (KKP-GT-03) from the total injected flow rate in KKP-GT-02 well are 25 % & 75% respectively].

There is no change in the flow rates of the 3 wells (KKP-GT-02, KKP-GT-01, and KKP-GT-03) from 2013 to 2121 for the simulation cases with an injection temperature of 20°C, 25°C and 35°C. The energy production rate of KKP-GT-01 is almost similar in the simulation cases with an injection temperature of 20°C, 25°C, and 35°C. The energy production rate of KKP-GT-03 on the longer term in case of an injection temperature of 35°C is higher than the simulation case with an injection temperature of 25°C and 20°C due to the cooling rate around the KKP-GT-03 well. The cooling rate in the vicinity of the production well (KKP-GT-03) changes with different injection temperatures. There is no change in the bottom hole pressures of the 3 wells (KKP-GT-02, KKP-GT-01, and KKP-GT-03) from 2013 to 2121 for the simulation cases with an injection temperature of 20°C, 25°C, and 35°C. The following results of the updated input thermal properties simulation case show the lifetime of the production well KKP-GT-03 related to different injection temperatures from 2024 with a discontinuous shut-off development strategy and the optimal guide rate ratio distribution.

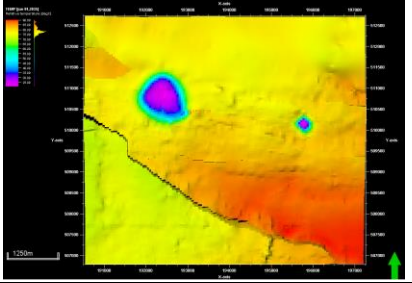
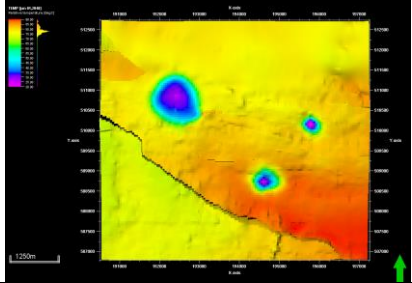
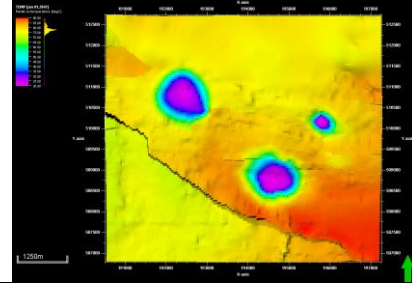
Injection temperature	20°C from 2024	25°C from 2024	30°C from 2024
Arrival of cold front at KKP-GT-03 (Predicted year of non-economical heat [55°C] production for KKP-GT-03)	2035	2040	2047
operation Interval from 2024 KKP-GT-03	11 years	16 years	23 years
Visualization in 3D			
Description	The lifetime of the third well “KKP-GT-03” is sensitive to the injection temperature of “KKP-GT-02”. By increasing the temperature of the injected water from 20°C to 25°C, the operation interval of the third production well “KKP-GT-03” will increase by 5 years, and in case of rising the temperature of the injected water from 20°C to 30°C, the operation interval of the third production well “KKP-GT-03” will increase by 12 years. In this regard, the injection temperature is directly proportioning to the lifetime of the doublet.		

Table 17: shows the sensitivity of the updated model towards different injection temperatures in terms of the arrival of the cold front according to the second production well “KKP-GT-03”.

For the KKP-GT-01 production well of the updated input thermal properties simulation case, the field will be operated in such a way that avoids non-economical water temperature production before 2121.

b- Injection pressure:

The results that are shown in the following table are obtained at an injection temperature of 20°C from 2024 at a guide flow rate ratio of 75% for KKP-GT-01 and 25% for KKP-GT-03.

Injection pressure	Maximum injection pressure (252 bar) at injection temperature of 20°C	Maximum injection pressure (252 bar) + 10 bar (262 bar) at injection temperature of 20°C
Flow rate [m ³ /day]		
Energy production rate [KJ/day]		
Bottom hole pressure (Bar)		
Description	<p>The flow rate of the injection well “KKP-GT-02” in case of an injection pressure equal to 262 bar for “KKP-GT-02” will reach the targeted flow rate of 6240 m³/day earlier than that in case of an injection pressure equal to 252 bar. There are no changes in the flow rates of the production well “KKP-GT-01” in both cases of injection pressures. In the case of an injection pressure equal to 262 bar, the flow rate and the energy production rate of the second production well “KKP-GT-03” will be higher than the flow rate and the energy production rate of the second production well “KKP-GT-03” in the case of an injection pressure equal to 252 bar in the period between 2024 and 2027. The energy production rate of the production well “KKP-GT-01” will remain the same in both cases of injection pressures.</p>	

Table 18: shows the sensitivity of the initial model towards different injection pressures of the first injection well “KKP-GT-02” in terms of the flow rate, energy production, and bottom hole pressure.

c- Thermal boundary conditions:

The results of the model with and without the thermal boundary conditions (confining layers and western boundary condition) are obtained at an injection temperature of 20°C from 2024 at a guide flow rate ratio of 75% for KKP-GT-01 and 25% for KKP-GT-03. The field energy production rate of the model with thermal boundaries conditions (confining layers and western boundary condition) is higher than the field energy production rate of the model without thermal boundaries conditions due to higher predicted and simulated bottom hole temperature in case of the model with thermal boundaries conditions than that of the model without thermal boundaries

conditions. Based on a continuous extraction of energy without any period dedicated for operational thermal recharge and without the initial velocity of the aquifer, the table which is indicated in Appendix 14 shows a comparison between the temperatures distribution in 2113 for the model with (confining layers and western thermal boundaries conditions) and the model without any thermal boundaries conditions, the lifetime of the first production well “KKP-GT-01” of the model with thermal boundaries conditions is longer with around 6 years than the model without thermal boundaries conditions. During the process of heat extraction, the forecasted reservoir temperature under the “recharge boundary condition” is slightly higher than that under the “no flow boundary condition”.

d- Initial velocity of the aquifer (with and without)

The KKP model which takes the initial velocity and direction of the aquifer is simulated from 2013 to 2121 by the constant flux aquifer method which is available in Petrel software. The effect of the initial velocity of the aquifer is studied on the following 2 properties (Comparison between the development of KKP field with and without the initial velocity of the aquifer according to):

I. Production Temperature:

Based on the temperature output results of the 2 wells (KKP-GT-01 and KKP-GT-07), the production temperature of KKP-GT-01 for several time steps is higher in the case of the model with an initial velocity effect of (0.0015 Celsius) than the production temperature of KKP-GT-01 in case of the model without initial velocity effect. The difference in the output temperature in the case of KKP-GT-07 is 0.013.

II. Doublet lifetime:

Wells names	Doublet lifetime of the model without initial velocity effect (constant flux aquifer model)	Doublet lifetime of the model with initial velocity effect (constant flux aquifer model)
(KKP-GT-01)	On 02/09/2039 (at 14:50:00) Temperature = 78.535 Celsius	On 04/09/2039 (at 21:30:00) Temperature = 78.535 Celsius (2 days, 6 hours extra lifetime)
(KKP-GT-03)	On 10/07/2042 (at 00:30:47) Temperature = 60 Celsius (1 day, 9 hours extra lifetime)	On 08/07/2042 (at 14:44:16) Temperature = 60 Celsius
Description	The doublet lifetime of the model without the initial velocity effect is lower than the doublet lifetime of the model with the initial velocity. However, in the case of the KKP-GT-03 well, the doublet lifetime of the model without initial velocity effect is higher than the doublet lifetime of the model with the initial velocity due to the well location. The difference is small because the initial velocity of the natural aquifer flow is 3.18 m ³ /day.	

Table 19: shows the sensitivity of the doublet lifetime towards the updated model with and without initial velocity of the aquifer in terms of bottom hole temperature value at a certain time according to the first and second production wells.

4.Results & Discussion

4.1 Production guide rate and temperature distribution:

Results that show the production energy of the first doublet (KKP-GT-02 & KKP-GT-01) as well as the third planned well (KKP-GT-03) under the field pressure constraints and variety of injection temperature are shown in table 18. A detailed comparison between these simulations is mentioned in the sensitivity analysis section. Amongst the numerous scenarios in appendix 12 with an injection temperature of 20°C from 2024, the following results show the different production guide rate ratio effect on the arrival of the cold front to the first production well “KKP-GT-01”.

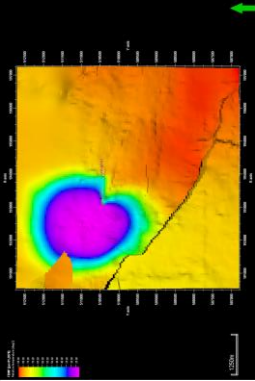
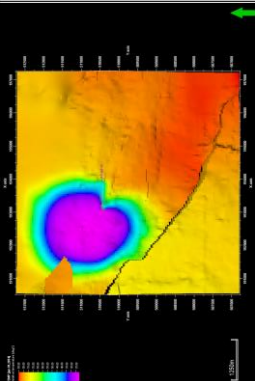
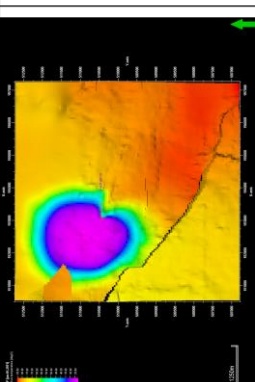
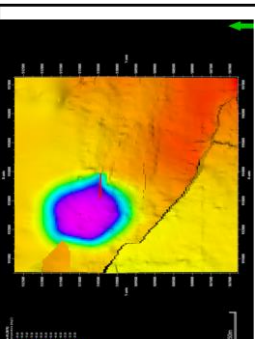
Guide rate ratio	KKP-GT-03:25% KKP-GT-01:75%	KKP-GT-03:50% KKP-GT-01:50%	KKP-GT-03:75% KKP-GT-01:25%	KKP-GT-01:100%
Arrival of cold front at KKP-GT-01 (Predicted year of non-economical heat production KKP-GT-01)	2079	2074	2071	2043
operation Interval from 2024 KKP-GT-01	55 years	50 years	47 years	19 years
Visualization in 2D				

Table 20: The effect of different production guide rate ratios on the arrival of the cold front to the second production well “KKP-GT-01” with an injection temperature of 20°C from 2024 to 2121.

As shown in table 20, the advantage of the location of the second production well KKP-GT-03 is that it retards the cold front propagation from arriving at the first production well KKP-GT-01.

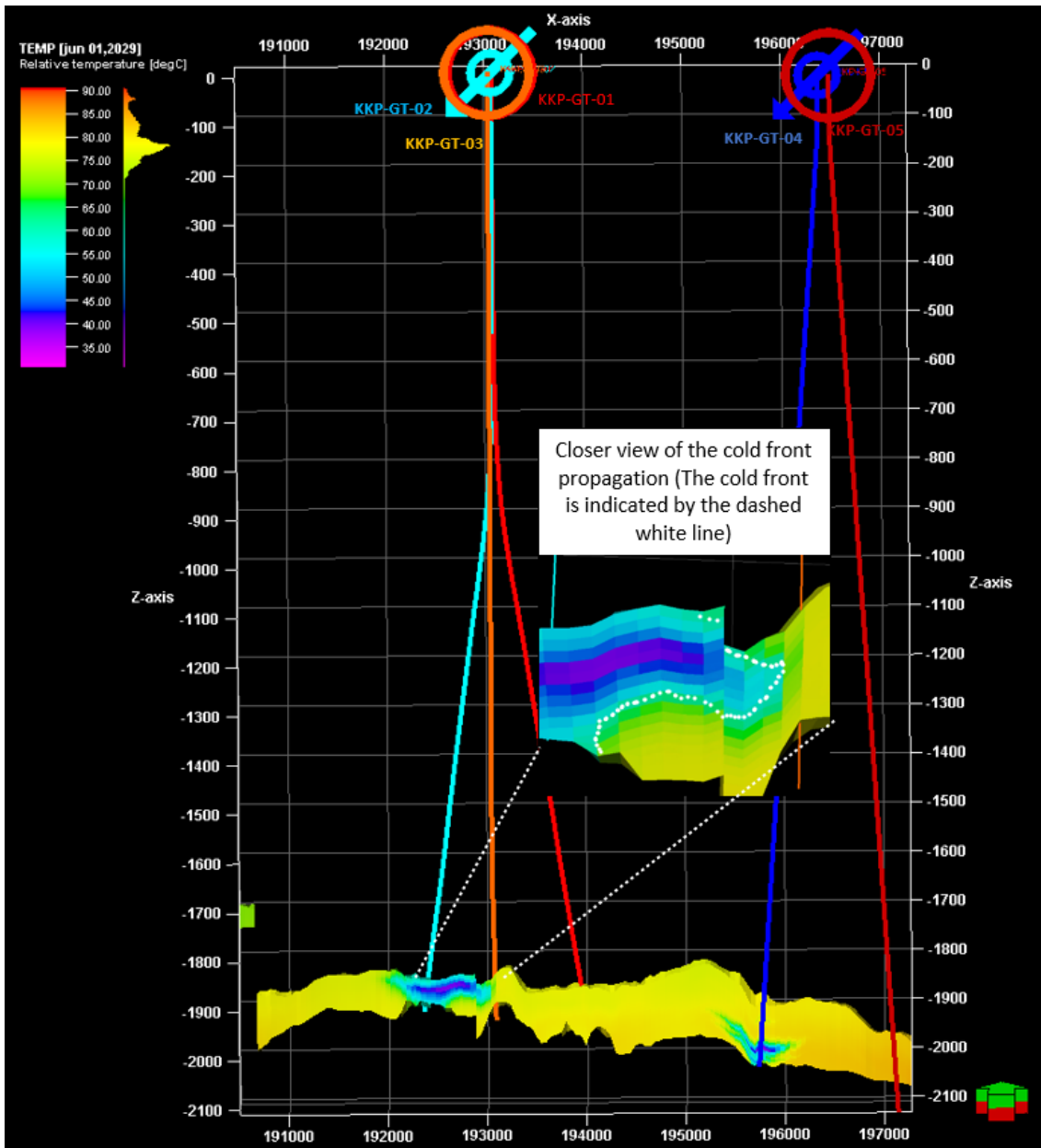


Figure 24: shows a cross sectional view of the updated temperature model along the j direction in the beginning of 2029 with the displayed wells (KKP-GT-02, KKP-GT-01, KKP-GT-03, KKP-GT-04 and KKP-GT-05) as well as a closer view of the cold front shape in January indicated by the white dashed line.

As shown in figure 24, the cold front is not a vertical straight line that propagates through the aquifer. It is irregular front propagation due to the heterogeneity of the reservoir properties and structure. The propagation of the reinjected cold water along the good quality sand with better porosity and permeability areas of reservoir is faster than the other parts of the reservoir. Based on the analysis of the results generated from the thermal model, a relation between the non-economical bottom hole temperature and the rock cold front temperature can be generated. At

the beginning of the year 2029, the bottom hole temperature of the second production well (KKP-GT-03) will be around 71.844°C and the average temperature of the aquifer in the vicinity of the third production well will be around 72.45125°C as shown in appendix 15. The cold front temperature of the aquifer is approximately 55.464878°C and it is determined based on the non-economical temperature defined by the owner of the field which is around 55°C. The cold front propagation is determined based on the non-economical temperature (The range of non-economical temperature extends from 60°C to 55°C). The initial model with a guide rate ratio of 25% for the third production well KKP-GT-03, and a 75% of production guide rate ratio for KKP-GT-01 production well has the longest operational interval for the second and the first production well (Interval before reaching the non economical temperature) from 2024. Therefore, this production guide rate ratio is considered the optimal guide rate ratio. The shape of cold front propagation from 2024 to 2121 in the case of the second production well “KKP-GT-03” placed between KKP-GT-02 and KKP-GT-01 is different than that of the first production well with 100% production guide rate which exhibits the presence of a second production well between the first injection well KKP-GT-02 and the first production well “KKP-GT-01”. The lifetime of the different doublets sets increased when the thermal properties were updated and corrected. For instance in the case of a guide rate ratio of 25% for the third production well KKP-GT-03 and 75% of production guide rate ratio for KKP-GT-01 production well, the arrival of the cold front at KKP-GT-03 is expected to be at the year 2036 instead of 2028. The following figure shows the flow rate and bottom hole pressure for the optimal guide rate of the first and second production wells “KKP-GT-01” and “KKP-GT-03”.

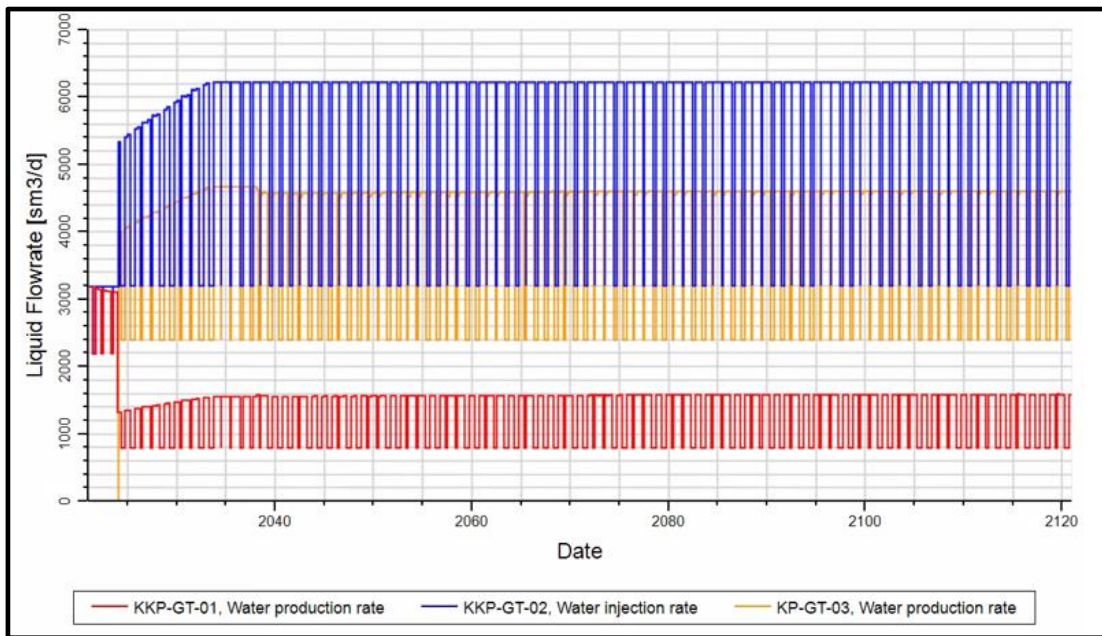


Figure 25: shows the flow rate of the optimal guide rate ratio of the first and second production wells “KKP-GT-01” and “KKP-GT-03”.

In figure 25, there is a small difference between the injected brine water volume of the KKP-GT-02 well and the production well KKP-GT-01 from the beginning of 2023 due to the pressure constraints of a minimum bottom hole pressure equal to 153 bar. If the BHP constraint of the production well “KKP-GT-01” will decrease, the small difference between the injected brine water volume of the KKP-GT-02 well and the production well KKP-GT-01 will decrease. The presence of the very small offset simulated between the injected and produced flow rates is due to the pressure constraints of the Koekeekspolder field. For instance, the results shown in appendix 16 for the period between 2021 to 2045 are with a lower production bottom hole

pressure around 140 bar while the other runs have a minimum production pressure of 153 bar. The simulated results is more reliable than the direct manual computation of the targeted extractable energy because the produced bottom hole temperature and flow rates may not reach the target in certain periods of the KKP field development due to the field constraints for example.

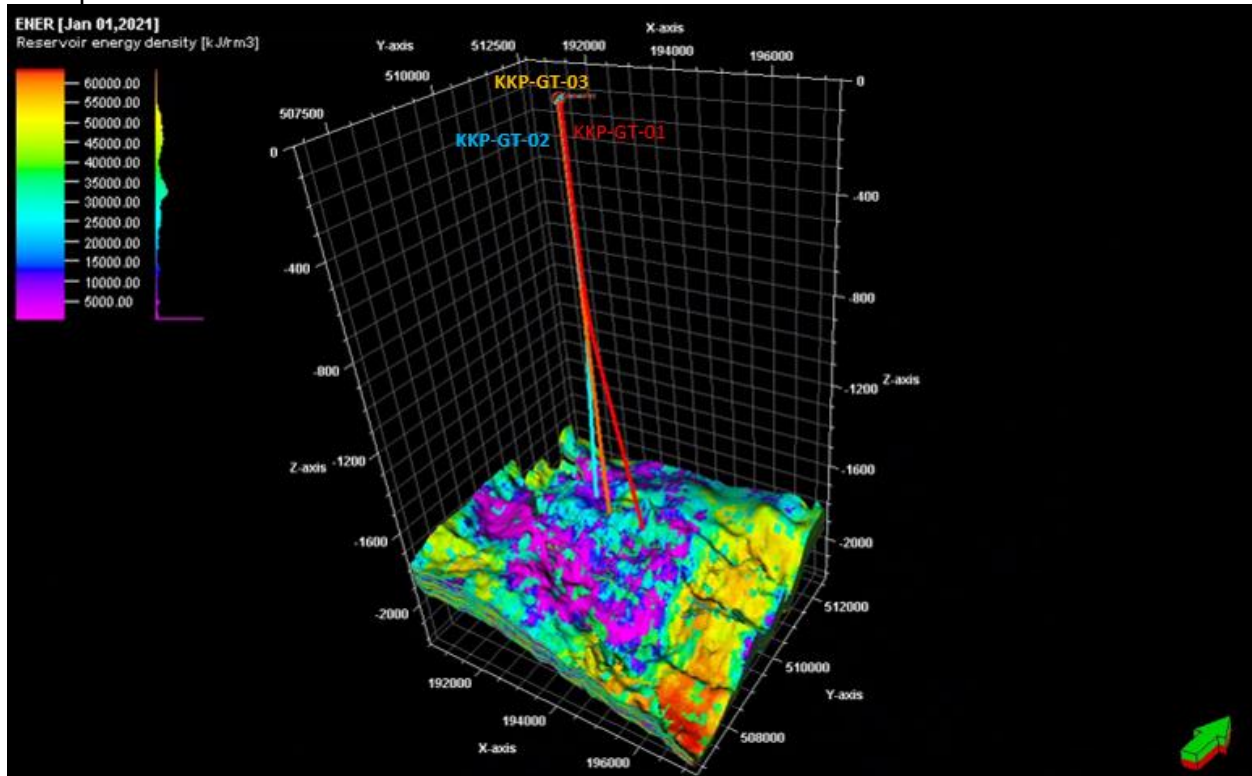


Figure 26: represents the energy distribution of the initial model in the month of January 2021.

As shown in the figure above, the simulated stored energy distribution has a wide range of variations due to the following factors:

- The temperature variation related to the depth of each location (Structure of the reservoir).
 - The heterogeneity in the aquifer that is resulted from the gypsum and sandstone deposits as well as the water content dissimilarity within the aquifer as a result of permeability distribution.
- The southern-eastern part of the aquifer has the highest energy values of the aquifer as shown in figure 26 and it has a low thickness as indicated in figure 5.

4.2 Direct & Indirect increase in doublets:

The following results are related to the geothermal continuous shut-off development strategy with the direct and indirect increase in doublets using the optimal forecasting strategy within the first doublet for the updated model. Based on the output bottom hole temperature of the production wells (KKP-GT-01/KKP-GT-03/KKP-GT-05/KKP-GT-07), the indirect increase in doublets with continuous recharge strategy has a higher simulated bottom hole temperature than the direct increase in doublets (separated doublets operation).

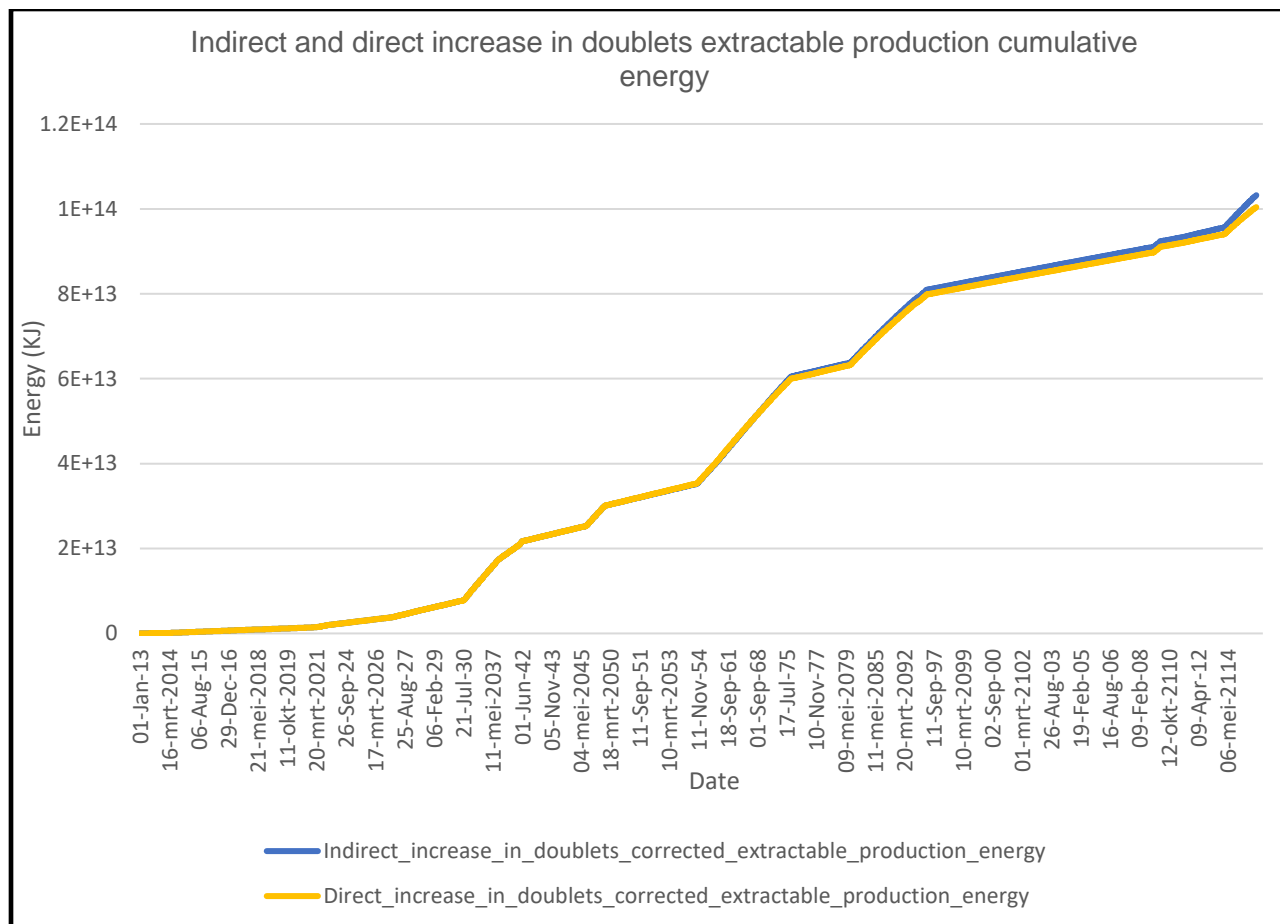


Figure 27: shows the cumulative energy for the direct and indirect increase of the continuous recharge strategy.

In addition, the indirect increase in doublets will slightly increase the output energy as seen in figure 27 but it is not taken into consideration for the optimal scenario because it is a new technology, and further drilling engineering studies are required to determine if it can be possible to have in the reality the well heads of the KKP field wells close to each other at the surface or to inject the excessive volume of produced water at KKP-GT-01 in KKP-GT-02 with predicting what will happen in the field in term of pressure distribution and subsidence. Based on the analysis of the pressure distribution results, the pressure around KKP-GT-05 and between the injection well KKP-GT-04 and KKP-GT-01 in case of indirect increase in doublet is lower than that in case of the direct increase in doublet with a minimum pressure that doesn't subceed the minimal allowed production pressure of 153 bar.

4.3 Unconventional geothermal field development:

The results of different types of development strategies (Continuous shut-off/ Discontinuous shut-off and low-pressure gradient) using the updated model that takes into account the thermal recharge are obtained for each production well to find the optimal scenario for the whole Koekoekspolder field. The following results are obtained using an injection temperature of 20°C from 2024.

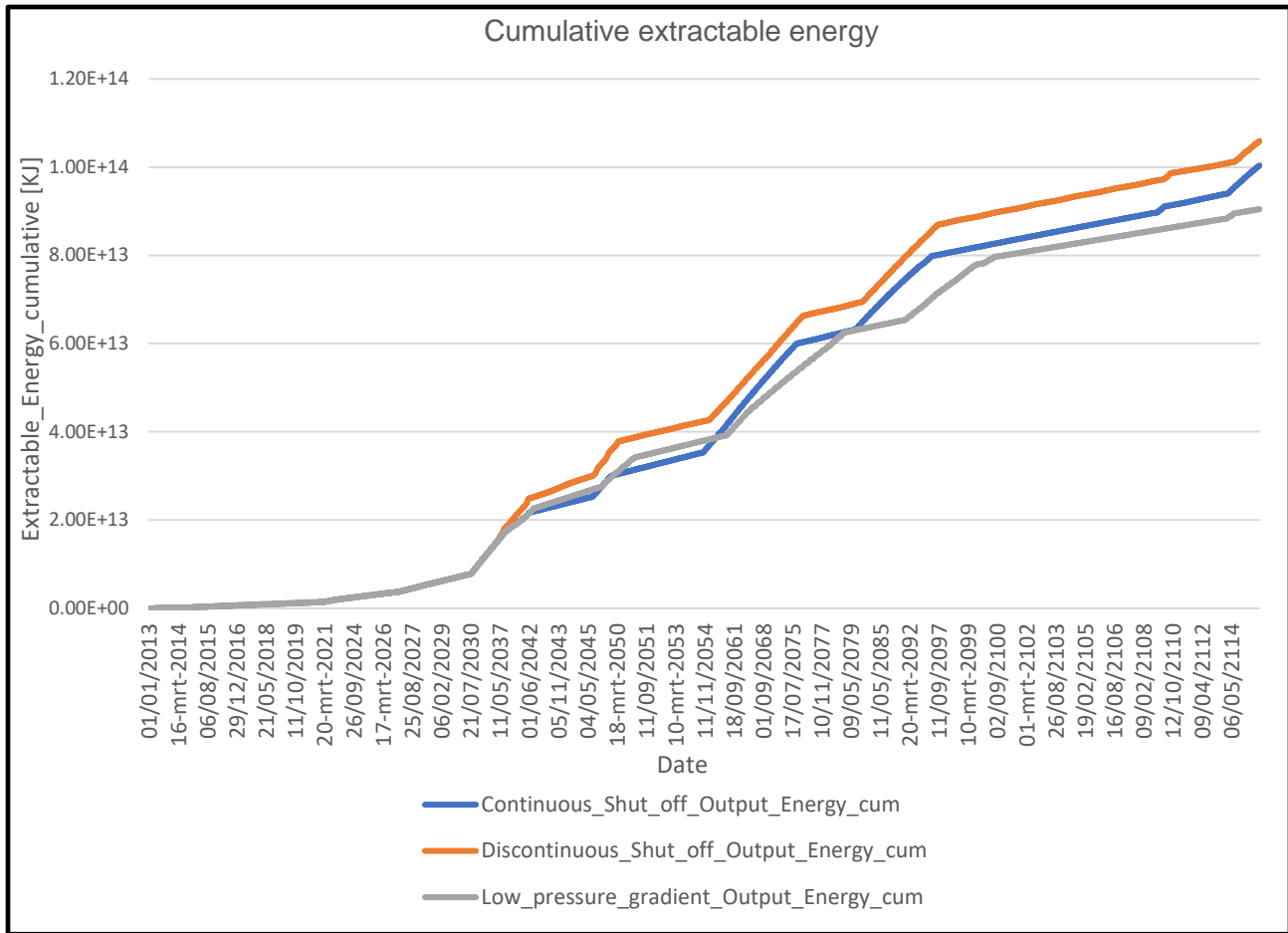


Figure 28: shows the cumulative extractable energy of the KKP field for the continuous, discontinuous, and low-pressure gradient geothermal operation.

In Figure 28, most of the changes in the slopes of the cumulative extractable energy for the different operational thermal recharge development strategies are due to the operational timing of the new doublets [(Injection well KKP-GT-04 & Production well KKP-GT-05) starting from 2027 and the third doublet starting in 2036 in the case of discontinuous shut development strategy and from 2050 in the case of continuous shut-off and low-pressure gradient development strategies which have higher enthalpy than the first doublet (Higher extraction water temperature) as well as a shift in operational parameters such as flow rates, doublets periods (assigned operational thermal recharge periods) which is reflected in different cumulative extractable energy pattern.

The discontinuous shut-off yields the largest cumulative extractable energy among the other operational strategies, the discontinuous shut-off operation is a powerful strategy that can overcome the high cooling rate expected for the KKP field due to the lower injection temperature of 20°C planned by the owner to increase the extractable energy production. Moreover, the discontinuous-shut off allows sustainable optimization with very low thermal depletion. A high cooling rate in the aquifer and especially around the faults of the KKP field can generate induced earthquakes which can be a major obstacle to the sustainable development of the KKP field [The discontinuous shut-off will provide a continuous fulfillment of energy demand (only certain doublets will be on and off for particular periods and this strategy is better than having an induced earthquake which can threaten the continuation of the project and a big loss in

investment)]. Also further studies are required to check if the discontinuous shut-off for doublets can extend the ESP replacement costs which can provide additional incentives. Thus, the KKP updated model is tested using the optimal discontinuous shut-off with an injection temperature equal to 20°C, 25°C, and 30°C from 2024 to 2121 to analyze the predicted cooling rate and extractable energy scenarios at 3 different locations. The cooling rate in the case of continuous injection temperature of 20°C is around 0.58777 °C/year. In the case of continuous injection temperature of 25°C, the cooling rate is approximately 0.278667 °C/year. The cooling rate is around 0.277 °C/year in the case of continuous injection temperature of 30°C. As illustrated in table 21, the discontinuous shut-off operation has a significant role in overcoming the high cooling rate using an injection temperature of around 20°C from the year 2036. The location near the KKP3 fault with the coordinates (X= 193116.67 m/ Y= 510539.44 m) is used to test the cooling rate generated by the different geothermal operational strategies involved in this research study such as the discontinuous shut-off, low-pressure gradient, and continuous shut-off operation.

Year	Aquifer temperature at the location with the coordinates (X= 193116.67 m/ Y= 510539.44 m) in the case of different geothermal operational strategies:					
	Discontinuous-shut off operation for operational thermal recharge* ¹		Continuous-shut off for operational thermal recharge* ¹		Low pressure gradient for operational thermal recharge* ¹	
	Aquifer temperature °C	Cooling rate per year °C/year	Aquifer temperature °C	Cooling rate per year °C/year	Aquifer temperature °C	Cooling rate per year °C/year
2036	75.60		75.60		75.60	
2037	75.45	0.15	75.27	0.33	75.27	0.33
2038	75.16	0.29	74.89	0.38	74.89	0.38
2039	75.12	0.04	74.65	0.24	74.65	0.24
2040	74.85	0.27	74.19	0.46	74.19	0.46
2041	74.67	0.18	73.67	0.52	73.78	0.41
2042	74.24	0.43	72.86	0.81	73.02	0.76
Average cooling rate °C/year	0.226666		0.456666		0.43	

Table 21: shows the predicted temperature and cooling rate at a location near the KKP3 fault with the coordinates (x= 193116.67 m/ y= 510539.44 m) in the updated 3D thermal model.

In table 21, the discontinuous shut-off operation for the geothermal doublets in the KKP field showed the lowest (< 0.3°C/year) average cooling rate among the other geothermal field development strategies with an injection temperature of 20°C from the year 2036. Based on the cooling rate values shown in table 21, the continuous-shut off and low-pressure gradient for operational thermal recharge*¹ from the year 2036 will generate almost the double value of the cooling rate generated by the discontinuous shut-off operation. The cooling rate varies from one place to another and it is very difficult and uncertain to represent one value of the cooling rate for the whole field because the cooling rate within the 5.2 km² area of the KKP field has a wide discrepancy. This is why a cooling rate distribution was generated based on the simulated temperature distribution of the updated Koekoekspolder thermal model as shown in the following figures.

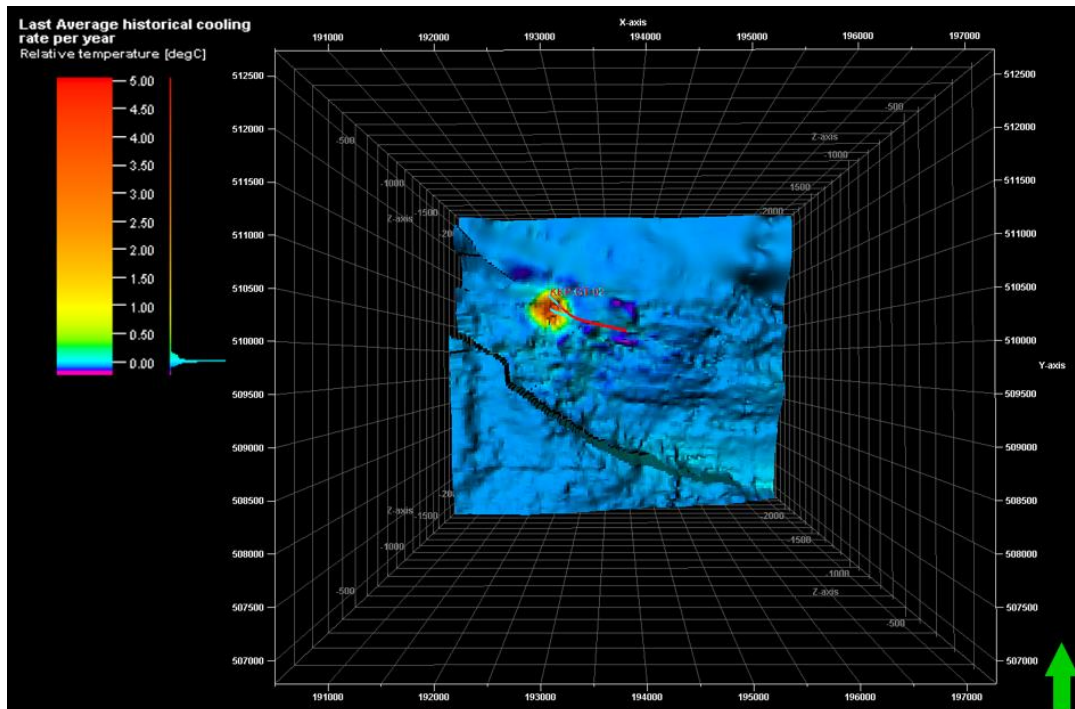


Figure 29: shows the average historical cooling rate per year from 2013 to 2021.

The average historical cooling rate distribution from 2013 to 2021 of the updated thermal model shown in figure 29 was obtained by subtracting the temperature distribution in 2021 from the temperature distribution in 2013 and then dividing it by the number of years between 2013 and 2021 to obtain the average historical cooling rate per year. From 2013 to 2021, no induced seismicity was recorded in the KKP field. Furthermore and with the same concept of computing the average historical cooling rate distribution, the predicted cooling rate distribution from 2024 to 2035 in the case of injection temperature scenario equal to (20°C, 25°C, and 30°C) was computed. The average cooling rate as a result of an injection temperature of 20°C, 25°C, and 30°C is obtained by subtracting the temperature distribution in 2036 from the temperature distribution in 2024 and then dividing the output by 11 to obtain the average cooling rate per year. Afterward, the difference between the predicted average cooling rate distribution for each injection temperature scenario and the average historical cooling rate per year distribution is obtained to have a general idea about which injection temperature can be used from 2024 to 2036 without major disturbance of the geothermal system.

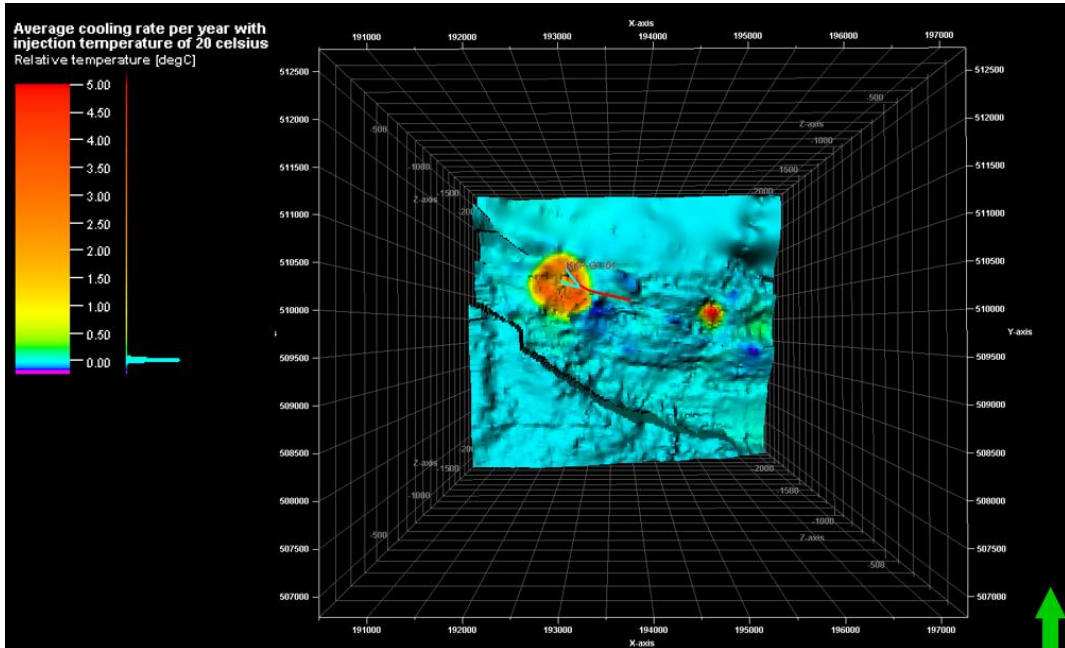


Figure 30: shows the average cooling rate per year distribution of the updated thermal model with an injection temperature of 20°C from 2024 to 2035.

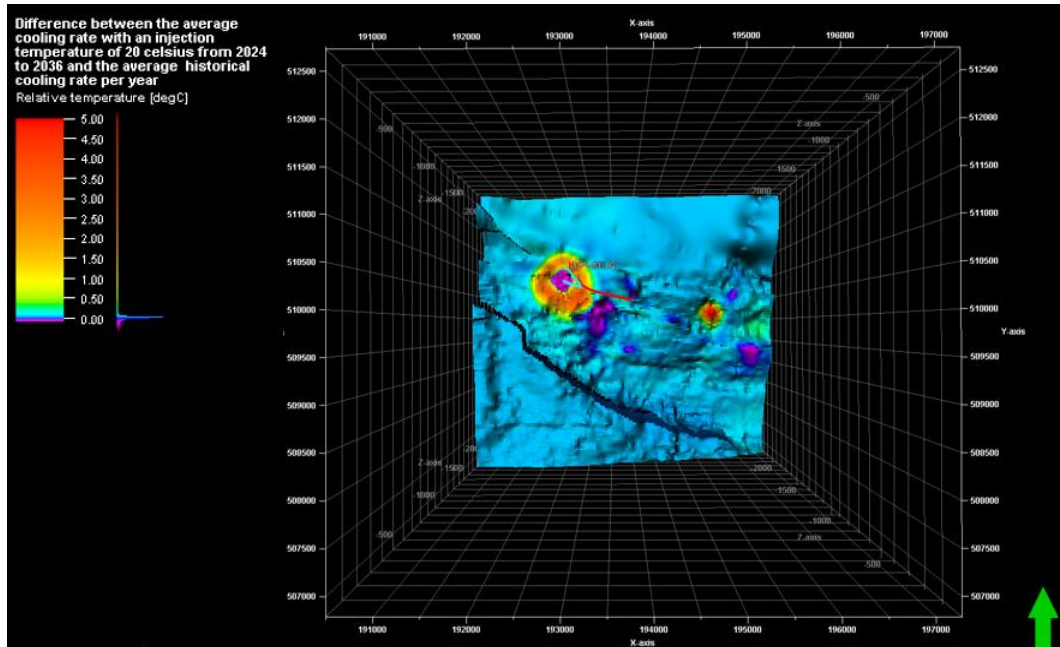


Figure 31: shows the difference between the average cooling rate per year distribution with an injection temperature of 20°C from 2024 to 2035 and the average historical cooling rate per year.

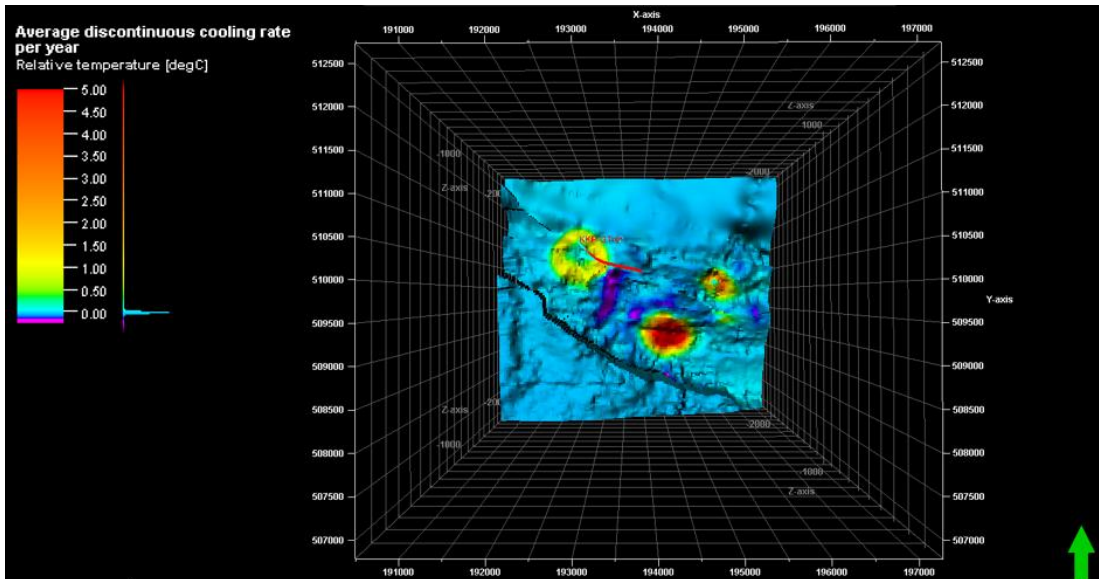


Figure 32: shows the average cooling rate per year distribution of the updated thermal model generated by the discontinuous shut-off operation for doublets using an injection temperature of 20°C from 2036 to 2042.

The average cooling rate distribution per year for discontinuous shut-off operation is obtained by subtracting the temperature distribution in 2042 from the temperature distribution in 2036 then the output value of subtraction is divided by the number of the years between them.

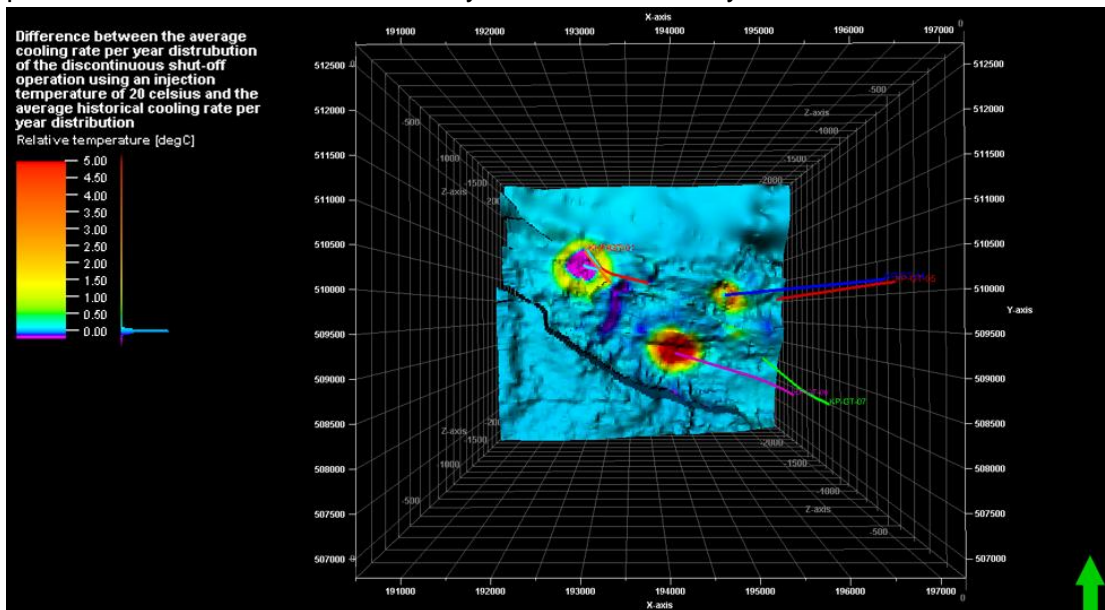


Figure 33: shows the difference between the average cooling rate per year distribution of the updated thermal model generated by the discontinuous shut-off operation for doublets using an injection temperature of 20°C from 2036 to 2042 and the average historical cooling rate per year.

The cooling rates vary based on the reservoir properties, thermal recharge boundary conditions around the geothermal aquifer as well as the operational parameters such as injection flow rates and injection temperatures. The cooling rate decreases as the distance from the injection well increases. The decrease in the cooling rate is not homogeneous because of the reservoir thermal properties as well as the effect of the recharge thermal boundaries which can generate the negative value of cooling rate in Slochteren aquifer as indicated in figure 32. There are a few cooling rates with negative values due to the increase in temperature because the Koekoekspolder reservoir is under realistic recharge thermal boundary conditions from the confining layers and the western thermal boundary. The historical cooling rate distribution can be used as a reference in case the minimum cooling rate cannot be determined especially for a field with 5.2 km² and by knowing that the cooling rate has a wide variation. Despite using the yearly discontinuous shut-off, one of the doublets which are not under operational thermal recharge^{*1} can generate a high cooling rate which can be solved by a creative solution such as the Jafer matrix for discontinuous shut-off operation. As shown in figures 29 and 32, the discontinuous shut-off operation for the first doublet showed a powerful technique to overcome a high cooling rate because the average cooling rate per year for the discontinuous shut-off operation is lower than the historical cooling rate per year. It is recommended that the field will operate with an injection temperature of 30°C instead of 20°C from 2024 to 2036 until the discontinuous shut-off operation will start. If any seismicity will be recorded then the owner must sustain the current injection temperature of 35.4 °C until the discontinuous shut-off will take place in the field. The discontinuous shut-off operation for this research study is based on one year of operation followed by one year of continuous shut off which overcomes the cooling rate caused by the 2 doublets but for the other third doublet, there is a chance to have a high cooling rate, this why a creative concept is introduced called “Jafer matrix for discontinuous shut off to overcome high cooling rate with the least number of doublets” because as already mentioned in chart 2, the target from the beginning is to reduce the amount of cash inflow and reaching a sustainable development of the Koekoekspolder field. The field can be operated by an injection temperature of 30°C in the third doublet with continuous operation and discontinuous shut-off for the first and second doublets with an injection temperature of 20°C or to sustain the injection temperature of 20°C by applying the concept of “Jafer matrix for discontinuous shut off to overcome high cooling rate with the least number of doublets” which ensure a high profit and safe sustainable development of the field.

The “Jafer matrix for discontinuous shut-off operation to overcome high cooling rate with the least number of doublets” can be structured based on the cooling rate constraints of any geothermal system. Shutting off the doublet can be represented by a zero value (0) while opening the doublet is represented by one value (1) [Binary numbers]. The switch between opening the doublets for operation and shutting the doublets for operational thermal recharge^{*1} must be done carefully in such a way that fulfills the energy demand. In the case of the Koekoekspolder field, it is required to operate 2 doublets in total from 2036 to 2121 to fulfill the upcoming desired energy demand. The shorter the period to switch between opening the doublet for operation and shutting off the doublet for operational thermal recharge^{*1} (discontinuous duration), the better, safer, and more sustainable the development of the geothermal field will be. The tables below are structured based on 2 types of constraints:

- The first type >>>>>>>>> Economical constraint which is operating at least 2 doublets in total from 2036 to 2121 to fulfill the upcoming desired energy demand
- Second type >>>>>>>>> Cooling rate constraint for safety which is not exceeding a period of 1 year for opening each doublet for continuous operation

Period (Year)	First doublet set (KKP-GT-02/KKP-GT-01/KKP-GT-03)	Second doublet (KKP-GT-04/KKP-GT-05)	Third doublet (KKP-GT-04/KKP-GT-05)
2036	Shut-off (For operational thermal recharge ^{*1}) [0]	Open (For operation) [1]	Open (For operation) [1]
2037	Open (For operation) [1]	Shut-off (For operational thermal recharge ^{*1}) [0]	
2038			
2039			
2040			

Table 22: shows the planned switch between opening the doublets for operation and shutting the doublets for operational thermal recharge^{*1} in the case of the KKP field development with a prerequisite of one year period to switch between opening and shutting-off for each doublet (discontinuous duration) and the cooling rate constraint of not exceeding a period of 1 year for opening the doublets in term of continuous operation.

The red color in table 22 indicates that there is a risk of a high cooling rate (A possible safety issue). In table 22, the KKP field followed a prerequisite of one year to switch between opening and shutting-off for each doublet. The green color in table 22 indicates the first doublet which is under operational thermal recharge^{*1}. It is recommended that any doublet under the discontinuous operational thermal recharge has a lower flow rate than the other 2 doublets. The same recommendation can be repeated for the other doublets when they are under operational thermal recharge^{*1}. The discontinuous operational thermal recharge for the first doublet set will start from 2036 to 2077 and the discontinuous operational thermal recharge for the second doublet will start from 2077 to 2094. Furthermore, the discontinuous operational thermal recharge for the third doublet will start from 2094 to 2111 which will be followed by the discontinuous operational thermal recharge for the first set of doublet again. The doublet under operational thermal recharge must have the biggest number of shut-off periods. The planned switch between opening the doublets for operation and shutting the doublets for operational thermal recharge is tested with a prerequisite of 6, 4 and 3 months to switch between opening and shutting-off for each doublet. A possible safety issue can take place in the KKP field with a prerequisite of 6 and 4 months to switch between opening and shutting-off for each doublet. The table below shows the planned switch between opening the doublets for operation and shutting the doublets for operational thermal recharge^{*1} with a prerequisite of 3 months to switch between opening and shutting-off for each doublet. The following Jafer matrix prohibits the KKP field to have 5 successive periods of continuous operation (open doublet) due to the second type constraint which is related to safety.

Period (From the start datum to the end datum)	First doublet set (KKP-GT-02/KKP-GT-01/KKP-GT-03)	Second doublet (KKP-GT-04/KKP-GT-05)	Third doublet (KKP-GT-04/KKP-GT-05)
From 1-January- 2036 to 31 March-2036	Open (For operation) [1]	Open (For operation) [1]	Shut-off (For operational thermal recharge ^{*1}) [0]
From 1-April-2036 to 30-June-2036	Open (For operation) [1]	Shut-off (For operational thermal recharge ^{*1}) [0]	Open (For operation) [1]
From 1-July-2036 to 30-September-2036	Open (For operation) [1]	Open (For operation) [1]	Shut-off (For operational thermal recharge ^{*1}) [0]
From 1-October-2036 to 31-December-2036	Shut-off (For operational thermal recharge ^{*1}) [0]	Open (For operation) [1]	Open (For operation) [1]
From 1-January- 2037 to 31 March-2037	Shut-off (For operational thermal recharge ^{*1}) [0]	Open (For operation) [1]	Open (For operation) [1]
From 1-April-2037 to 30-June-2037	Shut-off (For operational thermal recharge ^{*1}) [0]	Open (For operation) [1]	Open (For operation) [1]
From 1-July-2037 to 30-September-2037	Shut-off (For operational thermal recharge ^{*1}) [0]	Shut-off (For operational thermal recharge ^{*1}) [0]	Open (For operation) [1]
From 1-October-2037 to 31-December-2037	Open (For operation) [1]	Open (For operation) [1]	Shut-off (For operational thermal recharge ^{*1}) [0]
From 1-January- 2038 to 31 March-2038	Open (For operation) [1]	Shut-off (For operational thermal recharge ^{*1}) [0]	Open (For operation) [1]
From 1-April-2038 to 30-June-2038	Open (For operation) [1]	Shut-off (For operational thermal recharge ^{*1}) [0]	Open (For operation) [1]
From 1-July-2038 to 30-September-2038	Open (For operation) [1]	Open (For operation) [1]	Shut-off (For operational thermal recharge ^{*1}) [0]
From 1-October-2038 to 31-December-2038	Shut-off (For operational thermal recharge ^{*1}) [0]	Open (For operation) [1]	Open (For operation) [1]

Table 23: shows the planned switch between opening the doublets for operation and shutting the doublets for operational thermal recharge in the case of the KKP field development with a prerequisite period of 3 months to be able to switch between opening and shutting-off for each doublet (discontinuous duration) and the cooling rate constraint of not exceeding a period of 1 year for opening the doublets in term of continuous operation.

Besides knowing that the discontinuous shut-off is the optimal strategy in terms of energy output, it is also necessary for obtaining a lower cooling rate than the continuous and low-pressure gradient strategies. The discontinuous shut-off can start as soon as the 3 doublets can exist in the Koekoekspolder geothermal field but in this research study and according to the plan provided by the owner to drill an extra doublet from 2027, it is assumed that the discontinuous shut-off will start from 2036. As depicted in table 23, we can overcome the high cooling rate problem by discontinuous shut off based on months (a period of 3 months to be able to switch between opening and shutting-off) and not yearly basis if we need to stick with the plan of an injection temperature of 20°C from 2036.

4.4 Energy demand fulfilment using the discontinuous shut-off operation:

Before the start of the discontinuous shut-off in 2036 and by upholding the bottom hole pressure constraints, the energy demand can be fulfilled from 2027 either by increasing the flow rate with a higher injection temperature to avoid a high cooling rate or to decrease the injection temperature with relatively low flow rates but with a risk of high cooling rate, especially before the counter cooling rate effect of discontinuous shut-off operation of the doublets. The generated extractable energy of the updated thermal model is affected by the injection temperature. The updated development strategy is tested by an injection temperature of 20°C, 25°C, and 30°C to analyse the energy supply according to the energy demand.

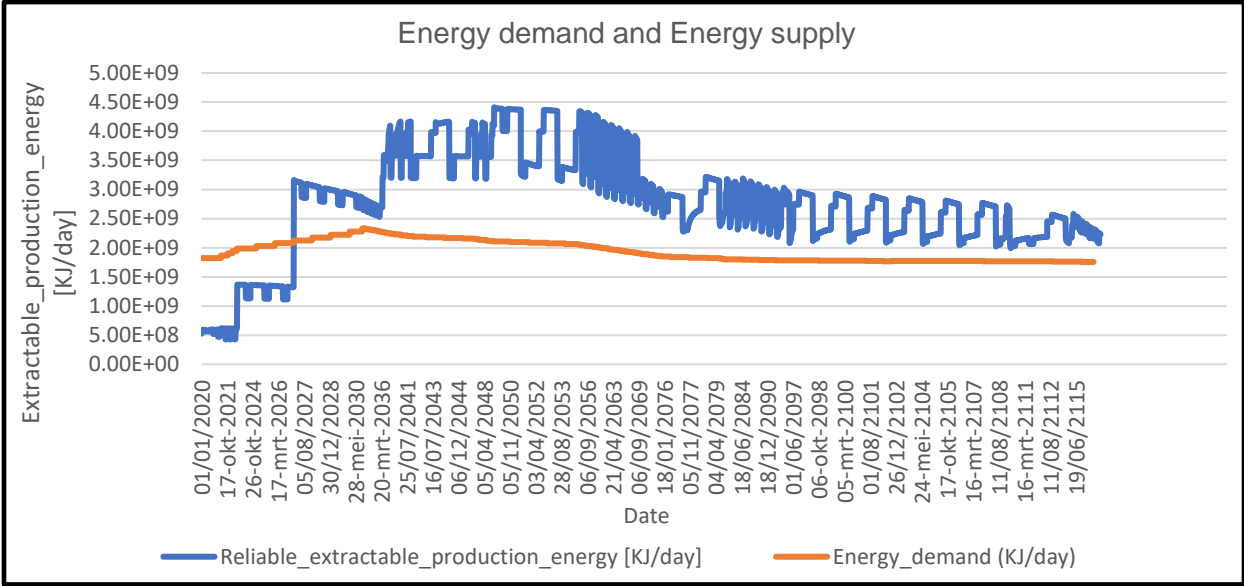


Figure 34: shows the predicted extractable production energy and the energy demand from 2020 to 2121 after applying the optimal discontinuous forecasting scenario for the development strategy using an injection of 30°C from 2024 to 2036 then an injection around 20°C from 2036 to 2121.

4.5 Well placement and stored energy distribution:

The extractable energy supply results from 2021 to 2121 in figure 34 are based on the initial planned doublets locations and the current locations of the first set of doublets (First set of doublet: KKP-GT-01/ KKP-GT-02/ KKP-GT-03, Second doublet: KKP-GT-04/ KKP-GT-05, Third doublet: KKP-GT-06/ KKP-GT-07) as shown in figure 35.

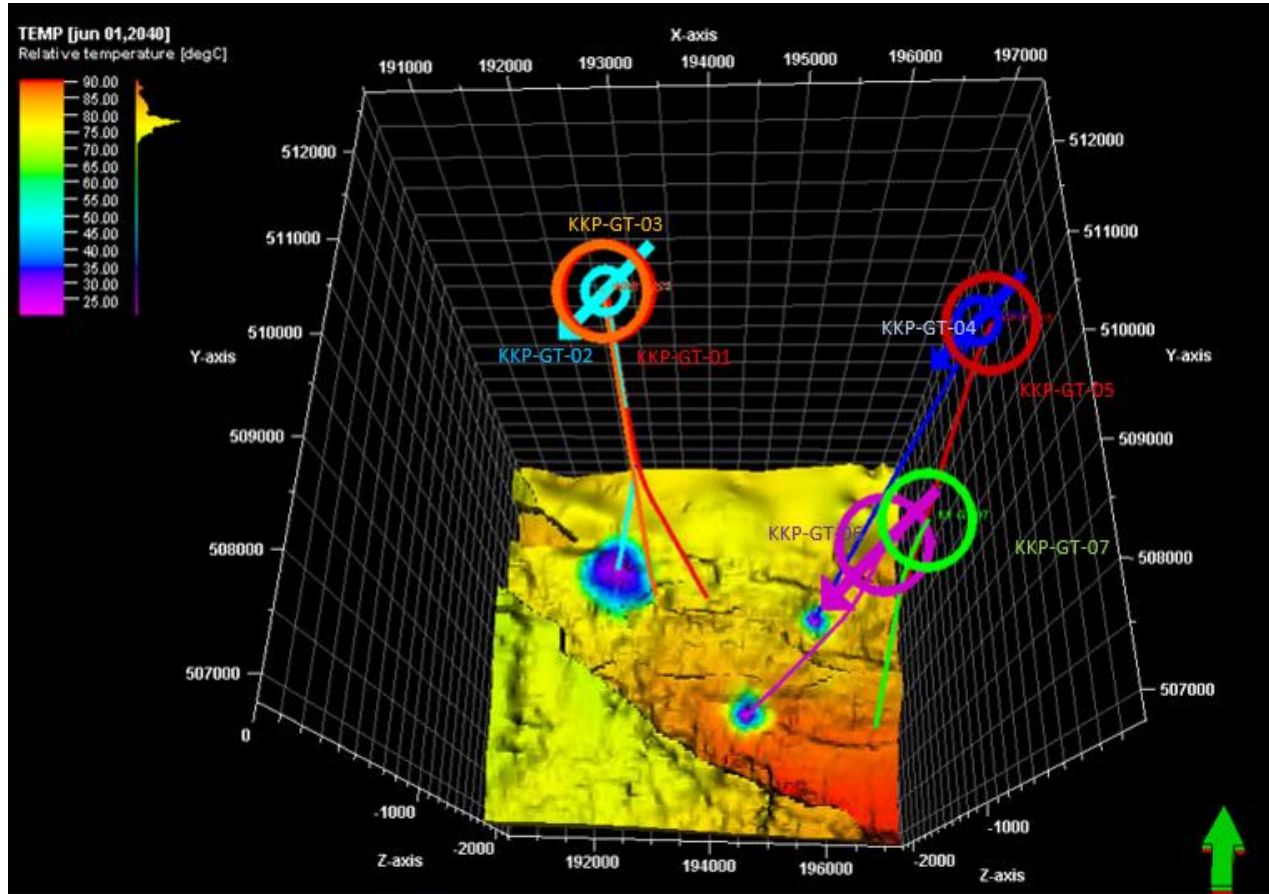


Figure 35: shows the temperature distribution on the 1st of June 2040 of the updated thermal model with the initial planned doublets locations and the current locations of the first set of doublets as well as the planned wells trajectories.

The temperature in the south-western part of the model is lower than the rest of the model because this part of the model is considered the hanging wall of the main fault SE-NW. This south-western part of the Slochteren aquifer is at a lower depth than the rest of the reservoir which means a lower temperature area that ranges on average from 60°C to 72°C.

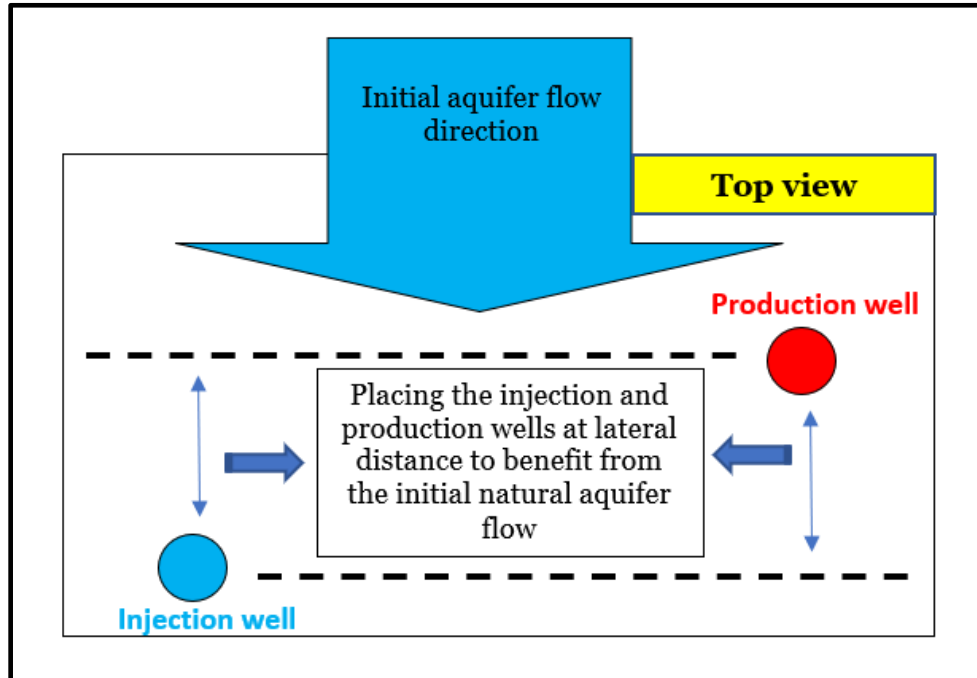


Figure 36: shows a top view theoretical sketch to emphasize how the operator can take advantage of the initial aquifer flow in the geothermal field.

Based on the concept illustrated by the sketch above in figure 36, alternative locations of KKP-GT-04, KKP-GT-05, and KKP-GT-06 are introduced to take advantage of the possible natural aquifer flow in the aquifer as shown in figure 36. When both the direction and velocity of the aquifer natural flux are taken into consideration, it is more efficient to put the injector toward the southern direction and the producer toward the northern direction to increase the lateral distance between them, to benefit from the natural aquifer velocity and direction. The natural aquifer flow in the KKP field is considered low flow because it has a small velocity.

After the year 2121, there will be recoverable energy areas, especially in the northern area which can be consumed. Based on the temperature distribution on 1st January 2121 especially around KKP-GT-04 and KKP-GT-05 as illustrated in figure 37, the effect of the initial aquifer velocity on the geometry of cold front propagation is more dominant around the production wells areas. This is why the shape of the cold front propagation and energy pattern around the production wells is different than near the injection wells.

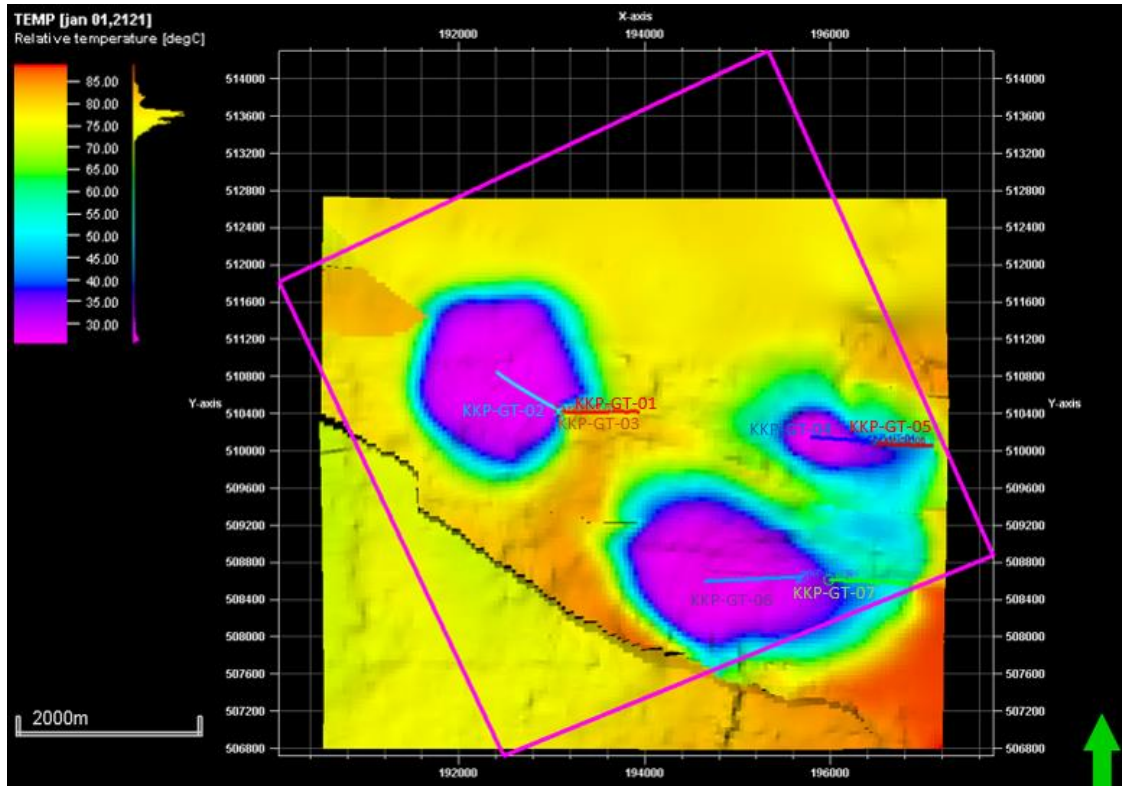


Figure 37: shows the temperature distribution of the updated thermal model on 1st January 2121 in the koekoekspolder concession boundaries indicated by the purple square.

As seen in figure 37 on 1st January 2121, the temperature distribution only at the south-eastern part outside the KKP field boundaries will be affected by the optimal geothermal development strategy suitable for the KKP field using the initial locations of the injection well KKP-GT-06 and the production well KKP-GT-07. The locations of the planned injection wells in the KKP field are chosen carefully to avoid significant depletion of another possible geothermal field next to the KKP field, the alternative location of KKP-GT-06 and KKP-GT-07 can be chosen as in the following table to avoid any thermal depletion of areas outside the KKP field concession area. The horizontal distance of the affected area outside the KKP concession is equal to 620.058 m, this is why the wells must be shifted with preserving the same distance of 2103.34 m between the injection and production wells.

Alternative possible Third doublet location	Coordinates at aquifer depth	Depth	Covered Thickness
Injection well (KP-GT-J6)	X= 194300.52 m/ Y = 508806.91 m	2136.81 m	71.1 m
Production well (KP-GT-J7)	X = 196283.35 m/ Y = 508878.82 m	2099.47 m	52.98 m

Table 24: Information related to the possible third doublet.

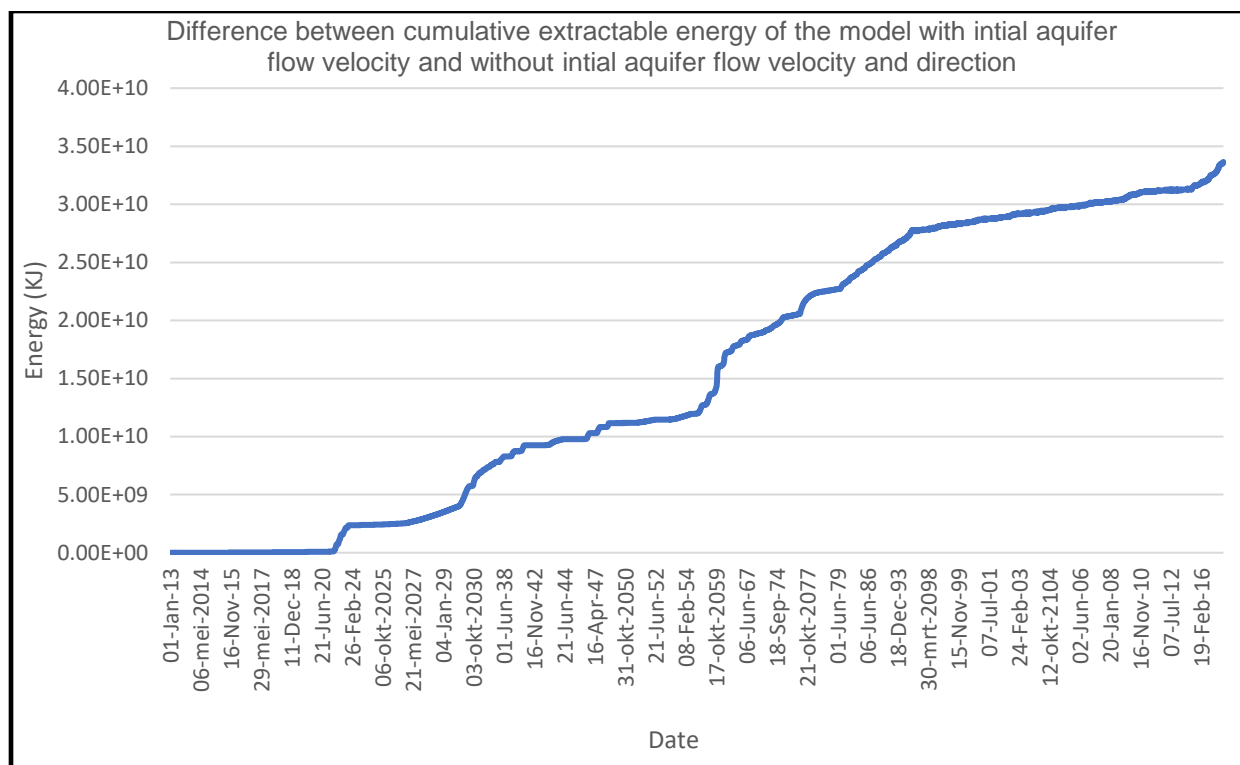


Figure 38: shows the difference between the simulated extractable cumulative energy of the model with natural aquifer flow and the model without natural aquifer flow.

The current location of the second production well “KKP-GT-03” which has been drilled since 28/05/2022 based on 2D seismic data could have an alternative better location for KKP-GT-03 as shown in table 9. Therefore, the realistic 3D geothermal reservoir modeling derived from seismic data is very crucial in optimizing the koekoekspolder field.

For instance, the planned current coordinates of the KKP-GT-03 were not the ideal location and instead of KKP-GT-03 location, an alternative location could be chosen such as the location of the hypothetical production well “KKP-GT-BB3” based on the results of forecasting scenarios. Moreover, the position of the new doublet can help in maintaining the production of an economical bottom hole temperature in “KKP-GT-BB3” for a longer period. A slight increment in the cumulative production energy is noticed over the long term in the case the initial velocity of the natural aquifer flow is taken into account. If the hypothetical and alternative second production well “KKP-GT-BB3” is chosen instead of the current second production well “KKP-GT-03”, the net present value will increase especially because of the depth of “KKP-GT-BB3” is lower than the depth of “KKP-GT-03” (Which means lower drilling costs). Therefore, it is significant to optimize the locations of the geothermal wells based on a 3D geothermal model to choose the best locations for the new wells.

5.Sustainability & Optimization

5.1 **Direct & Indirect factors on geothermal sustainability:**

The intake temperature at the bottom of the producer well is equal to 76.4 °C while the temperature at the surface before reaching the separator is equal to 74.3 °C which means that there is 2.1°C heat loss. Minimizing the heat loss in the injector and the producer wells can have a direct effect on the sustainability of heat extraction. According to the permit holder of the Koekoekspolder field, the minimal economical temperature is equal to 55°C. Therefore, planning either well-studied discontinuous shut-offs for the wells before reaching a non-economical produced water temperature or a continuous shut-off of the doublet after a non-economical produced water temperature or a predicted severe depletion due to cold fronts intersection can help in adequate operational thermal recharge^{*1}. The discontinuous shut-off for the wells might be better than the continuous shut-off in terms of maintenance of the doublet because the duration for non-operation will be repeatedly reduced but the continuous shut off might be better than the other shut-off method for short-term revenue and easier in term of field operation. Taking advantage of the natural aquifer properties like the initial aquifer velocity and direction as well as the highest heat anomalies spots of the aquifer can contribute to sustainable field development. In addition, choosing the best optimal locations for the new wells is very crucial in terms of sustainable field development. And to find an optimal sustainable strategy to develop any geothermal field, the doublets must be linked together in a certain way that allows systematic recharge without a contradiction to maintain the desired and predicted target ongoing with the lowest amount of investment as indicated in chart 5.

5.2 **Ranking of different optimized scenarios:**

Based on the forecasting results of the model, crucial decisions should be taken to operate the KKP field and to tackle the expected problems to get the maximum output energy of the subsurface by choosing the best realistic and optimal scenario. In order to choose the optimal development scenario for the entire field, the optimal operational scenario between the first 2 wells and the third production well (KKP-GT-03) must be first obtained then the optimal operational scenario between the current and the possible new doublets is to be achieved. The current production well KKP-GT-03 will have an economical heat production period lower than that of the first production well “KKP-GT-01”. On the other hand, this non-economical period of operation for heat production in KKP-GT-03 can indirectly contribute to the retardation of the arrival of the cold front to the first production well KKP-GT-01. In the case of KKP-GT-03 presence, the optimal operational scenario for the first 3 wells is achieved by the simulation case which distributes the flow among the producers with a 25% for KKP-GT-03 and 75% for KKP-GT-01. The 2 parameters that are chosen to determine what is the optimal forecasting operational thermal recharge strategy are the lifetime of the doublet in terms of economical output temperature and the extractable energy as well as the cooling rate of the wells. Among the different unconventional thermal development approaches such as the continuous shut-off operation and the low-pressure gradient operation, the discontinuous shut-off strategy for doublet operation showed the optimal way to develop the field as shown in table 25.

Geothermal development strategy types	Profit ranking	Safety ranking
Continuous shut-off operation	Moderate in term of profit	Lowest (worst) in term of safety (Highest cooling rate per year)
Discontinuous shut-off operation	Highest (best) in term of profit	Highest (Best) in term of safety (Lowest average cooling rate per year)
Low pressure gradient	Lowest in term of profit	Moderate (Almost lowest) in term of safety because it generates as well high average cooling rate per year.

Table 25: shows the ranking between the different types of geothermal development strategies tested in this research study.

5.3 Optimal field operation:

The Optimal strategy with an injection temperature of 30°C from 2024 to 2035 and an injection temperature of 20°C using the discontinuous shut-off from 2036 to 2121 needs a few adjustments as follows:

- 1) the total injected flow rate from 2027 to 2030 needs to be decreased by 500 m³/day. Whenever higher extractable energy than the energy demand is predicted, the permit holder can decrease the flow rate to preserve the energy for later unexpected energy demand anomalies.
- 2) an alternative location of KKP-GT-06 and KKP-GT-07 as mentioned in table 24 can be chosen to avoid any depletion of areas outside the Koekoekspolder field.
- 3) The “Jafer matrix for discontinuous shut-off operation to overcome high cooling rate with the least number of doublets” concept as shown in table 23 needs to be applied to the optimal development strategy in this research study from 2036 to 2121.
- 4) The concept of the optimal development strategy is flexible. For instance, if the owner of the field wants to fulfill the energy demand before 2027 then he can start earlier than 2027 drilling the other 2 doublets.

6. Effects of subsurface geothermal engineering

Effective, secured, and sustainable heat production requires the operator to avoid any major risks such as induced or triggered earthquakes resulting from reaching and exceeding the critical injection pressure or from the thermo-elastic stresses that reactivate major faults. In this section, the possible causes and risks that can induce seismicity in the KKP geothermal field are reviewed and assessed to reach a truly sustainable production by avoiding these causes to ensure safety for surface facilities and buildings around the KKP field geothermal site. There are different risks that needed to be studied in the case of the Koekoekspolder geothermal field which can be summarized by the following chart.

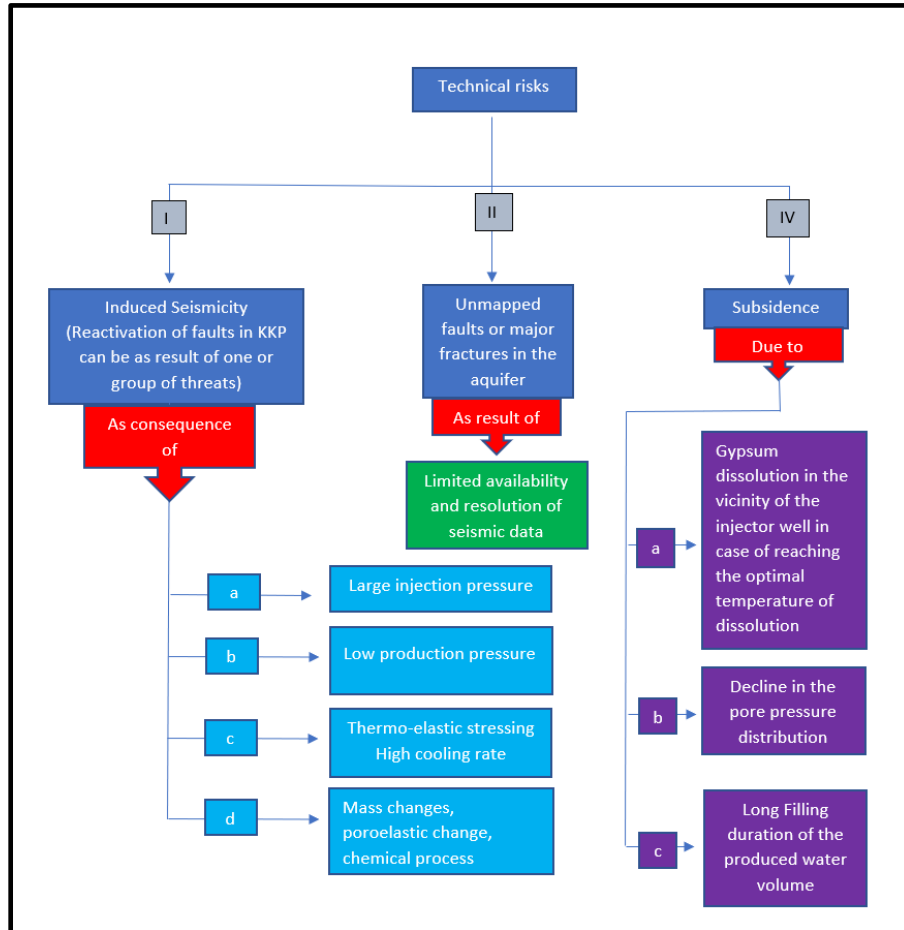


Chart 6: represents the possible technical risks and their causes.

There are expectations from the operator to reduce risks by following all possible measures to meet project goals. Therefore, there are several measures the owner of the field must take into consideration to avoid the technical risks shown in chart 6 and they are:

- 1- Avoid injection of brine water into the Slochteren aquifer with temperatures less than 30°C until operating the doublets with discontinuous shut-off to overcome the high cooling rate as a result of an injection temperature equal to 20°C.
- 2- Operating the field with Bottom hole pressures that don't exceed a maximum injection pressure of 252 bar according to SodM and a minimum production pressure of 153 bar.
- 3- Seismic monitoring regularly and especially when there is a shift in operational parameters like the flow rates and bottom hole pressures to prevent any escalation of possible threats.

- 4- Regular monitoring of the chemical composition of the produced water at the current and future production wells as well as comparing the currently produced water chemical composition with the initial water composition at the well name “KKP-GT-01” to understand if chemical dissolution of gypsum bodies is taking place or not.
- 5- Reducing the filling duration⁶ of the produced brine water.
- 6- Using the coordinates and well designs as in this research study and/or designing wells trajectory that don’t interfere with the faults plan in the Koekoekspolder field.
- 7- It is recommended to change the location of the third production well “KKP-GT-03” not only because it is not feasible by comparing it to other development scenarios in this research study but also because the location of the planned well “KKP-GT-03” at the reservoir level is very close to the fault KKP 1 as shown in the figure below. {Distance between the third production well “KKP-GT-03” and the nearest fault KKP 1 is around 108.883 meters}.

7. Feasibility study

To conduct a reliable economical model, all expenditures and revenues after applying depreciation value and discount rate from 2013 to 2121 must be taken into consideration. This feasibility study assumes that there are no Abandonment Expenditures (AbEx) to achieve sustainable operation of the KKP field. This feasibility study is based on the optimal development strategy for the KKP field so far. The steps used to create an economical model from 2013 to 2121 are (Van Wees *et al.*, 2012; Daniilidis, Nick and Bruhn, 2020; Zaal, 2020) :

- a- Predicting the reliable revenues
- b- Computing the capital expenditures (Capex)
- c- Calculating operational expenditures (Opex)
- d- Obtaining the pure profit in terms of net to present value

7.1 Predicting the reliable revenues:

The energy injection cumulative is subtracted from the energy production cumulative to obtain the cumulative extractable energy production. Based on the extractable cumulative energy rate of the optimal scenario, the revenue can be obtained from 2013 to 2121. The heat energy price in the Netherlands according to the Authority for Consumers and Markets (ACM) for 2022 is equal to 53.95 euro inclusive tax for every 1 GJ (Eneco, no date).

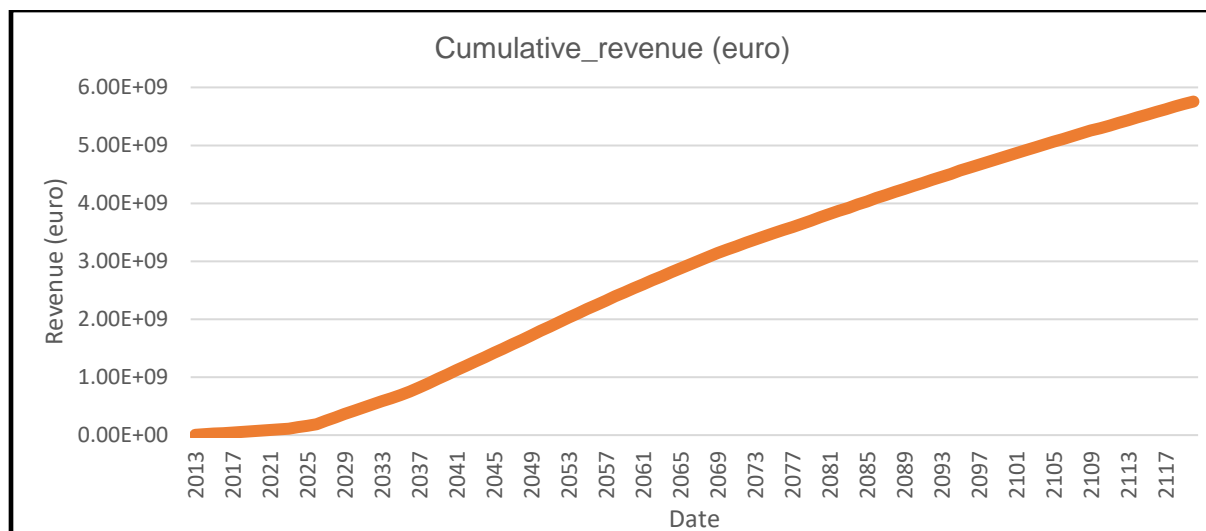


Figure 39: shows the cumulative revenue based on the current heat prices.

In the Netherlands, when the prices of gas and electricity increase, the heat prices escalate (Eneco, no date). This is why it is very difficult to predict what will be the heat prices in the future. It is predicted that the prices of electricity and heat according to high prices scenarios will remain more or less high till the end of 2030 after which they will decline due to the growing availability of renewable energy (Afman, Maarten Hers, Sebastiaan Scholten, 2017). A clever idea that determines the relation between the electricity price and the heating price can be implemented in case of a lack of forecasting scenarios of heat prices. The electricity price is equivalent to 0.247 euros for every 0.0036 GJ (GlobalPetrolPrices, 2022), or 68.611 euros for every 1 GJ. The relation between the heating price and electricity price is as follows.

$$(10) \quad HP = 0.786317 * EP$$

Where HP is the Heat price, 0.786317 is a constant derived from the relation between the current heat and electricity prices, and EP denotes the Electricity price.

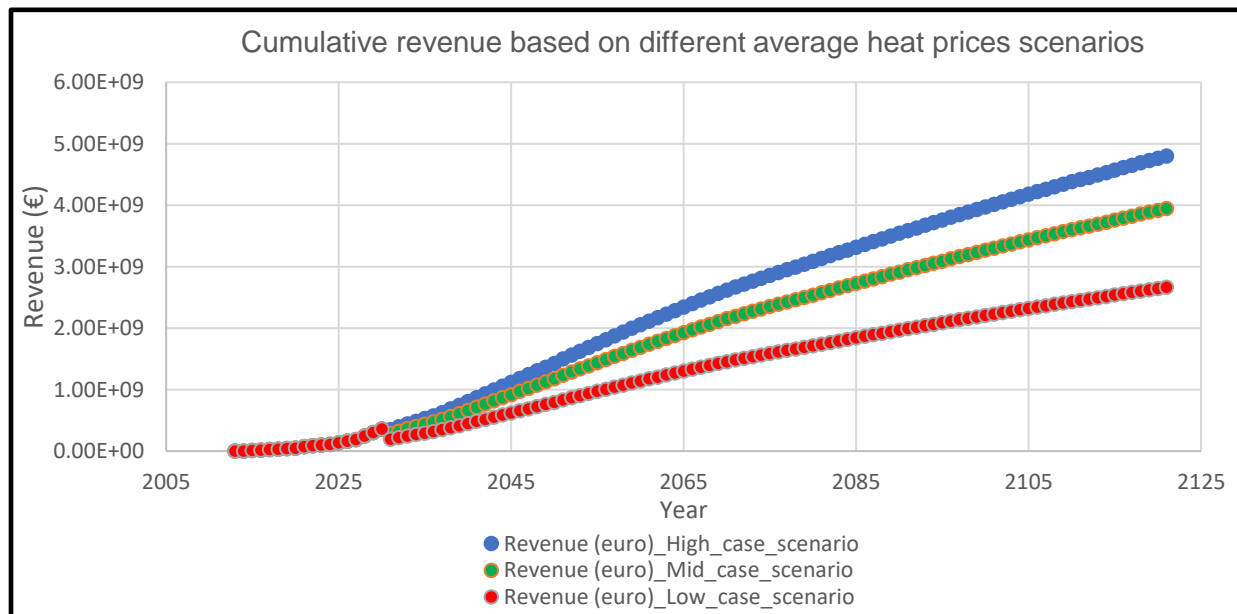


Figure 40: shows the cumulative revenue based on different scenarios for the average heat prices.

The revenue of the KKP field according to the optimal geothermal development strategy is based on 3 scenarios for the average heat price due to the wide range of uncertainty related to the predicted heat prices from 2023 to 2121. As shown in figure 40, there is a steep decline (Kink) in the revenue of the low case scenario due to the heat price projections assumption for every 1 GJ that will decrease from 53.95 euros to 37 euros in the case of Mid case scenario (31.41% decrease in heat prices) and from 53.95 euros to 25 euros in case of Low case scenario (46.3392% decrease in heat prices) as well as from 53.95 euros to 45 euros in case of High case scenario (16.589% decrease in heat price) in the period from 2031 to 2121.

7.2 Computing the capital expenditures:

The capital expenditures (Capex) costs include the well costs as well as other installation costs such as construction, site preparation, and equipment like pumps (*ThermoGIS*, no date). Also, the capital costs include research and exploratory phase costs that vary in total between € 135000 to € 460000 (van den Bosch, Flipse and Vorage, 2013; Zaal, 2020). It is assumed that the capital costs related to the research and exploratory phase are around € 460000. The

drilling costs of the new planned wells (KKP-GT-03 / KKP-GT-04 /KKP-GT-05 /KKP-GT-06 /KKP-GT-07) can be computed using the following relation (*ThermoGIS*, no date).

$$(11) \quad C_{drilling} = 375000 + 1150MD + 0.3MD^2$$

The following table shows the drilling costs of each well and the total drilling costs that are required for the Koekoekspolder field.

Well name	Measured depth (meters)	Well CAPEX(x 10 ⁶)[M€]
KKP-GT-01	2258	4.5012692
KKP-GT-02	2205.30	4.370099427
KKP-GT-03	1932.53	3.71781116
KKP-GT-04	2126.23	4.176420704
KKP-GT-05	2210.81	4.383735757
KKP-GT-06	2227.42	4.424952957
KKP-GT-07	2221.91	4.411261714
Total		29.98555092

Table 26: shows the drilling costs of each well and the total drilling costs of the configuration of the primitive wells.

The drilling costs that are required for the KKP field with an alternative positions for wells is more expensive than the drilling costs of the primitive wells. The other capital costs include drilling location and surface facilities costs such as pumps and ESP. The drilling location costs are the costs related to the placement of production facilities and buildings and these costs as well as preparation, installation and drilling on the particular location (Zaal, 2020). The total drilling location costs range from € 150000 to € 300000 (van den Bosch, Flipse and Vorage, 2013). An average value of € 225000 is chosen for the 7 predicted drilling locations. For the geothermal wells in the Netherlands, an average ESP lifetime of about 5 years is predicted (Van 't Spijker and Ungemach, 2016). The initial costs of the Electrosubmersible pump are taken into account while the replacement costs are included in the operational expenditures. Based on the estimated costs of ESP (van Dongen, 2019; Zaal, 2020), the estimated costs for the ESP of the future production wells (KKP-GT-05 and KKP-GT-07) are assumed to have a high capacity which means that the estimated cost for each ESP is equal to 1200 k€ while the ESP for KKP-GT-01 is assumed to be 1000 k€ and 800 k€ for KKP-GT-03 production well. The surface facilities consist of an injection pump, circulation pump, screens, and filter as well as a heat exchanger (Zaal, 2020). The costs of surface facilities are between € 500000 as the minimum and € 1500000 as the maximum amount (van den Bosch, Flipse and Vorage, 2013). The value of surface facilities is considered to be € 1500000 for each doublet.

Capital Item	Capital costs	Number of items	Total costs
Drilling location	€ 225000	7	€ 1575000
ESP for KKP-GT-01	1000 k€	1	€ 1000000
ESP for KKP-GT-03	800 k€	1	€ 800000
ESPs for KKP-GT-05 and KKP-GT-07 production wells	1200 k€ each	2	€ 2400000
Surface facilities for every doublet	€ 1500000	3	€ 4500000

Table 27: shows the other capital expenditures costs.

7.3 Calculating Operational expenditures:

The operational expenditure can be divided into **Fixed operational expenditures** and **variable operational expenditures**. **The fixed Operational costs** include maintenance costs (For example repairing cost of the geothermal wells and pump replacement every number of years), workover costs (company consultancy is included), insurance, price of renting facilities, staff payment, and insurance costs (Zaal, 2020). One of the main ESP Opex costs is the ESP replacement costs that varies between 35 k€ and 60 k€ per year (Van 't Spijker and Ungemach, 2016). The Opex costs are estimated and assumed to be around 5 % of Capex costs (Zaal, 2020). The electricity price in the Netherlands in 2022 for business purposes is equal to 0.247 euros for every 1 KWh [(GlobalPetrolPrices, 2022)]. **The variable Opex costs** include the electrical energy needed for the ESP and injection pump (Zaal, 2020). By assuming that the total consumed power of the ESP pump is around 605 KW (Van 't Spijker and Ungemach, 2016) which is around 5.2272×10^7 KJ/day and 19079.28 GJ per year for every ESP pump. The ESP pump during operational thermal recharge^{*1} periods will work only for certain wells and the other wells will be shut. Furthermore, the electrical energy required for the operations of the injection pumps is obtained from knowing the pump power calculated using the following equation (Van 't Spijker and Ungemach, 2016; Zaal, 2020).

$$(12) \quad P_{pump} = \frac{Q \Delta P}{\eta}$$

Where P_{pump} : power needed for the pump (W), ΔP : pressure difference between ESP, and injector (Pa), Q : volume flow rate (m^3/s) and η : pump efficiency (an overall pump efficiency is considered to be around 65% as a starting point (Van 't Spijker and Ungemach, 2016; Zaal, 2020))

The following steps are used to compute the variable Capex related to the required electrical energy of each injection pump from 2013 to 2121:

- I- Distributing the flow rates in (m^3/day) predicted from the optimal geothermal development strategy of each injection well (KKP-GT-02 / KKP-GT-04 / KKP-GT-06) from 2013 to 2121 by taking into consideration that there are discontinuous shut-off planned for the injection wells over the whole development period.
- II- Multiplying the summer and winter flow rates of each year from 2013 to 2121 by 273 and 92 days to obtain the flow rates in ($m^3/year$).
- III- Converting the flow rates of each year from ($m^3/year$) to (kg/s).
- IV- Calculating the average predicted pressure difference between the wellhead above ESP and the injection well based on the relationship between THP and flow rates.
- V- Computing approximately the yearly required power in watts for each injection pump and ESP pump then computing the costs of the required electrical energy from 2013 to 2121 based on the estimated heat price obtained from equation (10).

By using equation (10) and based on the mid-case scenario of estimated heat prices indicated in section 7.1, the electricity price of the mid-case scenario is around 40 euros from 2013 to 2020 and 53.95 euros from 2021 to 2030 then 37 euros from 2031 to 2121. The estimated tubing head pressure of each injection well is obtained based on applying several iterations of the suitable Tubing head pressure value that generate the available simulated and predicted BHP with taking into consideration the corresponding flow rates and the pressure drop relation shown in equation (8) as well as the density and viscosity of the brine water. The relation between measured tubing head pressures and calculated bottom hole pressure is used to compute the rest of the tubing head pressures based on the available estimated bottom hole pressures. The same procedures are applied on the other injection wells "KKP-GT-04" and "KKP-GT-06". The estimated ESP pressure of each production well is obtained based on applying several iterations of the suitable ESP difference in pressure value that generates the available simulated and predicted BHP with taking into consideration the corresponding flow

rates and the pressure drop relation shown in equation (8) as well as ESP depth, density, and viscosity of the brine water. The ESP pressure is computed based on the flow rate assuming that the wellhead pressure is equal to 2.30 and the ESP depth is around 413 with no constraints on the difference in ESP pressures for all production wells. The ESP pressure is computed based on the tubing head pressure relationship with flow rate. This relationship is applied to obtain the tubing head pressure of the other wells due to the same well diameter and ESP depth. After computing the estimated required electrical power for the KKP field injection and ESP pumps, the costs of the required electrical energy for the KKP field injection and ESP pumps can be obtained based on the mid-case scenario for energy prices.

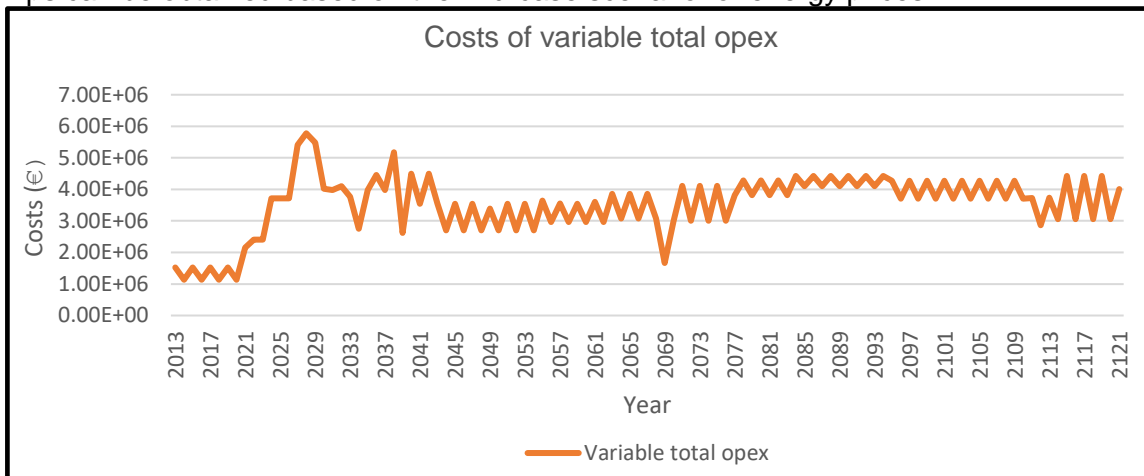


Figure 41: shows the total variable operational expenditures estimated for the KKP field based on the mid-heat price scenario.

In figure 41, the cost of total variable operational expenditures is related to the electricity price. This is why the highest values of total variable Opex are in the period between 2021 and 2030 because of the electricity price variation.

7.4 Obtaining the pure profit in term of net to present value:

The subsidy can be valid for 15 years. The reference heat price expected is around 0.051 euro for every 1 KWh, and any heat price below this value for 15 years will be recompensated and covered by the SDE+ amount for geothermal energy (*ThermoGIS*, no date). The subsidy can be included for 15 years in case of extremely low case scenario for heat prices with a reference heat price of 10.6111 euro for every 1 GJ based on a subsidy of € 0.0380/ KWh (RVO, 2020). However, the average heat price of the low case scenario is around 25 euros from 2031 to 2121 which is predicted to be above the reference heat price of 10.6111 euro for every 1 GJ.

Therefore, the subsidy is not taken into consideration in the very low case scenario. The depreciation value indicates how much an asset value has been utilized over a certain period (TUOVILA, 2022). The discount rate represents the interest rate utilized in Discounted Cash Flow (DCF) analysis to decide the present value of future cash flows (MAJASKI, 2022). The cash flow can be calculated simply by subtracting all expenditures from the revenue plus subsidy in case of heat prices are less than the reference heat price. The cash flow in this research study is calculated without taking the depreciation value into account. The cash flow and both fixed and operational expenditure are represented in a cumulative pattern to be able to subtract the cumulative expenditure from the cumulative revenue. First, the capital expenditures and the total variable opex are converted to a cumulative pattern then the fixed opex is computed based on the cumulative capex from 2013 to 2121.

The discounted Cash Flow (DCF) can be calculated using the following equation (Zaal, 2020):

$$(13) \quad DCF_cumulative = \sum_{t=0}^n \frac{C_t}{(1+r)^t}$$

Where C_t : cashflow generated at time t (Euro), r : Yearly discount rate [-], t : Duration of time (total number of years = 108) from the start of the project, n : number of years, r and t must have the same basis (either monthly or yearly basis).

The inflation rate is assumed to be equal to 2% from 2028 to 2030, then 1.12 % from 2031 to 2121 due to the rise in the infeed of renewable energy from 2031 (Afman, Maarten Hers, Sebastiaan Scholten, 2017). From 01/05/2004 to 31/12/2006, the discount rate in the Netherlands was varying between 3.70 % to 4.43 % (European Commission, no date).

Period	Discount rates	Motivations
From 2013 to 2030	Assumed to be 4 %	By knowing that the social discount rate of the European commission is 4 % (Farmer and Russi, 2018), and based on (Energy Education, 2019).
From 2031 to 2050	Assumed to be 4.5%	
From 2051 to 2121	Assumed to be 4.7 %	Furthermore, the discount rate is assumed to be around 4.7% from 2051 to 2121 due to the expected increase in renewables energy supply which will probably lead to lower energy prices and probably a lower inflation rate (Afman, Maarten Hers, Sebastiaan Scholten, 2017).

Table 28: shows the discount rates assumed for the KKP field and their motivations.

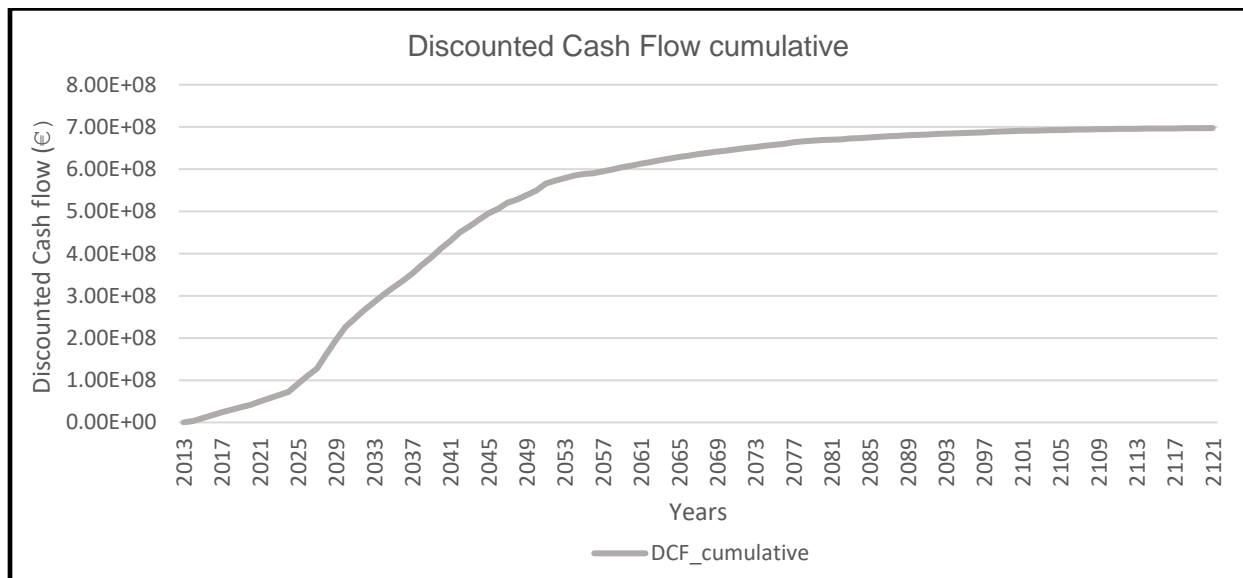


Figure 42: shows the mid-case scenario cumulative discounted cash flow estimated for the KKP field from 2013 to 2121.

In figure 42, the discounted cash flow will probably have a steep increase from 2027 to 2052 due to the high heat price in this period as previously indicated then the discounted cash flow will probably have a lower discounted cash flow pattern. The peak value of the cumulative discounted cash flow is in the year 2121. Thereafter, the cumulative net present value (NPV_cumulative) can be generated by subtracting the cumulative Capex and Opex from the cumulative discounted Cash Flow (DCF_cumulative) (Zaal, 2020) as shown in equation 14.

$$(14) \quad NPV_{cumulative} = DCF_{cumulative} - Investment\ costs$$

The investment costs include all current and estimated expenditures.

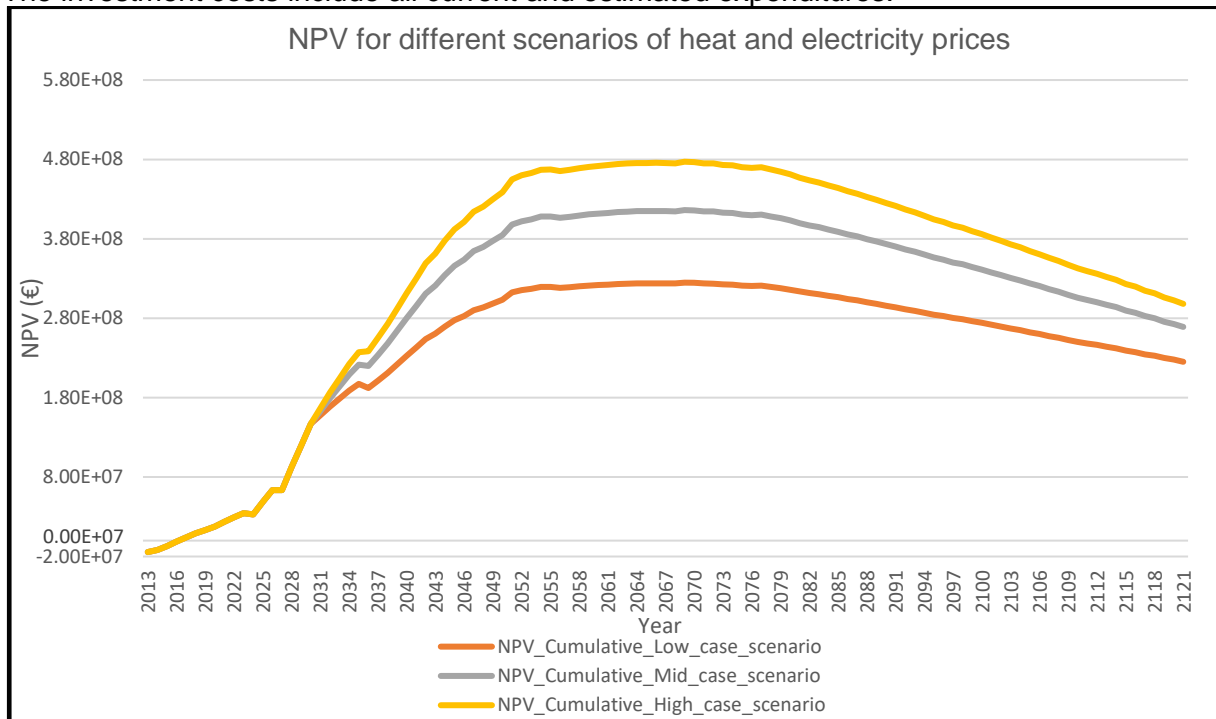


Figure 43: shows the cumulative net present value from 2013 to 2121 for different scenarios of heat and electricity prices.

According to the NPV results of the mid-case scenario as shown in figure 43, it is profitable and worth to developing the field according to the assigned optimal development strategy. Based on the sustainable optimization conducted in this research study on the KKP field , there is no contradiction between sustainable development of KKP field and long term revenue. The cumulative net to present value is predicted to be positive which means profitable from January 2018 to January 2121. However, the net to present value has a steep decrease from the beginning of 2079 to 2121 due to several reasons as:

- 1- Expected heat price decrease
- 2- Cumulative electricity purchase price

The owner of the field cannot control the first reason (Expected heat price decrease). But the owner of the field can control the second reason (Electricity purchase price) in terms of buying renewable sources of electricity such as solar panels which can contribute to decreasing the total variable opex costs. Thus, a higher net to present value can be achieved. According to the addressed assumptions in this study, the owner of the field might choose to stop the project in the year 2079 because the net-to-present value will probably start declining which means that if the project is continued the commercial entity will lose money. However, financial incentives, not accounted for in the addressed assumptions, might make the process profitable for the whole period. The period between 2013 to 2018 has a negative NPV because of the initial capital and operational expenditures. The NPV value for the simulation cases with natural aquifer flow is slightly higher than the NPV without natural aquifer flow due to the expected higher cumulative discounted cash flow as a result of the difference between their cumulative extractable energy. The mid scenario is used to compare the old wells distribution and the distribution of the alternative wells with a lateral distance that takes advantage of natural aquifer flow direction and velocity. The simulation case with natural aquifer flow and old wells distribution shows higher field cumulative energy than the simulation case with natural aquifer flow and the distribution of

the alternative doublets. In addition, the capital expenditures of the old wells locations are lower than the capital expenditures of the alternative wells locations. As shown in figure 44, the discontinuous shut-off development strategy shows a significant higher net to present value than the continuous shut-off strategy.

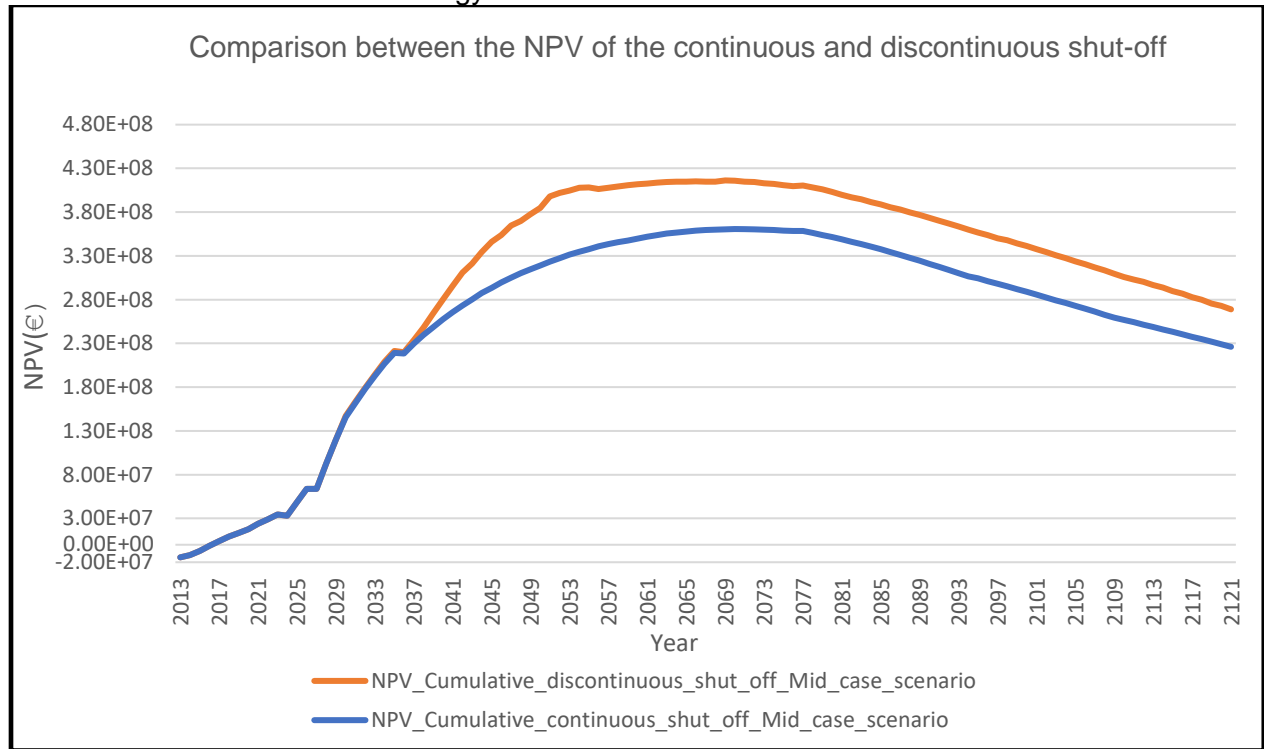


Figure 44: shows the cumulative net present value from 2013 to 2121 of the continuous and discontinuous shut-off development strategy using 3 doublets in total and the second production well “KKP-GT-03”.

The owner of the field can change any economical input or assumption in case there is an update in expenditures, revenues, and subsidy conditions or the interest of the bank if there is a debt to predict the net present value in the future. The NPV can be very promising if the expected discount rates will be lower than the assumed discount rates. The capital expenditures related to the gas separation and burning equipment are not taken into account for this economical model. The Net to present value is expected to be higher because the owner of the field uses the CO₂ volume that is produced from burning the diluted gas in agriculture and the output gas volume is burned to produce extra heat energy as well as the depreciation value of capex that can be added on the revenue is not taken in consideration .

8. Conclusion

The static, dynamic, and thermal models of the KKP field are history matched with high accuracy based on the measured and approximated data to create a robust model that can generate a reliable prediction from 2022 to 2121. The aquifer that is under recharge from different boundary conditions has big potential for heat extraction, and this research study emphasizes the importance and benefits of considering reservoir boundary conditions. The Slochteren geothermal model takes into consideration different boundary conditions such as the

thermal effect of the confining layers and the pinch-out surface like the western thermal boundary as well as the natural aquifer flow velocity and direction. The initial energy content of the aquifer as well as the available energy distribution of the Slochteren aquifer into the KKP field from 2013 to 2121 are obtained using the continuous, discontinuous, and low-pressure gradient geothermal development strategies.

This research study shows that a sustainable and economical heat extraction for the KKP field which can meet the energy demand is possible. The optimal discontinuous shut-off operation from 2036 to 2121 generates a heat supply that fulfills the heat demand and offers a chance to overcome any risk as a result of the high cooling rate. Based on the study related to the effects of geothermal engineering on the subsurface, feasibility study, and the results of the different geothermal development strategies applied to the robust Koekoekspolder model, the long-term discontinuous shut-off operation of the doublets showed an optimal, economical and sustainable development strategy of the Koekoekspolder geothermal field. The KKP field can be sustainably developed using 3 doublets and the second production well of the first doublet "KKP-GT-03" based on the optimization of the number and type of wells as well as the rate and timing at which the heat is extracted, combined with the alignment between subsurface heat extraction and local heat demand. Thus, sustainable situations where heat extraction and thermal recharge of the koekoekspolder reservoir are in balance from 2021 to 2121. The workflow used in this research study to answer the research questions and to tackle the complexity of the KKP field as well as overcome different technical challenges related to this study can be implemented in other geothermal fields.

9.Recommendation

1- As mentioned in section 2.2, the permeability in the NE direction can be higher than in the other permeability direction due to the wind direction during deposition, this is why laboratory studies are needed to prove if this assumption can be considered valid in the reservoir modelling. A new method as taking the resultant of the permeability distribution in the x and y directions {Permeability in NE direction = (Permeability in x direction * cos(45)) + (Permeability in y direction * cos(45))} can be alternative for permeability prediction in the NE direction.

2-A detailed study of the connectivity of the faults zones is needed especially the major faults that connect the Slochteren formation with deeper aquifers due to high reservoir temperature. As well as the hitherto continuous extraction of gas dissolved in the Slochteren aquifer. There is a continuous supply of gas coproduced which is dissolved in the brine water. There are possibilities that the hot gas from the Limburg group migrates through the faults toward Slochteren formation to dissolve in the targeted aquifer and release heat, this is why there should be a comparison between the composition of the Slochteren aquifer and the composition of gas of the Limburg group. The following links show the gas composition map of the Upper Rotliegend group and the Limburg group according to NLOG:

A- https://www.nlog.nl/sites/default/files/gascompro_ce.pdf

B- https://www.nlog.nl/sites/default/files/gascompdc_ce.pdf

The second reason is the composition of gas according to the available NLOG data (https://www.nlog.nl/sites/default/files/gascompdc_ce.pdf), methane and nitrogen take up a big proportion of the total gas composition in the Limburg group in areas near the KKP field which is similar to the gas composition of Slochteren formation in Koekoekspolder field. Moreover, there is a chromatograph analysis of a gas sample in appendix 17.

3- Further studies are needed for the classification of faults that allow migration of gas from the Limburg group based on displacement and horizontal connection (shale smear thickness computation) to be able to understand the flow across faults that are hydraulically connected

and faults that are not hydraulically connected. A relation between displacement and connectivity of the different faulted blocks can be created with the following assumptions:

- When there is a small fault displacement (< the thickness of Slochteren reservoir), the fault most probably will have a good permeability due to the same formation horizontal connection (sandstone connection).
- When there is a big fault displacement (> the thickness of Slochteren reservoir), the major faults will have a very low permeability [no hydraulic connection] because there is (big displacement) and there is no connection with the same sandstone body.

The horizontal permeability across the faults that are not hydraulically connected with the reservoir can be very low while the vertical permeability across the fault can be higher than the horizontal permeability which allows gas inflow from lower layers. (An outcrop with the same reservoir properties could be used as a reference to understand extensively the flow across these faults). The faults that are hydraulically connected probably have a horizontal permeability higher than the vertical permeability because the hanging wall and the foot-wall reservoir section are horizontally more or less connected.

4- More experiments are needed to be conducted to test the cooling rate effect on the stability of the geothermal reservoir to quantitatively determine the maximum cooling rate allowed in the KKP field to determine the maximum cooling rate required for the KKP field not based on just assumptions. The cooling rate can vary from one place to another, it is recommended as well to obtain a representative element value for the cooling rate distribution. If the experiments results showed that 20°C as an injection temperature won't cause any subsurface problems then the optimal development strategy with an injection temperature of 20°C can be used from 2024 to 2121 without the concept of the "Jafer matrix for discontinuous shut-off operation to overcome high cooling rate with the least number of doublets" but in case of 20°C as an injection temperature will cause subsurface problems as expected and backed up in this research study then the development strategy with the concept of "Jafer matrix for discontinuous shut-off operation to overcome high cooling rate with the least number of doublets" shown in table 24 is recommended to be used instead. The flow rate for doublet in the period under operational thermal recharge¹ can be lower than the flow rates of another doublet to ensure ultimate economical development using the concept of "Jafer matrix for discontinuous shut-off operation to overcome high cooling rate with the least number of doublets".

5- Based on the rate and state friction law, it is a remarkable truth that extra physical or chemical impacts of fluids may lead to the weakening of materials in fault zones (Kang, Zhu and Zhao, 2019b). This is why further studies and experiments are needed to understand if there will be unstable slip behaviour or stable slip behaviour of faults around the injections wells in the KKP field with higher injection pressure that range from 207.82 bar to the maximum bottom hole pressure of 252 bar allowed by SODM with a detailed study on the effect of fluid pressure on the frictional parameters (a-b) related to the fault composition and conditions in Koekoekspolder field. (In case of encountering difficulties related to the experiments then several scenarios can be studied by checking the type of clay minerals along the major faults by obtaining the cuttings description of the Silverpit formation which is the seal of Koekoekspolder reservoir.

6- For a more accurate distribution of permeability, the fractures in the fault zone area must be taken into consideration because they might affect the flow pattern near the major faults. It is expected to find many minor fractures in the fault zones area (A region that ranges from several meters to kilometers with minor faults and fractures that could be present below the seismic resolution)

7- Further studies are needed to be conducted on the fluid interaction with the reservoir rock in the vicinity of the injection well to be able to model if the dissolution of gypsum is going to take place or not, especially in the area around the injector where the temperature is decreased because the temperature affects the dissolution. Moreover, Further studies might be useful to check if there are other or optimal solutions rather than the one provided in this study to tackle

any predicted dissolution or precipitation due to changes in reservoir conditions, especially around the operating wells.

8- Before the discontinuous shut-off operation will start, it is recommended to gradually decrease the injection temperature from 35.4 to 30. The sudden change in injection temperature and the gradual change in injection temperature effect can be further studied.

9- The technical challenges or expected problems related to the operational equipment using the discontinuous shut-off operation or other unconventional thermal development approaches need to be well studied.

10- Another approach to develop the field that meet the same energy demand would be to drill fewer doublets at the start and produce them at high rate and when the non economical cold water breaks through in a doublet, more doublets can be drilled over the 100 years. This approach can delay the expenditures costs with minor or no change to income.

11- If the owner of the field wants to increase the extractable energy for any reason in the future or to supply other greenhouses, it is recommended to drill the extra wells in the north-eastern part of the KKP field.

12- The materials used for the wells should be carefully chosen for the new planned wells to minimize corrosion and to attain sustainable production without major obstacles such as leaking and other unexpected problems.

13- Continuous history matching is very important to update the subsurface aquifer model. In addition, applying quantitative uncertainty analysis via tornado charts and not only depending on the qualitative uncertainty analysis.

14- The short and long-term impact of cyclic injection pressure on the geothermal reservoir needs to be studied and experimented due to the cyclic reinjection after shutting the doublet for a certain period (discontinuous shut-off). In addition, checking if the gradual increase of injection pressure to reach the desired injection pressure can represent an effective solution.

10. New technology

- I) Indirect increase in doublets either by:
 - a- *The coordinates of the new doublets at the surface can be near the first existing doublet to have a relation and connection between doublets.
 - b- *Injecting the excessive volume of produced water at KKP-GT-01 in KKP-GT-02 with predicting what will happen in the field in terms of pressure distribution and subsidence.
- II) Discontinuous shut-off of doublets for geothermal operation: Powerful technique that yields the largest amount of cumulative energy./ *Creative technology that can overcome high cooling rates. Therefore, the discontinuous shut-off can decrease the restrictions on the injection temperature which in turn increases the profit of the owner of the field. / *The maintenance of the injector well under operational thermal recharge^{*1} can be done by a periodic flush to avoid any decrease in the injectivity index as a result of geochemical problems related to the precipitation and clogging of permeability near the injector well. The fluid temperature must be above 40 degrees to allow the dissolution of the precipitated gypsum in the pore spaces.
- III) Using the low pressure gradient concept for operational thermal recharge^{*1} (lower injection pressure and higher production pressure for operational thermal recharge^{*1}).
- IV) Incorporating the boundaries of the sides layers, where pinch-outs take place can have an important role in thermal recharge because they can act as western,

- eastern, southern, or northern recharge boundaries as well as the confining layers of the geothermal aquifer. It was very important to find the areas with zeros thickness where pinch out takes place to introduce new terms in thermal boundaries like “thermal boundaries at the sides of the aquifer”.
- V) Generating a historical cooling rate distribution in the geothermal aquifer to use it as a reference to compare it with the predicted and simulated cooling rates in the future.
- VI) How to incorporate the idea of the possible natural aquifer flow direction and velocity in the geothermal aquifer model.
- VII) Applying the oversaturation concept for a certain component in the fluid on the injected brine water to avoid dissolution of rock component such as gypsum which can lead to subsidence and/or other undepicted risks.
- VIII) A creative concept is introduced called “Jafer matrix for discontinuous shut off to overcome high cooling rate with the least number of doublets” as illustrated in table 54 because as already mentioned in chart 2, the target from the beginning is to reduce the amount of cash inflow and reaching a sustainable development of the Koekoekspolder field.
- IX) Jafer Periodic counter cooling rate effect [This concept simply means injecting and producing with the same production temperature (For instance injecting with the current production temperature of 75.4°C) [It is a new concept that needs to be studied to resist the high cooling rate around the injection wells], [The operator of the field can do that at least few days in a year. It is for sure non-economical but it can increase sustainability in the long term.
- X) Based on this study, there can be an extra second type of history matching in the Koekoekspolder geothermal field: - First known type of history matching: requires identic simulated and measured flow rates as well as bottom hole pressures.
- Second type of history matching: requires the same historical extractable energy as well as estimated and measured timing and temperature of the produced water for the 2 production wells (KKP-GT-01 & KKP-GT-03) after the year the second production well starts operation.

11. References

- Van 't Spijker, H. and Ungemach, P. (2016) 'Definition of Electrosubmersible pump (ESP) design and selection workflow', (June), pp. 1–38. Available at: https://www.kasalsenergiebron.nl/content/user_upload/Definition_of_ESP_design-_final_version_20160629_-public_v2.pdf.
- Aardwarmtecluster 1 KKP BV (no date) *Winningsplan Aardwarmte Kampen*. Available at: <https://docplayer.nl/204021763-Winningsplan-aardwarmte-kampen.html>.
- Afman, Maarten Hers, Sebastiaan Scholten, T. (2017) 'Power-to-Ammonia: Energy and electricity price scenarios 2020-2023-2030'. Available at: <https://www.ce.nl/publicaties/1912/power-to-ammonia-energy-and-electricity-prices-scenarios-2020-2023-2030>.
- Arisona, A. *et al.* (2018) 'Assessment of Microgravity Anomalies of Soil Structure for Geotechnical 2D Models', *Journal of Geoscience, Engineering, Environment, and Technology*, 3(3), p. 151. doi: 10.24273/jgeet.2018.3.3.2058.
- Bonté, D., Van Wees, J. D. and Verweij, J. M. (2012) 'Subsurface temperature of the onshore Netherlands: New temperature dataset and modelling', *Geologie en Mijnbouw/Netherlands Journal of Geosciences*, 91(4), pp. 491–515. doi: 10.1017/S0016774600000354.
- van den Bosch, R., Flipse, B. and Vorage, R. (2013) 'Stappenplan Winning Aardwarmte voor

Glastuinbouw', *Kas als Energiebron*, (December).

Byerlee, J (1978) 'Friction of rocks', *Pure and Applied Geophysics PAGEOPH*, 116(4–5), pp. 615–626. doi: 10.1007/BF00876528.

Byerlee, J. (1978) 'Friction of rocks', *Pure and Applied Geophysics PAGEOPH*, 116(4–5), pp. 615–626. doi: 10.1007/BF00876528.

Chekhonin, E. *et al.* (2012) 'When rocks get hot: Thermal properties of reservoir rocks', *Oilfield Review*, 24(3), pp. 20–37.

Chen, T., Liu, G. and Liao, S. (2019) 'A comparison study of reservoir boundary conditions of enhanced geothermal systems(EGS)', *Energy Procedia*, 160, pp. 301–309. doi: 10.1016/j.egypro.2019.02.157.

Daniilidis, A., Nick, H. M. and Bruhn, D. F. (2020) 'Interdependencies between physical, design and operational parameters for direct use geothermal heat in faulted hydrothermal reservoirs', *Geothermics*, 86(January), p. 101806. doi: 10.1016/j.geothermics.2020.101806.

Dirkx, R. and Buik, N. (2019) 'Well trajectory KKP-GT-03', 2019(March).

van Dongen, B. (2019) 'Personal communication from Pipeline engineer (van Dongen,B) with Caroline'.

Emujakporue, G. O. and Enyenihi, E. E. (2020) 'Identification of seismic attributes for hydrocarbon prospecting of Akos field, Niger Delta, Nigeria', *SN Applied Sciences*, 2(5), pp. 1–11. doi: 10.1007/s42452-020-2570-1.

en Klimaat, M. van E. Z. and Warmte en Ondergrond; TNO (2019) 'Advies instemming winningsplan geothermie Kampen'.

Eneco (no date) *Eneco*. Available at: <https://news.eneco.com/enecos-heat-prices-remain-well-below-cap-set-by-acm/>.

Energy Education (2019) 'Discounting. 2019.', (Sept), p. 150.

European Commission (no date) *European Commission*. Available at: https://ec.europa.eu/competition-policy/system/files/2021-04/reference_rates_eu25_en.pdf.

Evans, P. (2016) *Specific heat capacity of materials*. Available at: <https://theengineeringmindset.com/specific-heat-capacity-of-materials/>.

Farmer, A. and Russi, D. (2018) 'Annex I-IV KTMs as detailed in WFD Reporting Guidance , examples of discount rates and measures chosen , and outcomes assessed in eight', (July).

Franco, A. and Donatini, F. (2017) 'Methods for the estimation of the energy stored in geothermal reservoirs', *Journal of Physics: Conference Series*, 796(1).

Glennie, K. (1982) *Early Permian (Rotliegendes) palaeowinds of the North Sea: Sedimentary Geology*. Available at: [https://doi.org/10.1016/0037-0738\(83\)90088-X](https://doi.org/10.1016/0037-0738(83)90088-X).

GlobalPetrolPrices (2022) *GlobalPetrolPrices.com*. Available at: https://www.globalpetrolprices.com/Netherlands/electricity_prices/#:~:text=Netherlands%2C%20September%202021%3A%20The%20price,%20of%20power%20distribution%20and%20taxes.

Hazel, W. (2017) 'On the impact of reservoir overburden heterogeneity on subsidence modelling', p. 153.

Henares, S. *et al.* (2014) 'The role of detrital anhydrite in diagenesis of aeolian sandstones (Upper Rotliegend, The Netherlands): Implications for reservoir-quality prediction', *Sedimentary Geology*, 314, pp. 60–74. doi: 10.1016/j.sedgeo.2014.10.001.

Hulen, Jeffrey B., and D. L. N. (1995) "HYDROTHERMAL FACTORS IN POROSITY EVOLUTION AND INSIGHT FROM THE GEYSERS CORING PROJECT." TWENTIETH WORKSHOP GEOTHERMAL RESERVOIR ENGINEERING.'

Ikari, M. J., Saffer, D. M. and Marone, C. (2007) 'Effect of hydration state on the frictional properties of montmorillonite-based fault gouge', *Journal of Geophysical Research: Solid Earth*, 112(6), pp. 1–12. doi: 10.1029/2006JB004748.

J.Jansen (2017) *Nodal Analysis of Oil and Gas Production Systems*. Available at: <https://research.tudelft.nl/en/publications/nodal-analysis-of-oil-and-gas-production-systems>.

Kang, J. Q., Zhu, J. B. and Zhao, J. (2019a) 'A review of mechanisms of induced earthquakes:

from a view of rock mechanics', *Geomechanics and Geophysics for Geo-Energy and Geo-Resources*, 5(2), pp. 171–196. doi: 10.1007/s40948-018-00102-z.

Kang, J. Q., Zhu, J. B. and Zhao, J. (2019b) 'A review of mechanisms of induced earthquakes: from a view of rock mechanics', *Geomechanics and Geophysics for Geo-Energy and Geo-Resources*, 5(2), pp. 171–196. doi: 10.1007/s40948-018-00102-z.

Kiersnowski, H. (2013) 'Late permian aeolian sand seas from the polish upper rotliegend basin in the context of palaeoclimatic periodicity', *Geological Society Special Publication*, 376(1), pp. 431–456. doi: 10.1144/SP376.20.

Kirk, S. S. and Williamson, D. M. (2012) 'Structure and thermal properties of porous geological materials', *AIP Conference Proceedings*, 1426(March 2012), pp. 867–870. doi: 10.1063/1.3686415.

Klimaat, M. van E. Z. en and Warmte en Ondergrond; TNO (2019a) *Advies instemming winningsplan geothermie Kampen*. Available at: https://www.nlog.nl/sites/default/files/2020-08/191016_advies_tno_wp_kampen_gelakt.pdf.

Klimaat, M. van E. Z. en and Warmte en Ondergrond; TNO (2019b) 'Advies instemming winningsplan geothermie Kampen'. Available at: https://www.nlog.nl/sites/default/files/2020-08/191016_advies_tno_wp_kampen_gelakt.pdf.

Maharaja, A. (2007) 'Global Net-To-Gross Uncertainty Assessment At Reservoir Appraisal Stage', (June), pp. 1–162.

MAJASKI, C. (2022) *Investopedia*. Available at: <https://www.investopedia.com/ask/answers/052715/what-difference-between-cost-capital-and-discount-rate.asp>.

Mansur, G. M. (2018) 'Master Thesis in Applied Earth Sciences Flow in Fractured Media : a Darcy-Stokes-Brinkman Modelling Approach'.

Mechelse, E. and Hettema, M. (2017) 'The in-situ stress field in the Netherlands : Regional trends , local deviations and an analysis of the stress regimes in the northeast of the Netherlands', (August).

Peacock, J. R. *et al.* (2019) 'Geophysical characterization of the heat source in the Northwest Geysers, California', *44th Workshop on Geothermal Reservoir Engineering*, p. 7. Available at: <https://pangea.stanford.edu/ERE/db/GeoConf/papers/SGW/2019/Peacock.pdf>.

Power Technology (2012) *The Geysers Geothermal Field, California, 11-04-2012*. Available at: <https://www.power-technology.com/projects/the-geysers-geothermal-california/>.

Redjosentono, E. A. (2014) *AES / TG / 14-03 Static aquifer modelling of a Rotliegend Aeolian Sandstone for the Koekoekspolder Geothermal project . Copyright © 2014 Section for Applied Geology All rights reserved . Without the prior written permission of the.*

Reinhard, P. L. (2019) 'Pressure and Temperature Interference for Geothermal Projects in Dense Production Areas'. Available at: <http://resolver.tudelft.nl/uuid:7a0b0c31-1ee8-4678-9aa2-f354b375ebec>.

Reith, D. F. H. (2019) 'Dynamic simulation of a geothermal reservoir Dynamic simulation of a geothermal reservoir', *TU Delft*. Available at: <http://resolver.tudelft.nl/uuid:e38ecf05-dfc1-4bcc-b995-875e178609dc>.

Rutqvist, J. *et al.* (2008) 'Analysis of thermally induced changes in fractured rock permeability during 8 years of heating and cooling at the Yucca Mountain Drift Scale Test', *International Journal of Rock Mechanics and Mining Sciences*, 45(8), pp. 1373–1389. doi: 10.1016/j.ijrmms.2008.01.016.

RVO (2020) 'SDE++ 2020 Stimulation of Sustainable Energy Production and Climate Transition', (December).

Scuderi, M. M. and Colletini, C. (2016) 'The role of fluid pressure in induced vs. triggered seismicity: Insights from rock deformation experiments on carbonates', *Scientific Reports*, 6(January), pp. 1–9. doi: 10.1038/srep24852.

Segall, P. and Fitzgerald, S. D. (1998) 'A note on induced stress changes in hydrocarbon and

geothermal reservoirs', *Tectonophysics*, 289(1–3), pp. 117–128. doi: 10.1016/S0040-1951(97)00311-9.

SIMMELINK, E. and UNDERSCHULTZ, J. (2015) *Integrated pressure information system for the onshore and offshore Netherlands Final report*.
ThermoGIS (no date). Available at: <https://www.thermogis.nl/en/economic-model>.

TNO-AGE; SodM (2013) *Protocol bepaling maximale injectiedrukken bij aardwarmtewinning – versie 2*.

TNO-GSN (2020) 'In: Stratigraphic Nomenclature of the Netherlands; TNO – Geological Survey of the Netherlands.', 31-12-2020. Available at: <http://www.dinoloket.nl/en/stratigraphic-nomenclature/slochteren-formation>.

TNO; Minister of Economic Affairs and Climate (no date) *NLOG Dutch Oil and Gas Production, 07-10-1969*.

TUOVILA, A. (2022) <https://www.investopedia.com/alicia-tuovila-4687215>. Available at: <https://www.investopedia.com/terms/d/depreciation.asp>.

Verweij, H., Simmelink, E. and Underschultz, J. (2011) 'Pressure and fluid flow systems in the Permian Rotliegend in the Netherlands onshore and offshore', *SEPM Special Publications*, 98(June 2015), pp. 247–263. doi: 10.2110/pec.11.98.0247.

Verweij, J. M., Echternach, M. S. C. and Witmans, N. (2010) 'Central Offshore Platform - Area NCP2E Burial history, temperature, source rock maturity and hydrocarbon generation', *Offshore (Conroe, TX)*.

Warren, J. K. (2020) 'Brine density & persistence: Part 1 Physical properties of a brine', *Salty Matters*, pp. 1–10. Available at: www.saltworksconsultants.com.

Van Wees, J. D. et al. (2012) 'Geothermal aquifer performance assessment for direct heat production-Methodology and application to Rotliegend aquifers', *Geologie en Mijnbouw/Netherlands Journal of Geosciences*, 91(4), pp. 651–665. doi: 10.1017/S0016774600000433.

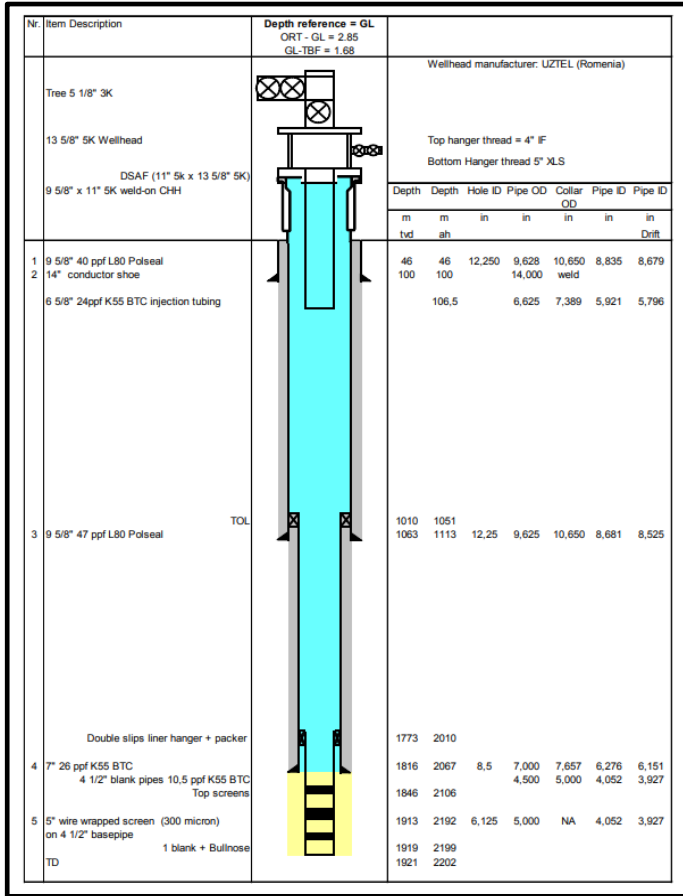
Well Engineering Partners (no date) 'End Of Well Report Koekoekspolder', *End of Well Report*, (August), p. 25. Available at: <https://docplayer.nl/40526637-End-of-well-report-koekoekspolder.html>.

Willems, Cees; Donselaar, Rick; Weltje, G. J. (2014) *Delft University of Technology Reservoir modelling of Lower Cretaceous West Netherland Basin aquifers for geothermal energy production Rijnland*.

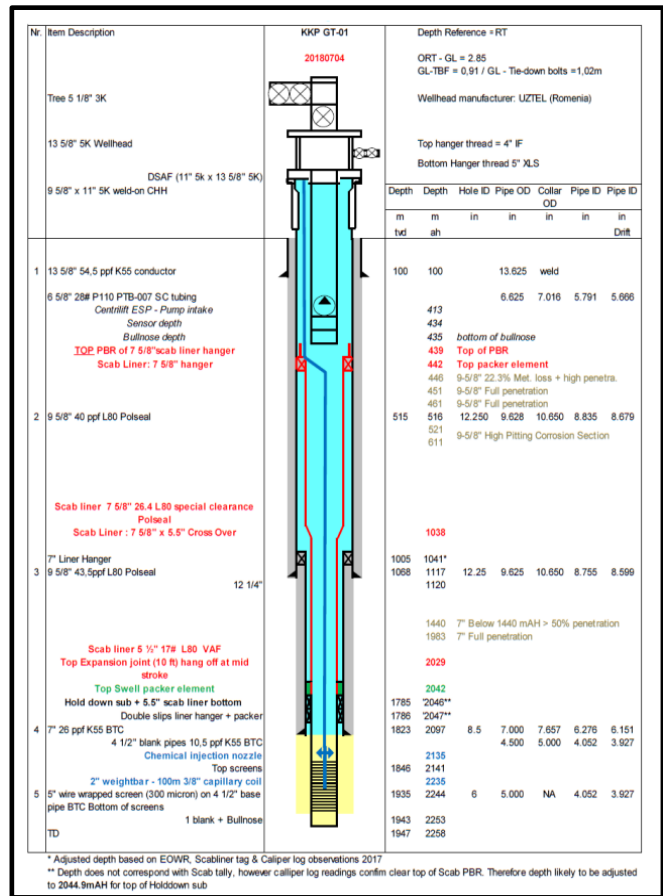
Zaal, C. (2020) 'Geothermal Field Development Strategies Based on Economic and Fault Stability Analysis A Case Study for the Delft Sandstone Area', (May). Available at: <http://repository.tudelft.nl/>.

Ziegler, K. (2006) 'Clay minerals of the Permian Rotliegend Group in the North Sea and adjacent areas', *Clay Minerals*, 41(1), pp. 355–393. doi: 10.1180/0009855064110200.

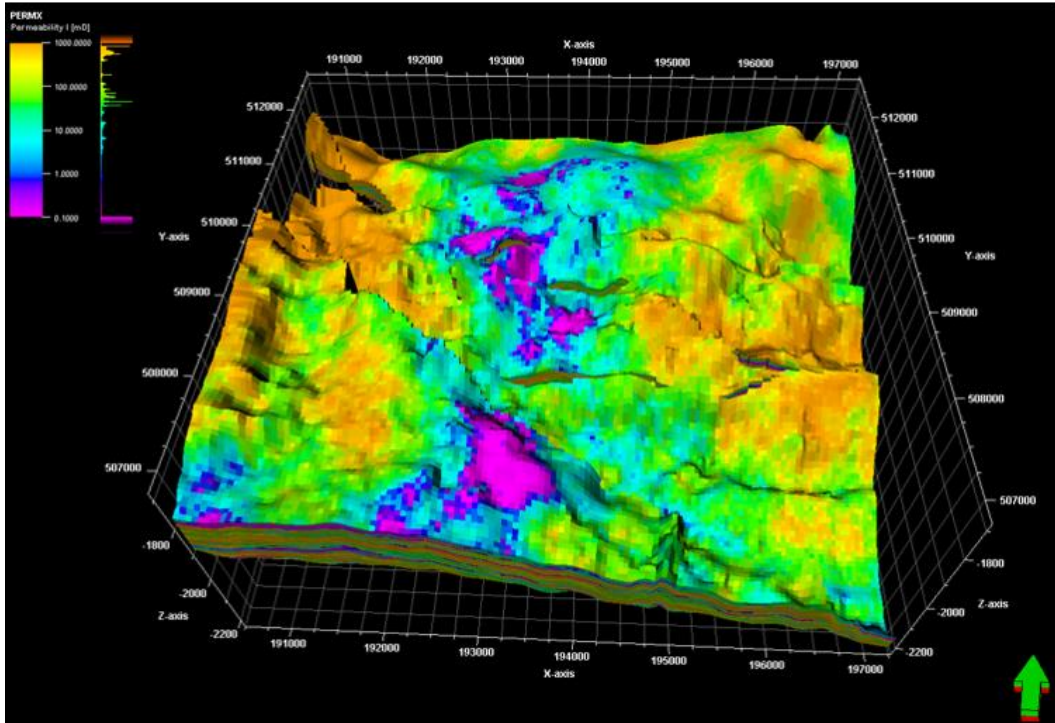
12. Appendices



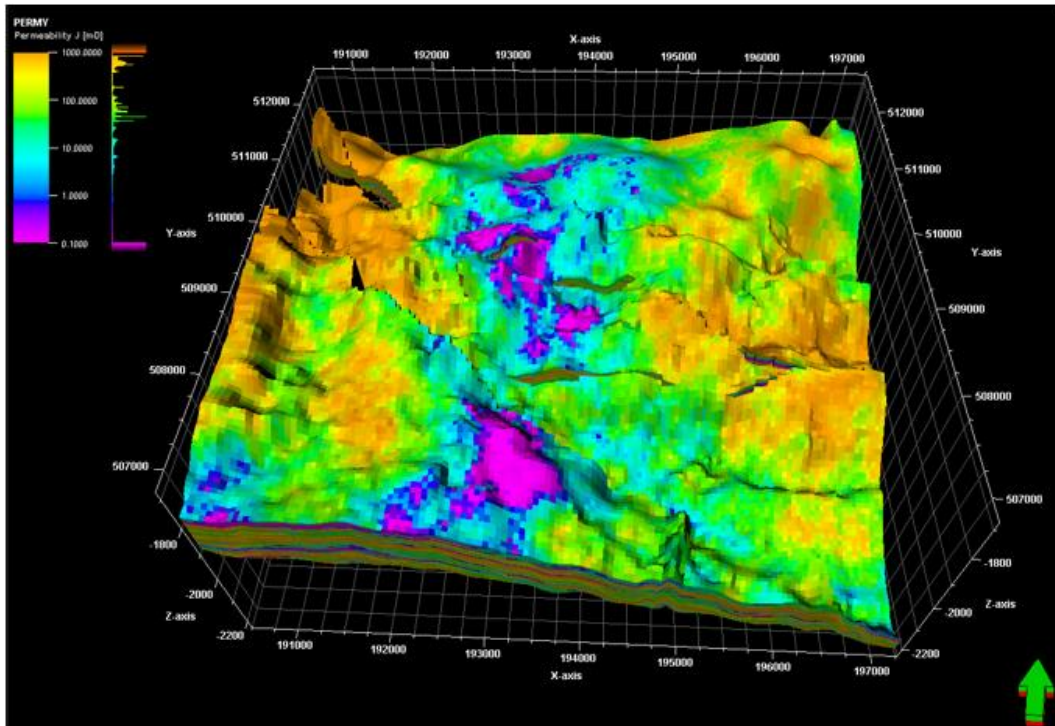
Appendix 1: KKP-GT-02 Injection well schematic (Well Engineering Partners, no date).



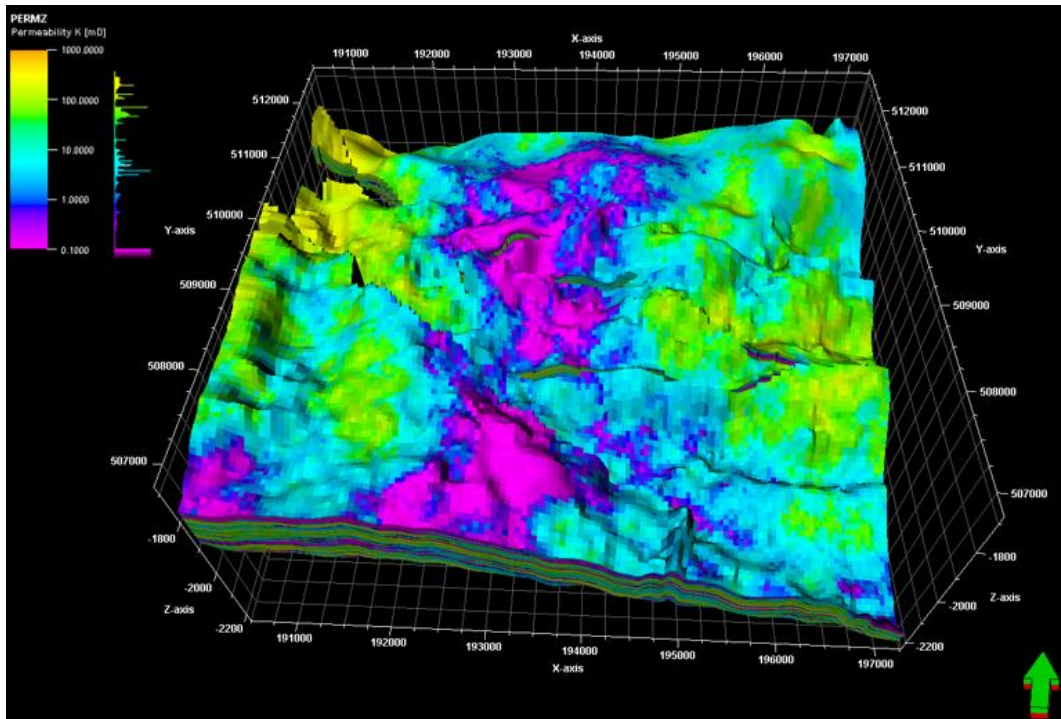
Appendix 2: KKP-GT-01 production well schematic (Aardwarmtecluster 1 KKP BV, no date).



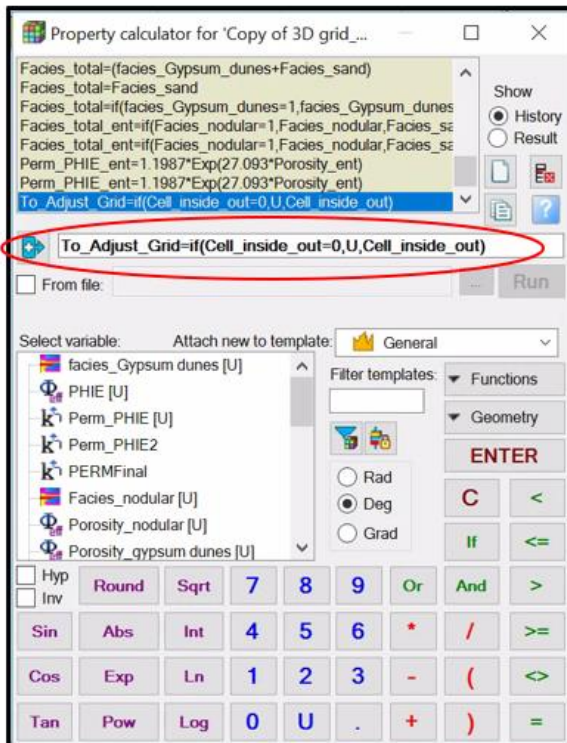
Appendix 2a: Adjusted permeability distribution in the X direction.



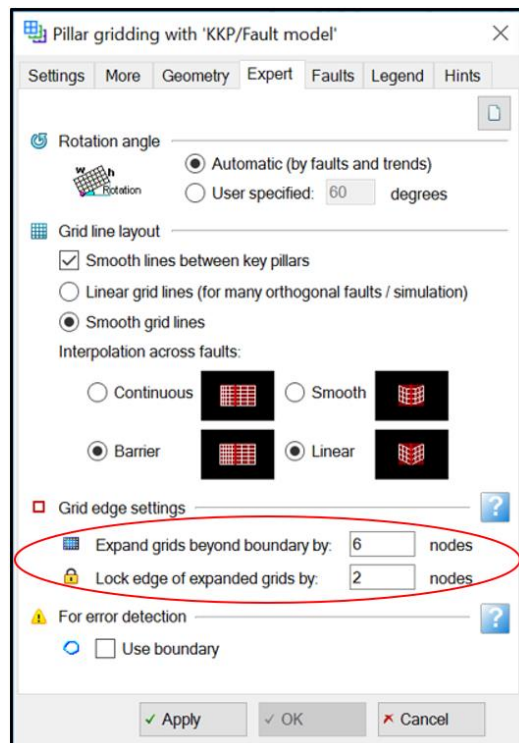
Appendix 2b: Adjusted permeability distribution in the Y direction.



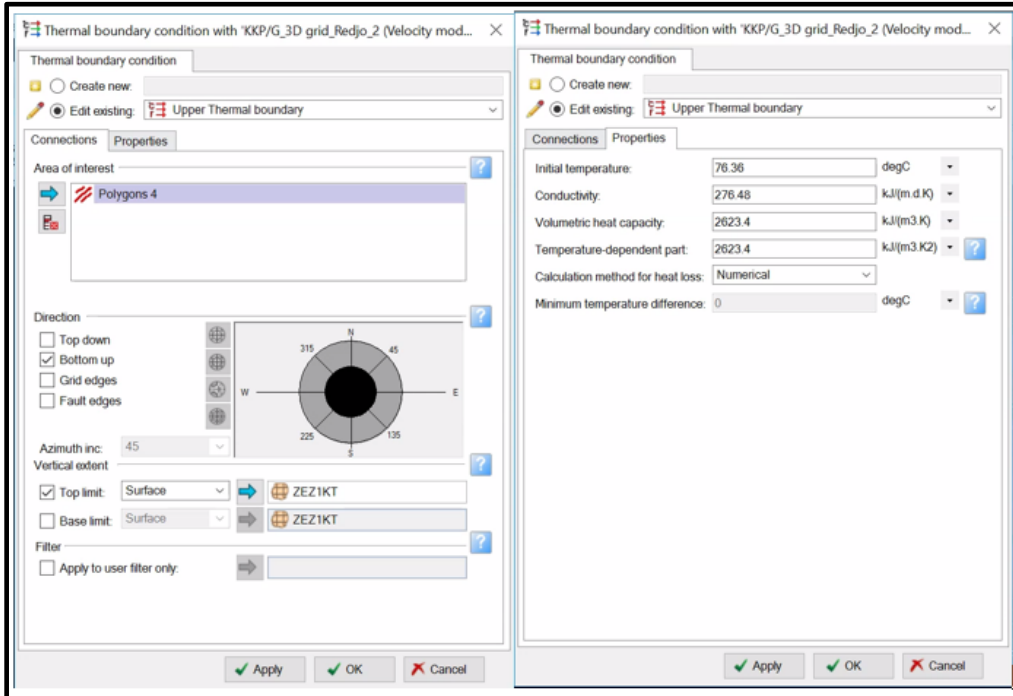
Appendix 2c: Adjusted permeability distribution in the Z direction.



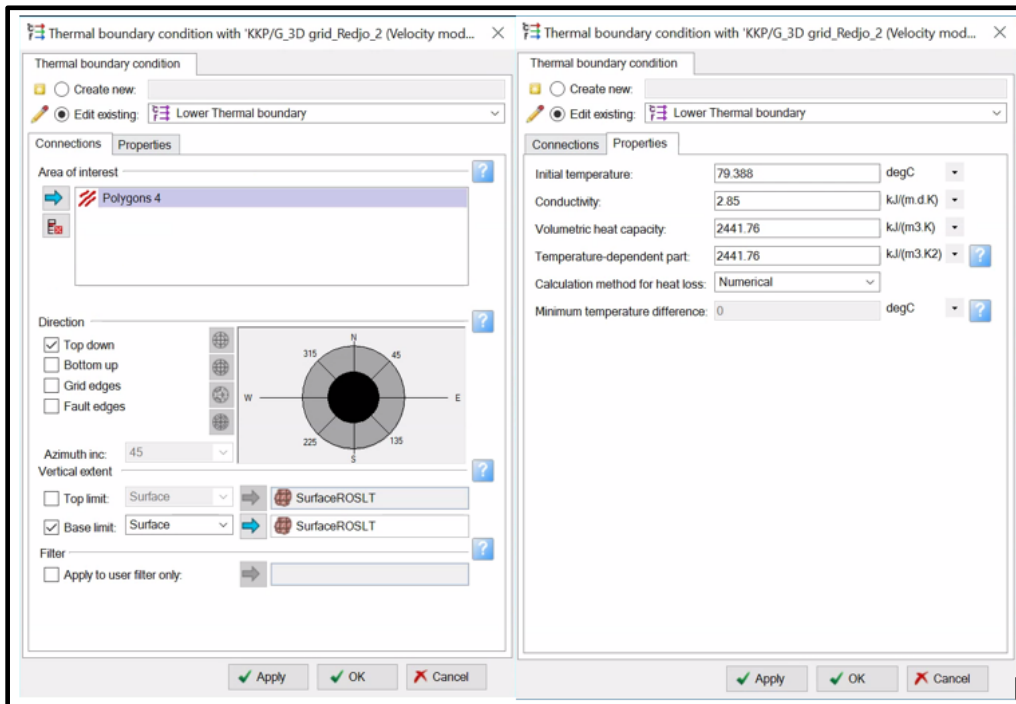
Appendix 3: represents the simple code used to neglect the skewed grids.



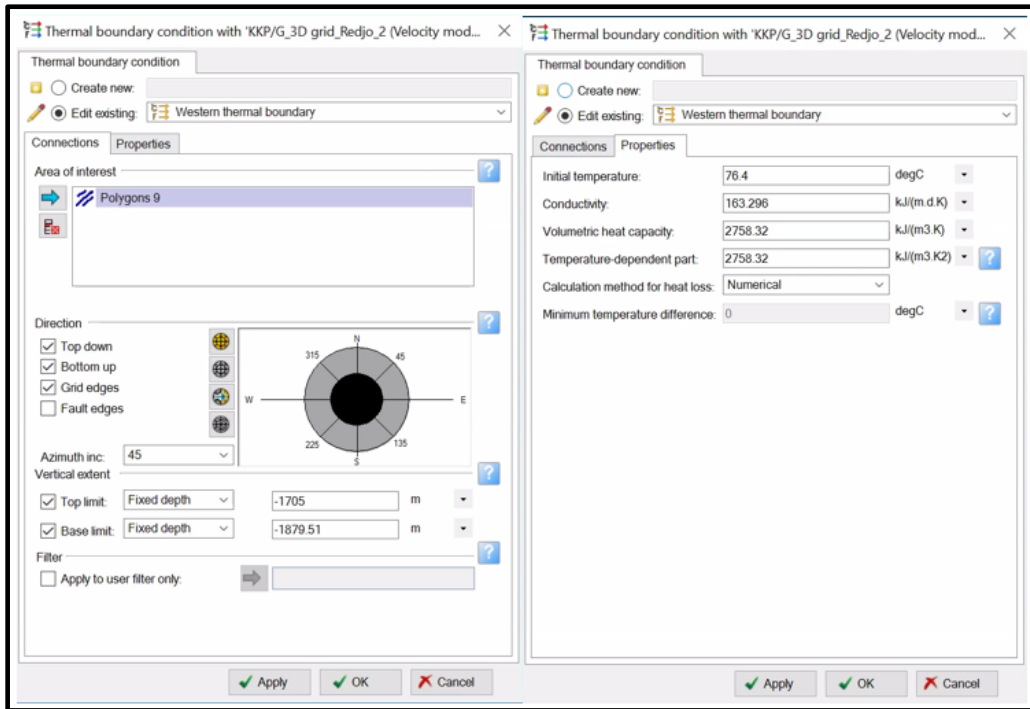
Appendix 4: illustrates the values of nodes used to adjust the grid edge settings. According to Petrel software, there is a complete freedom for the edges once the value of grids expansion beyond boundary is set to zero.



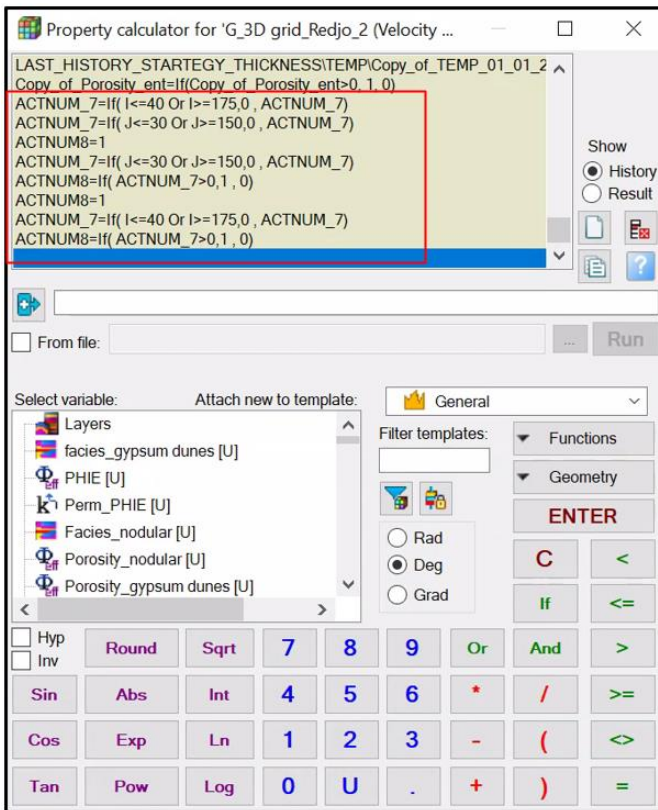
Appendix 5-a: represents the input data and adjustments applied for the upper thermal boundary.



Appendix 5-b: represents the input data and adjustments applied for the lower thermal boundary.



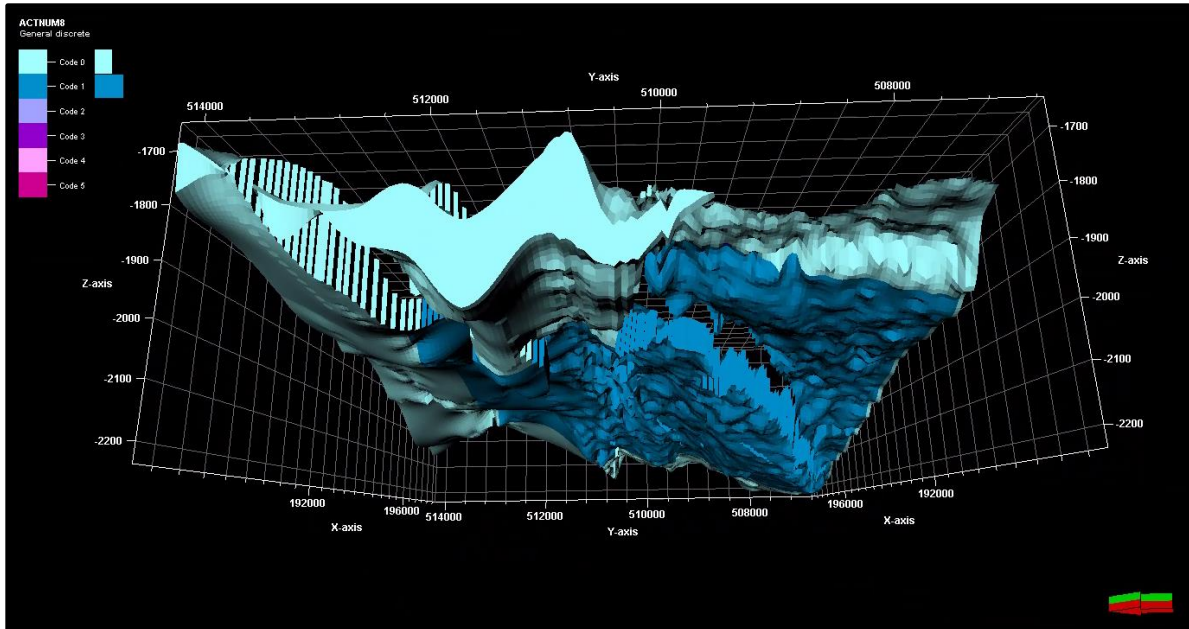
Appendix 5-c: shows the input data and adjustments applied for the western thermal boundary.



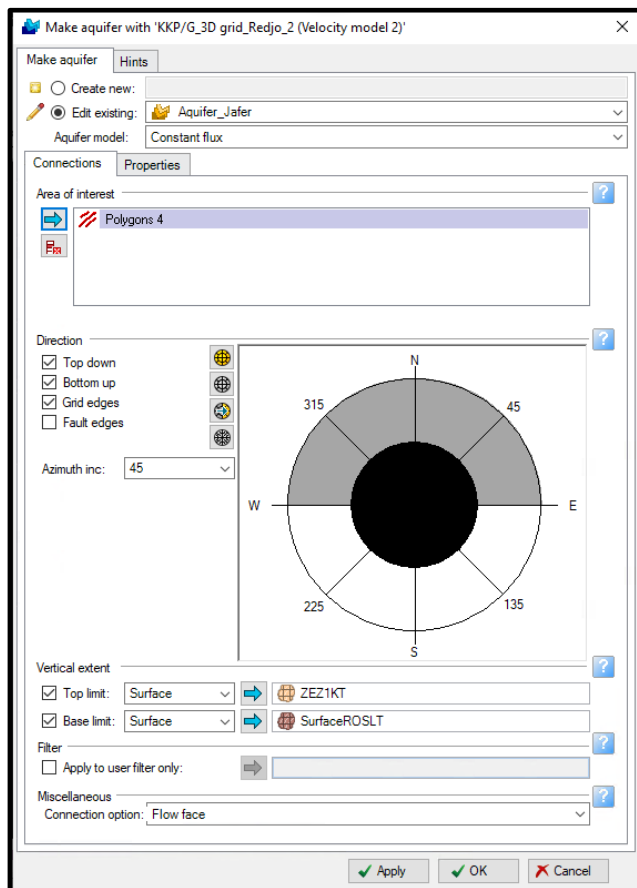
Appendix 6: represents the code used to define the extension of the smaller active sector.



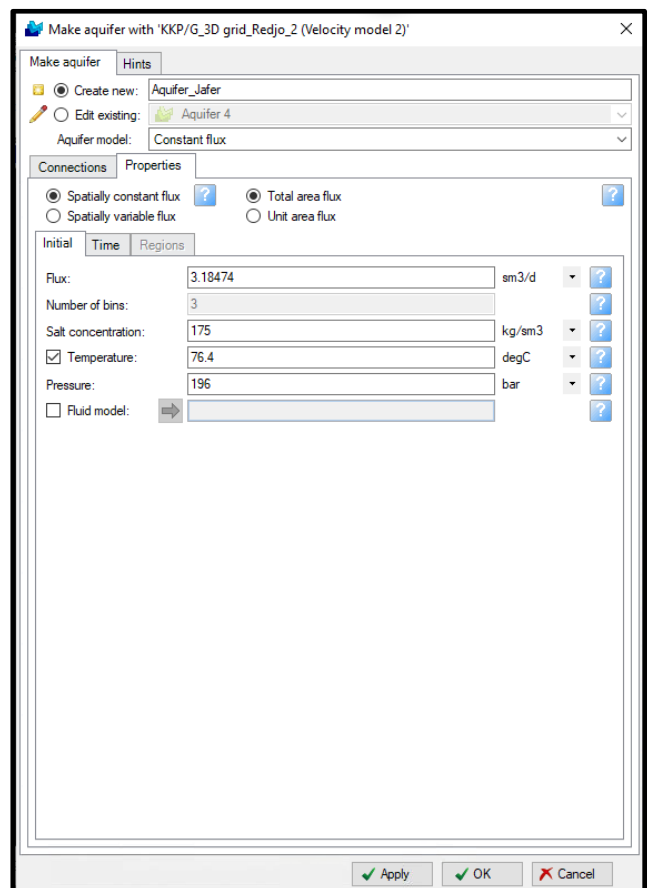
Appendix 6-a: shows the areas with colour coding where the owner of the field is interested to know their future energy distribution.



Appendix 7: shows the new smaller sector model that takes into consideration the upper and lower thermal boundaries as well as western thermal boundary due to pinching out.



Appendix 8: shows the needed adjustments for the connections of the aquifer.



Appendix 9: shows the input data for the properties of the constant flux aquifer model.

Alternative possible second doublet location	Coordinates at aquifer depth	Depth	Covered Thickness
Injection well (KP-GT-BB4)	X= 195748.87 m/ Y =510035.94 m	-2038.01 m	114.89 m
Production well (KP-GT- BB5)	X = 197135.99 m/ Y =510154.40 m	-2082.24 m	80 m

Appendix 10: Information related to the possible second doublet.

Alternative possible Third doublet location	Coordinates at aquifer depth	Depth	Covered Thickness
Injection well (KP-GT-BB6)	X= 194601.35 m/ Y = 508593.93 m	-2179.85 m	56.63 m
Production well (KP-GT-07)	X = 196885.61 m/ Y = 508578.19 m	-2094.88 m	47.4741 m

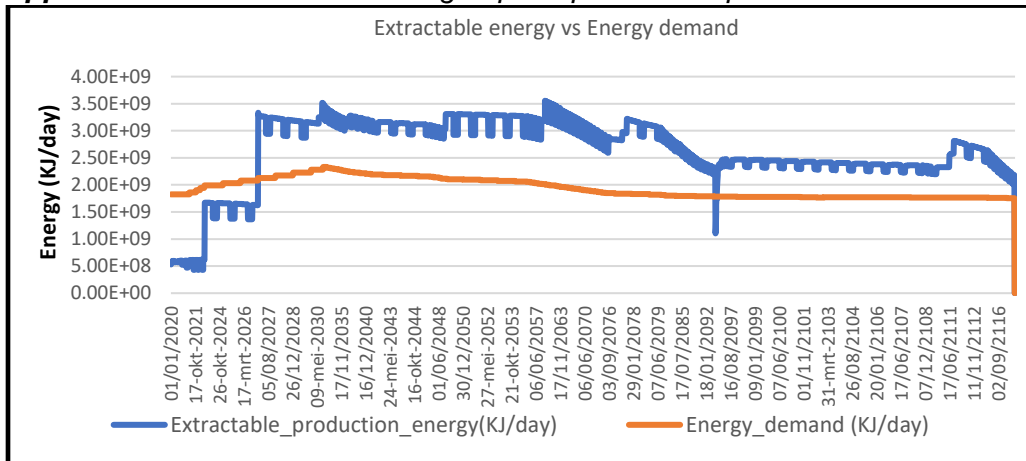
Appendix 11: Information related to the possible third doublet.

#####	Injection temperature (°C)	Number of wells	Injection pressure	Distribution of flow amongst the production wells
1 (Base case)	35	3	max	Distribution based on the Kh of both producers
2	35	2	max	n.a.
3	35	3	max	25% - 75%
4	35	3	max	50% - 50%
5	35	3	max	75% - 25%
6	25	3	max	Distribution based on the Kh of both producers
7	25	2	max	n.a.
8	25	3	max	25% - 75%
9	25	3	max	50% - 50%
10	25	3	max	75% - 25%
11	20	3	max	Distribution based on the Kh of both producers
12	20	2	max	n.a.
13	20	3	max	25% - 75%
14	20	3	max	50% - 50%
15	20	3	max	75% - 25%
16	35	3	max+10 bar	Distribution based on the Kh of both producers
17	35	2	max+10 bar	n.a.
18	35	3	max+10 bar	25% - 75%
19	35	3	max+10 bar	50% - 50%
20	35	3	max+10 bar	75% - 25%
21	25	3	max+10 bar	Distribution based on the Kh of both producers
22	25	2	max+10 bar	n.a.
23	25	3	max+10 bar	25% - 75%
24	25	3	max+10 bar	50% - 50%
25	25	3	max+10 bar	75% - 25%
26	20	3	max+10 bar	Distribution based on the Kh of both producers
27	20	2	max+10 bar	n.a.
28	20	3	max+10 bar	25% - 75%
29	20	3	max+10 bar	50% - 50%
30	20	3	max+10 bar	75% - 25%

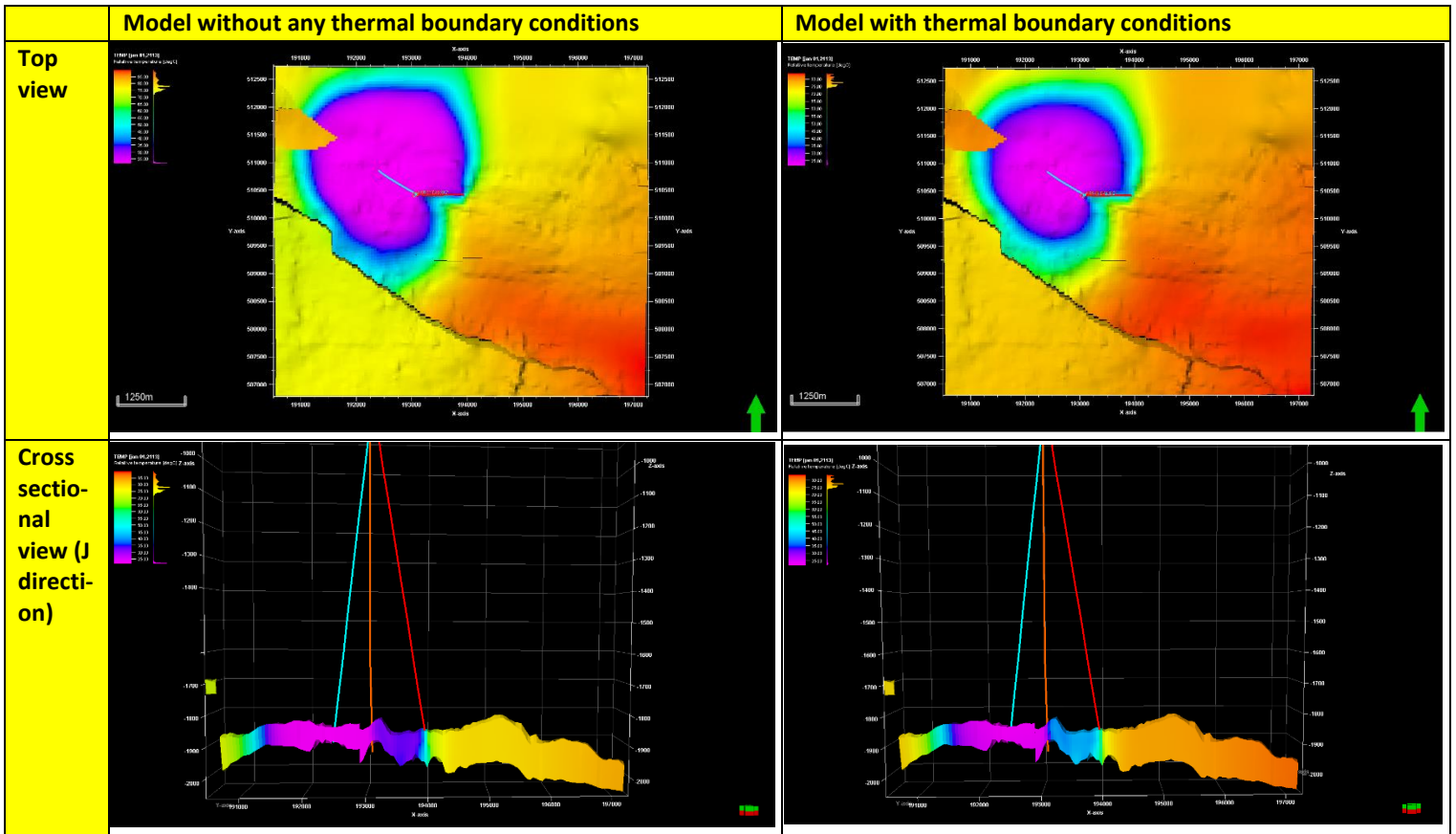
Appendix 12: shows the planned simulation cases scenarios.

Simulation case number	Forecasting strategy for operational thermal recharge*1	Properties
31	Continuous shut offs	Without natural aquifer velocity and direction
32	Continuous shut offs	Without natural aquifer velocity and direction but with updated flow rates (The flow rates were updated to fulfill the energy demand)
33	Continuous shut offs	With constant flux aquifer velocity method in Petrel
34	Continuous shut offs	With numerical aquifer velocity method in Petrel
35	Continuous shut offs	Without initial velocities but with indirect increase in doublets
36	Discontinuous shut offs	Without natural aquifer velocity and direction
37	Low pressure gradient	Without natural aquifer velocity and direction
38	Optimal forecasting strategy for the whole field	with natural constant flux aquifer velocity but with lateral distant doublets and KKP-GT-03 in the same position
39	Optimal forecasting strategy for the whole field	with natural constant flux aquifer velocity but with lateral distant doublets and alternative position of KKP-GT-03
40	Optimal forecasting strategy for the whole field	Without natural aquifer velocity but with alternative position of all wells and KKP-GT-03 in the same position
41	Optimal forecasting strategy for the whole field	Without natural aquifer velocity but with alternative position of all wells and KKP-GT-03 in an alternative position

Appendix 13: shows the second group of updated and planned simulation cases.



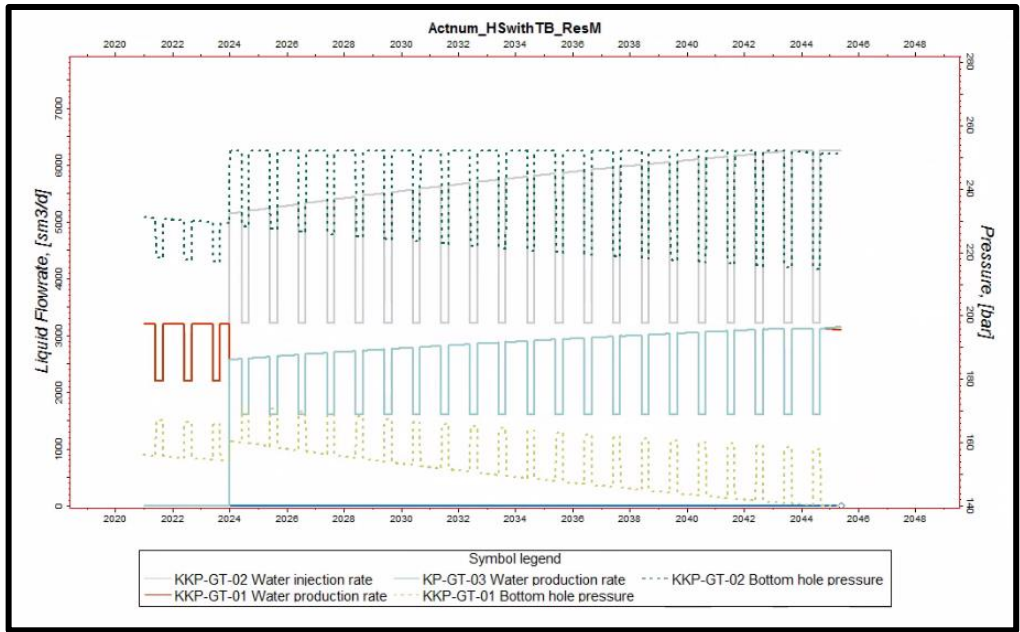
Appendix 13-a: shows the extractable energy with the energy demand after applying the updated forecasting scenario for the continuous shut-off development strategy.



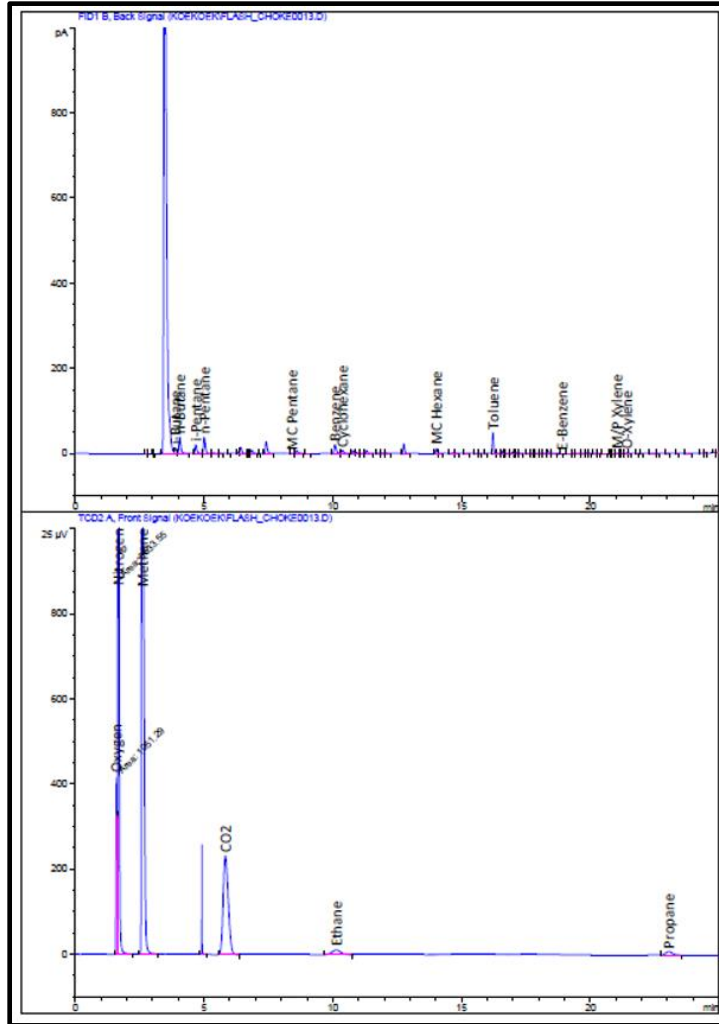
Appendix 14: Table which shows the top and cross-sectional views of the temperature distribution for the model with (confining layers and western thermal boundaries conditions) and the model without any thermal boundaries conditions in the year 2113.

Aquifer depth (m)	Temperature (°C)
-1836.96	74.24
-1843.24	73.30
-1849.52	71.35
-1855.8	68.55
-1862.31	70.71
-1868.11	71.32
-1874.64	74.29
-1886.92	75.85
Average temperature	72.45125

Appendix 15: Information about the predicted temperature in the vicinity of the second production well “KKP-GT-03” for several depths as well as the average temperature.



Appendix 16: shows the injection flow rate of KKP-GT02 and the production flow rate of the production wells KKP-GT-01 and KKP-GT-03 and their bottom hole pressure profile from 2021 to 2045 using a 140 bar as a minimum bottom hole production pressure constraint.



Appendix 17: shows a chromatogram Flashed gas sample (Well Engineering Partners, no date).